Closed-loop System Identification with Operator Intervention

by

Xunqing Jiang

A thesis submitted in conformity with the requirements
for the degree of Master of Applied Science
Graduate Department of Chemical Engineering & Applied Chemistry
University of Toronto

to my parents Wensheng Jiang and Mingyuan Sun

Abstract

During a process identification experiment, it often occurs that the process output variable drifts outside the acceptable operating region due to process disturbances. In this situation, the operator will attempt to bring the process output variable back inside the desired operating region by adjusting the manipulated input variable. This thesis studies the effects of such operator intervention on the accuracy of the identification results and proposes the use of correct noise models in the design of a process input-output data prefilter to remove the resulting biasing effects. In addition, this thesis develops a modified generalized least squares algorithm to simultaneously estimate the process model and the noise model.

Acknowledgements

I would like to take this opportunity to offer my sincere thanks to my wonderful supervisors, Dr. William R. Cluett and Dr. Liuping Wang for their friendship, supervision and assistance throughout the course of my graduate work.

I would also like to thank all my colleagues at the University of Toronto who have made my study in the master program productive and enjoyable. Special thanks to the fellow control group students for their excellent company and talented assistance. They are Michelle Desarmo, Dave Houser, Marshall Khan, Alex Kalafatis, Sophie McQueen, Raj Mutha, Steve Niu, Sharon Pate, Kim Stangeby and Joe Tseng.

Finally, I thank my family members for all their unselfish support during this endeavor. In addition, I must thank my close friends for the joy they brought to me besides my life in school.

I would also like to acknowledge financial support from Imperial Oil, Sunoco, Noranda and NSERC under their University-Industry Partnership program.

Contents

List of Figures

Nomenclature

a_t	White noise sequence
$C(z)$	Transfer function of the controller
E	Expected value
$e_{t,-t}$	PRESS residuals
e_t	Prediction error
F_k	Frequency sampling filter
$G(z)$	Transfer function from u_t to y_t
$G(z,\theta)$	Transfer function in a model structure
$G(e^{j\omega_k})$	Frequency response at sampling frequency ω_k
g_m	Step response coefficient
$H(z)$	Transfer function of the noise
h_i	Impulse response coefficient
$\pm$LIM	Acceptable range of process output
M	Number of data points
n	Effective order of FSF model
n_f	Noise model order
N	Order of FIR model
$R_{\alpha\beta}(\tau)$	Cross-covariance function of α and β at time lag τ
T_s	Settling time
u_t	Process input
v_t	Disturbance sequence
y'_t	Noise free process output
y_t	Measured process output
y_{sp}	Desired setpoint value for process output
z^{-1}	Back shift operator

Greeks

Δt	Sampling interval
σ^2	Variance of white noise
θ	Parameter vector
θ_0	True parameter vector
$\hat{\theta}$	Estimated parameter vector
ϕ_t	Regressor vector
$\Phi_u(\omega)$	Spectrum of u_t
ω_k	Discrete frequency $\frac{2\pi k}{N}$ (radians)

Superscripts

T	Transpose
-1	Inverse
$*$	Complex conjugate transpose
$\wedge$	Estimated quantity

Subscripts

f	Prefiltered quantity
0	True quantity
sp	Desired setpoint value
t	Sampling instant

Abbreviations

AIC	Akaike's Information Criterion
ACF	Autocorrelation Function
AR	AutoRegressive
ARI	AutoRegressive-Integrated
ARIMA	AutoRegressive-Integrated-Moving Average
ARMA	AutoRegressive-Moving Average
DFT	Discrete Fourier Transform

FIR	Finite Impulse Response
FPE	Final prediction error
FSF	Frequency Sampling Filter model
GLS	Generalized Least Squares
I	Integrated
IMA	Integrated-Moving Average
LS	Least Squares
MA	Moving Average
MPC	Model Predictive Control
MIMO	Multi-input Multi-output System
MISO	Multi-input Single-output System
PACF	Partial autocorrelation function
PEM	Prediction Error Method
PLS	Projection to latent structures
PRESS	PREdiction Sum of Squares
SISO	Single-Input, Single-Output system
TS	Two-Step Method for Closed-loop System Identification

Chapter 1

Introduction

1.1 Motivation

In the chemical process industries, design of a control system requires a mathematical model of the process. The process model may be used as the basis for controller design, or incorporated directly in the control law. Not all process control strategies use a model explicitly in their implementation. However, most strategies are "model-based" in the sense that some characteristics of the process must be known in order to carry out the design. Model Predictive Control (MPC) represents a family of process control algorithms which make direct use of an explicit and separately identifiable model (Prett and Garcia, 1988).

To develop a dynamic model of the process, either a first principles approach, or a black-box approach may be used. With the first principles approach, the process model is derived from physical and chemical principles such as the conservation laws. With the black-box approach, the model is developed directly from process input-output data. There exist many identification techniques for obtaining a process model from black-box experiments (Ljung, 1987). In this thesis, process modelling using the black-box approach is considered.

Data used to identify a mathematical model of the process are obtained from plant experiments, where the process inputs are perturbed and process outputs are measured. The identification experiment can be carried out in open-loop, where a pre-

determined input signal is applied to the process without any concern for whether the process output drifts outside a desired operating range. However, many systems must remain in closed-loop under feedback control due to safety and production restrictions. The feedback control can be either continuous or intermittent. Feedback control caused by an operator who intervenes and adjusts the process input when the process output drifts out of a desired range is an example of intermittent feedback.

Several important issues related to closed-loop identification have been reviewed in the recent paper by MacGregor and Fogal (1995). In this paper, the authors indicated that problems arise with the identification of high order finite impulse response (FIR) models under closed-loop conditions. Because these conditions are typical of how identification experiments are conducted in the chemical process industries combined with the popularity of FIR-type models in the design of many modern control strategies, the problems cited by MacGregor and Fogal (1995) have raised many questions about the proper use of these types of models. This thesis will revisit and attempt to clarify some of the issues raised by MacGregor and Fogal and will also examine some new issues which go beyond the scope of their earlier work.

1.2 Literature Review

1.2.1 Closed-loop System Identification

Much of the existing theory on system identification was developed in the 1970's (Gustavsson et al., 1977). Several methods have been proposed and can be categorized as either non-parametric or parametric methods. With non-parametric methods, a finite-dimensional parameter vector is not explicitly used in the search for the best model description. With parametric methods, a candidate model structure must be first selected.

The popular non-parametric approaches are commonly known as correlation analysis and spectral analysis. These methods can be successfully used to identify a process using data obtained from open-loop experiments. It is well known that these techniques yield no information about the true system if the data are generated from purely feed-

back operation. It has been shown in the literature that the presence of an external signal or dither signal is necessary in the closed-loop case in order to make a process identifiable (Wellstead, 1977; Fang and Xiao, 1988).

The most well-known parametric approach is the prediction error method (PEM). Within the prediction error method, three different approaches are available for identifying a system working in closed-loop: the direct method, the indirect method, and the joint input-output method. With the direct method, the experimental data are used as if no feedback was present, i.e. knowledge of the controller is not required. With the indirect method, the external setpoint must be measurable and the feedback law must be known. With the joint input-output method, the input-output process is first modelled jointly as the output of a system driven by white noise. The plant dynamics are subsequently derived from the joint model by matrix operations. The direct method has a major advantage over the other two in that it allows for a wider variety of possible structures for the unknown regulator, namely the regulator can be time varying, whereas the indirect method requires prior knowledge of the regulator and the joint input-output method is limited to systems with a linear and time-invariant regulator (Anderson and Gevers, 1982). In the case of the intermittent feedback introduced via operator intervention, the dynamics of the feedback controller may be quite complicated (e.g. perhaps nonlinear and time varying). Therefore, the direct method will be adopted in this thesis.

A few new closed-loop identification methods have been developed recently. Based on the concept of an observer for reducing the effect of noise in the identification of a state-space representation of the process working in open-loop (Chen et al., 1992; Juang et al., 1993) , Phan et al. (1994) proposed an identification technique dealing with the case where the feedback controller is known. To deal with the case where the feedback controller is unknown and assumed to be linear and time-invariant, Juang and Phan (1994) developed a similar method. These methods result in an unbiased estimate of the process model for systems working in closed-loop operation as long as the excitation signals are sufficiently rich, and the measurement noises are white, zero-mean, and Gaussian. Moreover, Van Den Hof and Schrama (1993) proposed a Two-Step method

(TS) which consistently estimates the process transfer function regardless of whether the noise contribution to the data can be modelled exactly. They also formulated an explicit expression for the asymptotic bias distribution of the identified model when the transfer function of the system cannot be modelled exactly. With different identification objectives, Huang and Shah (1996) proposed a similar two-step closed-loop identification method which asymptotically retains the accuracy of open-loop identification through the design of the sensitivity function decoupling filter.

1.2.2 Operator Intervention

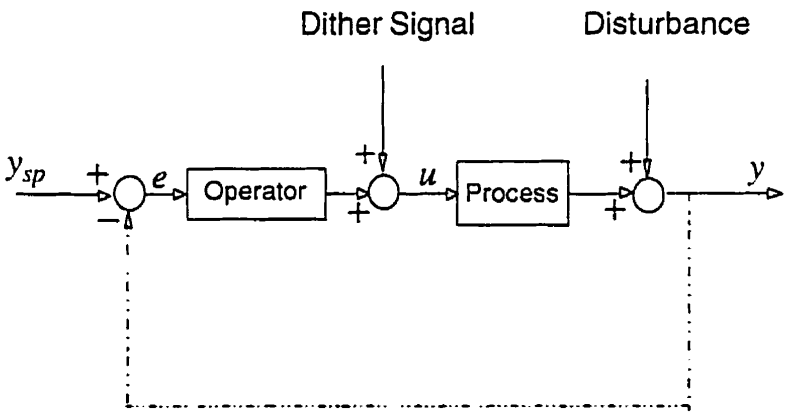

Figure 1.1: Conceptual block diagram of the procedure of operator intervention

The procedure of operator intervention can be described using Figure 1.1. During an identification experiment, a dither signal is introduced to the system input to excite the process, while the process output, y, is observed and compared with a set-point value, y_{sp}. When the difference between the set-point and the measured output (error, e) is outside an acceptable range, the operator makes an adjustment to the process input

to bring the process output back towards the target value. Because the operator intervention is not continuous, i.e. it happens only at the sampling instants when the process output is outside its acceptable range, we use a dashed line in Figure 1.1 to represent this intermittent feedback path. In the chemical process industries, identification experiments are often performed under such conditions. In this thesis, "open-loop" will refer to the situation where a pre-determined input signal is applied to the process without any concern for whether the process output drifts outside the desired operating range. "Closed-loop" will refer to the situation where the input is a combination of a pre-determined sequence or dither signal plus additional moves made by an operator to bring the process output back into the desired operating region.

As mentioned previously, several important issues related to process identification using data collected under various closed-loop conditions have been reviewed by MacGregor and Fogal (1995). They analyzed the role of the noise model and data prefilters on the identifiability of the process model. Also, they estimated higher order FIR-type models with data containing operator intervention, and implied that identification problems arise when trying to estimate high order FIR-type models under closed-loop conditions even when the data is properly prefiltered.

If the identification experiment is carried out entirely under open-loop conditions, Ljung (1987) shows in his Theorem 8.4 that the process model can be consistently estimated using the PEM approach without careful attention to the estimation of the noise transfer function as long as the process model and noise model are independently parameterized, the process model is sufficiently complex to capture the true process transfer function, and the noise model is stable. When the data is collected under closed-loop conditions, Ljung shows in his Theorem 8.2 and 8.3 that both process model and noise model can be consistently estimated using a PEM approach as long as the process and noise models are sufficiently complex to capture the true process and noise transfer functions. An alternative approach under closed-loop conditions is to estimate just the process model using prefiltered data. However, to obtain consistent estimates for the process model, the prefilter must be designed using a good estimate of the true

noise model. Otherwise, the process model will be estimated incorrectly (Ljung, 1987).

1.2.3 Process Model Representation

High order finite step response (FSR) or FIR models estimated directly from plant data are frequently used to characterize the process dynamics. The reasons for their popularity are that these types of models fit naturally into the design of many MPC algorithms, and the multivariable processes on which these algorithms are typically applied are not well represented by lower order transfer function models (Cutler and Yocum, 1991; MacGregor et al., 1991). In addition, these models are a straightforward representation of the process dynamics, and the parameters of these models, such as the sampling period and the model order, have a relatively simple physical interpretation.

Although FSR/FIR type models have their advantages, they have a few widely recognized problems. Firstly, it is difficult to obtain good estimates for their respective parameters due to their high dimensionality (Ricker, 1988). Secondly, these model structures often result in ill-conditioned solutions when applying a least squares estimator since the data matrices associated with these models are often poorly conditioned (MacGregor et al., 1991). MacGregor et al. (1991) have studied biased regression techniques (e.g. ridge regression) and the projection to latent structures (PLS) method as alternatives to least squares. Ricker (1988) studied the use of PLS and a method based on the singular value decomposition (SVD). All these approaches attempt to reduce the variances and improve the numerical stability of the solution with the result being biased parameters.

The frequency sampling filter (FSF) model structure is a candidate model structure which has many of the same attributes as the FSR/FIR type models but does not suffer from their problems to anywhere near the same degree. The FSF model is obtained from a linear transformation of the FIR model and consists of a set of narrow bandpass filters. Combined with a standard least squares estimator, the FSF model can be used to directly estimate the process frequency response. Recent work by Wang and Cluett (1996a) has shown that the FSF model is a much more efficient way to estimate

the process step response. The advantages of the FSF model structure over the popular FIR model are that the number of parameters to be estimated is independent of the choice of sampling interval and is generally far fewer than the number required by the FIR model to obtain an accurate estimate of the step response. In addition, the general conditioning of the correlation matrix is better with the FSF model due to the reduction in the number of parameters that need to be estimated and to the narrow bandpass nature of the frequency sampling filters themselves. Furthermore, with the assumption that the errors in the estimated process model are largely due to the presence of noise and disturbances, Cluett et al. (1996) extended the statistical confidence bound in Goberdhansingh et al. (1992) from a set of point-wise bounds to a bound over the entire frequency region. From this frequency domain model information, a time domain uncertainty bound for the corresponding step response model was also derived.

1.2.4 Process and Noise Model Structure Determination

Model structure determination is an important step in system identification. For parametric methods, most of the existing identification methods assume that the structure of the system is known a priori, (i.e. transfer function order and delay), or that the selected model structure is at least within the true model class. At this point, the identification scheme is in reality a parameter estimation procedure. Alternatively, high order FIR models can be used but lead to the estimation problems mentioned above. With the FSF model, lower order models maybe used but the question remains how to choose the best order of the FSF model.

A natural approach to searching for a suitable model structure is to test a number of different model structures and to compare the resulting models. To perform such comparisons, a discriminating criterion and data sets are needed. For example, with a cross-validation approach, the criterion could be the sum of squared prediction errors or the misfits between the actual outputs and the model predicted outputs using a fresh data set. An attractive feature of this method is that the comparison makes sense without any probabilistic arguments and without any assumptions about the true system. The only

disadvantage is that we have to save a fresh data set for the comparisons and therefore we are not using all of the available information to build the model in the first place.

When we cannot spare fresh data sets for cross-validation purposes, other methods can be applied. An extensive survey of the literature regarding model structure selection was given by Stoica et al. (1986). The rank test is a method which is independent of the estimates of parameters (Fang and Xiao, 1988). Other methods which are dependent on the parameter estimates are the F-test, Akaike's information criterion (AIC), the final prediction error criterion (FPE), penalty for model complexity, etc. (Ljung, 1987). In practice, one should not use just one method for model structure selection but it is recommended that a combination of statistical tests and plots of relevant signals be used (Söderström and Stoica, 1989).

For noise model structure selection, it is standard practice to examine auto-correlation functions (ACFs) and/or partial auto-correlation functions (PACFs) (Box and Jenkins, 1976). This is an off-line procedure which requires a certain amount of expertise to interpret these plots.

To take the advantage of cross-validation without suffering the loss of data information, PRESS is a candidate model structure selector for linear regression type problems (Wang and Cluett, 1996b). PRESS is defined as the sum of the squared true prediction errors, where the true prediction error is calculated using data which is not part of the data set used to estimate the process model. Unlike the cross-validation approach where the entire data set is split into two parts, PRESS is calculated on each and every data point with the remaining data points used for model estimation. Wang and Cluett (1996b) show that the PRESS criterion provides a consistent and robust estimate of the model order. Application examples of the PRESS statistic for model structure selection are available in Patel et al. (1996).

1.3 Contributions of this Thesis

The first major contribution of the thesis (Chapter 2) is a thorough study of the role of operator intervention in process identification. In industry, when estimating step re-

sponse models for model predictive control applications, sometimes the test data which contains operator intervention is discarded. In addition, research by MacGregor and Fogal (1995) implied that non-parametric models lead to biased step response estimates due to the presence of operator intervention. In this thesis, we have shown that operator intervention may lead to better models due to the fact that operator intervention often improves the overall signal-to-noise ratio. With proper data prefiltering, there is certainly no need to discard data which contains feedback when estimating FIR models. In addition, we show that there are some factors which can affect the process identifiability, e.g., whether the operator intervention is delayed or immediate, and if the unit delay is included in the model.

The second major contribution of the thesis (Chapter 3) is the study of the design of the prefilter. Both theoretical analysis and simulation examples are used to illustrate that the process input-output data must be prefiltered using an accurate estimate of the true noise model. In addition, the study shows that the autoregressive-type dynamics of the noise model are the most important components when it comes to designing the prefilter.

The third major contribution of the thesis (Chapter 4) is that a modification of the well-known generalized least squares algorithm (GLS) is proposed for simultaneous identification of both process and noise models. The proposed algorithm provides a simple approach to remove the effect of any feedback on the process step response estimate, and to produce "white" residuals to permit presentation of statistical confidence bounds for the step response models. This algorithm makes novel use of the PRESS criterion for both process and noise model order selection. The performance of the proposed algorithm is demonstrated using simulation examples and by application to an industrial data set.

Chapter 2

The Role of Operator Intervention in Process Identification

2.1 Introduction

In this chapter, the topic of closed-loop system identification is investigated with particular emphasis on the case where the feedback is introduced via operator intervention. A description of the procedure of operator intervention is given in section 2.2. In section 2.3, the identifiability of non-parametric models versus parametric models under these types of closed-loop conditions is investigated. In section 2.4, the effect of the extent of operator intervention on the resulting model quality is studied. In section 2.5, the effect of different types of intervention strategies is examined. Concluding remarks are given in section 2.6.

2.2 The Procedure of Operator Intervention

The closed-loop system under operator intervention can be conceptually described using Figure 2.1 from a process identification point of view. In this diagram, the process is represented by the transfer function $G_0(z)$, the process output target value is given by the set-point, $y_{sp,t}$ and the process input and output variables are denoted by u_t and y_t, respectively. All unmeasurable process disturbances are characterized by a white noise sequence a_t filtered through a noise model transfer function, $H_0(z)$.

In the identification experiment, we add a dither signal to the process input to

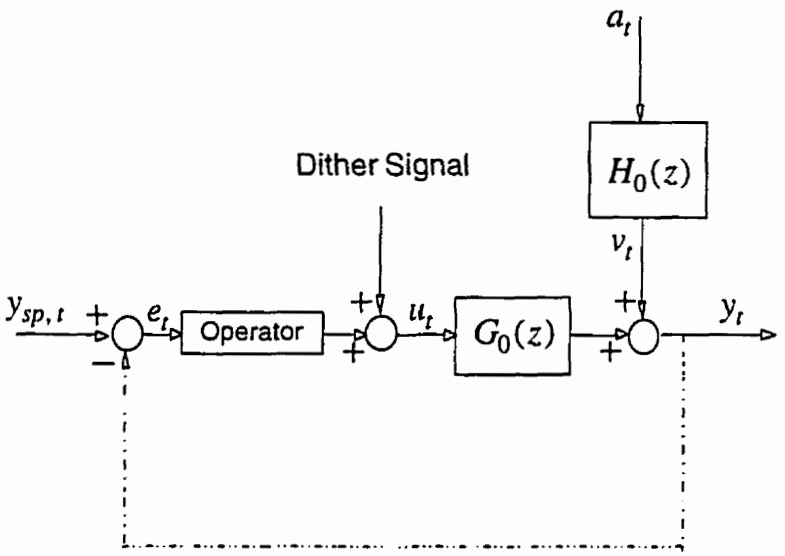

Figure 2.1: Closed-loop system under operator intervention

excite the process. The dither signal is typically a random binary signal with some specified magnitude and switching frequency. The process output, y_t, is measured and compared with a set-point value, $y_{sp,t}$. When the process output y_t is outside an acceptable range, which is specified by $\pm$ LIM in this thesis, the operator adjusts the input to draw the process output back towards the target. Here we assume that the operator has knowledge of the sign of the process gain and makes a step change adjustment. Therefore, the input signal u_t is the combination of the dither signal and the step changes introduced by operator. In order to determine whether the adjustment has the desired effect, the operator waits a certain period of time between two successive adjustments. This operator intervention procedure can be illustrated using the following simulation example.

Simulation Example 2.2.1:

Consider the system described by

$$y_t = \frac{0.1z^{-1}}{1 - 0.9z^{-1}}u_t + v_t \tag{2.1}$$

$$v_t = \frac{1}{1 - 0.97z^{-1}}a_t \tag{2.2}$$

where y_t is the measured process output, u_t is the process input, v_t represents the effect of all unmeasured disturbances on y_t, a_t is a white noise sequence with zero mean and variance of 0.3, and z is the mathematical shift operator defined by $z^{-1}y_t = y_{t-1}$.

The dither signal used to excite the process is a binary signal with a magnitude of 1, minimum switching time of 10 sampling intervals, and a 50% probability of switching. During the experiment, when the measured process output moves out of $\pm$ LIM from its target value at a given sampling instant, a step change of magnitude ± 5 is superimposed on the dither signal at the next sampling instant to attempt to bring the process output back to its target value. The operator then waits 25 sampling intervals after giving an adjustment to determine whether the action has the desired effect. For one experiment, 10 000 sets of input-output data are collected. In order to simulate different realizations of the stochastic disturbance, repeated experiments are performed by using the same random binary signal but with different seeds for generating the white noise sequence $\{a_t\}$.

This simulation example closely matches Example 2 in MacGregor and Fogal (1995) and will be used frequently throughout this chapter.

2.3 Estimating Process Step Response Under Closed-loop Conditions

The true process is assumed to be given by:

$$y_t = G_0(z)u_t + v_t \tag{2.3}$$

$$v_t = H_0(z)a_t \tag{2.4}$$

The system is then estimated using the assumed model structure

$$y_t = G(z,\theta)u_t + H(z,\theta)a_t \tag{2.5}$$

where θ can be either an infinite or a finite dimensional vector of parameters.

Taking $H(z,\theta) = H(z)$ as a user-selected prefilter, so that $y_{f,t} = H^{-1}(z)y_t$, $u_{f,t} = H^{-1}(z)u_t$, we have

$$y_{f,t} = G(z,\theta)u_{f,t} + a_t \tag{2.6}$$

Ljung (1987) shows in his Theorem 8.2 and 8.3 that both G_0 and H_0 can be consistently estimated from data collected under closed-loop conditions using a PEM approach provided that the models $G(z,\theta)$ and $H(z,\theta)$ are sufficiently complex to capture the true process and noise transfer functions, $G_0(z)$ and $H_0(z)$. This indicates that $G(z,\theta)$ can be estimated using Equation (2.6) with the prefiltered process input-output data provided that the prefilter $H(z)$ is designed using a good estimate of the true noise transfer function $H_0(z)$.

2.3.1 Non-parametric and Parametric Models

For a linear, time-invariant process, the process transfer function can be written as

$$G_0(z) = \sum_{k=0}^{\infty} h(k)z^{-k} \tag{2.7}$$

where the sequence $\{h(k)\}$ is the impulse response of the process.

Another example of a popular non-parametric model of the process is the step response model $\{g(k)\}$ where

$$g(k) = \sum_{i=0}^{k} h(i) \tag{2.8}$$

for $k = 0, 1, \cdots, \infty$.

Two examples of popular parametric models are the equation error or ARX model structure

$$A(z)y_t = B(z)u_t + a_t \tag{2.9}$$

and the output error (OE) model structure

$$y_t = \frac{B(z)}{D(z)} u_t + a_t \tag{2.10}$$

where $A(z) = 1 + a_1 z^{-1} + \cdots + a_{n_a} z^{-n_a}$, $B(z) = b_1 z^{-1} + \cdots + b_{n_b} z^{-n_b}$ and $D(z) = 1 + d_1 z^{-1} + \cdots + d_{n_d} z^{-n_d}$.

Another popular parametric model used to represent stable processes is the finite impulse response model (FIR), where

$$y_t = B(z) u_t + a_t \tag{2.11}$$

and $n_b = N$, where N is an estimate of the process settling time. From Equations (2.9), (2.10) and (2.11) we can see that the FIR model can be considered a special case of the OE model structure with $D = 1$, or a special case of the ARX model structure with $A = 1$.

2.3.2 Non-parametric and Parametric Estimation Methods

Methods for determining estimates of nonparametric models are called non-parametric methods since they do not explicitly use a finite-dimensional parameter vector in the search for a model (Ljung, 1987). For estimating a finite number (N) of terms in the impulse response $\{h(k)\}$, correlation analysis is a popular non-parametric method. This method produces an estimate of the first $N + 1$ impulse response coefficients by solving

$$\hat{R}_{uy}(\tau) = \sum_{k=0}^{N} \hat{h}(k) \hat{R}_{uu}(k - \tau) \tag{2.12}$$

for $0 \leq \tau \leq N$, where

$$\hat{R}_{uy}(\tau) = \frac{1}{M} \sum_{t=1}^{M} u_{t-\tau} y_t \tag{2.13}$$

$$\hat{R}_{uu}(\tau) = \frac{1}{M} \sum_{t=1}^{M} u_{t-\tau} u_t \tag{2.14}$$

and M is the number of observed sets of input-output data. Using a matrix form, Equation (2.12) is equivalent to

$$\begin{bmatrix} \hat{R}_{uy}(0) \\ \hat{R}_{uy}(1) \\ \vdots \\ \hat{R}_{uy}(N) \end{bmatrix} = \begin{bmatrix} \hat{R}_{uu}(0) & \hat{R}_{uu}(1) & \cdots & \hat{R}_{uu}(N) \\ \hat{R}_{uu}(1) & \hat{R}_{uu}(0) & \cdots & \hat{R}_{uu}(N-1) \\ \cdots & & & \\ \hat{R}_{uu}(N) & \hat{R}_{uu}(N-1) & \cdots & \hat{R}_{uu}(0) \end{bmatrix} \begin{bmatrix} \hat{h}(0) \\ \hat{h}(1) \\ \vdots \\ \hat{h}(N) \end{bmatrix} \tag{2.15}$$

These equations are derived from Equations (2.3) and (2.7) under the assumption that the identification experiment has been carried out under open-loop conditions, thereby,

$$\hat{R}_{uv}(\tau) = \frac{1}{M} \sum_{t=1}^{M} u_{t-\tau} v_t \approx 0 \tag{2.16}$$

i.e. the process input u_t and the disturbance v_t are uncorrelated for all lags $\tau \geq 0$. When the experiment is carried out under closed-loop conditions, this assumption does not hold because u_t and v_t are no longer independent, and correlation analysis will produce erroneous results.

Methods for estimating the parameters within a selected model structure (e.g. ARX, OE, FIR) are called parametric estimation methods. To evaluate the quality of the estimated model, the concept of the prediction error is often used. The prediction error, e_t, is defined by:

$$e_t = y_t - \hat{y}_t(\hat{\theta}) \tag{2.17}$$

With prediction error identification methods (PEM), the objective is to choose $\hat{\theta}$ such that some measure of the size of $\{e_t\}$ is minimized. We often use a quadratic norm where $\hat{\theta}$ is chosen to minimize $\frac{1}{M}\sum_{t=1}^{M} e_t^2$. For the ARX and FIR model structures, this can be accomplished with the well-known least squares method (LS). For example, the equivalent linear regression form of the FIR model is given by:

$$y_t = \phi_t^T \theta_0 + v_t \tag{2.18}$$

where

$$\phi_t^T = [u_{t-1} \quad u_{t-2} \cdots u_{t-N}] \tag{2.19}$$

and

$$\theta_0^T = [b_1 \quad b_2 \cdots b_N] \tag{2.20}$$

The LS estimate for the parameters θ is given by

$$\hat{\theta} = [\frac{1}{M}\sum_{t=1}^{M}\phi_t\phi_t^T]^{-1}\frac{1}{M}\sum_{t=1}^{M}\phi_t y_t \tag{2.21}$$

By comparing Equation (2.15) for estimating the impulse response model $\{h(k)\}$ and Equation (2.21) for estimating the N parameters in the FIR model, it can be seen that the correlation analysis estimates and the LS estimates are identical ($\hat{h}(k) = \hat{b}_k$) except for the fact that the leading coefficient, b_0, of the FIR is not estimated. This discrepancy arises from the fact that the unit delay has been included in the FIR model. However, the nonparametric method of estimating the impulse response model and the parameter estimation method (i.e. least squares) for estimating the FIR model can be made identical by either estimating b_0 in the FIR model or by forcing $h(0) = 0$ in Equation (2.7).

2.3.3 Comparison of Estimation Results Using Parametric and Non-parametric Models

In simulation example 2.2.1, LIM was set equal to 6 which matches the value chosen by MacGregor and Fogal (1995). A section of 1000 sample periods is plotted in Figure 2.2. The input-output data was prefiltered with the inverse of the correct noise model as illustrated in Equation (2.6). The impulse response model in Equation (2.18) was estimated using the LS method with u_t and y_t replaced by $u_{f,t}$ and $y_{f,t}$ in Equation (2.21). The estimation was performed using the MATLAB ARX command with $NN = [0 \;\; 50 \;\; 1]$ (see Appendix B). Fifty different experiments with 50 different seeds for the white noise sequence were performed yielding 50 estimates of the impulse response model. The corresponding unit step response estimates were generated from Equation (2.8) (with the unit step occurring at the first sampling interval) and the results are plotted in Figure 2.3. Compared with the true process step response shown in Figure 2.4, the estimates are clearly unbiased.

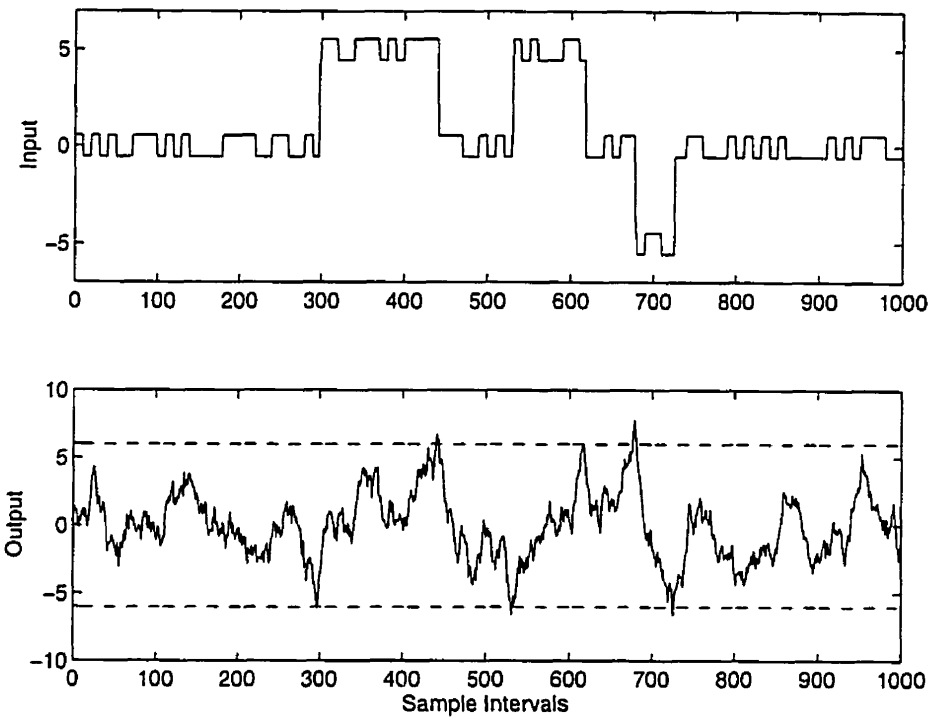

Figure 2.2: Process input-output data with LIM= 6.

MacGregor and Fogal (1995) suggest that, even if the prefilter is designed using the true noise model, when estimating a "non-parametric" model such as the impulse response, one might expect to identify some weighted combination of the process model and the negative inverse of the controller. Our result would seem to contradict the suggestions made by MacGregor and Fogal (1995), but it can be validated by the following explanation. Due to the nature of the operator intervention in this simulation example, correlation exists between $\{u_{t+1}\}$ and $\{v_t\}$. Because the disturbance $\{v_t\}$ is autocorrelated, then $\hat{R}_{uv}(\tau) \neq 0$ for all $\tau \geq 0$. Therefore, estimates of the impulse response would be biased if they had been generated from Equation (2.21) using u_t and y_t. However, with u_t and y_t being filtered by the inverse of the correct noise model, the impulse response model is estimated using the LS method with u_t and y_t replaced by $u_{f,t}$ and $y_{f,t}$ in Equation (2.21). Because correlation exists between $\{u_{t+1}\}$ and $\{v_t\}$, then correlation also exists between $\{u_{f,t+1}\}$ and $\{a_t\}$. However, because $\{a_t\}$ is a white noise sequence, $\hat{R}_{u_f a}(\tau) \approx 0$ for all $\tau \geq 0$. Then the estimated models are unbiased according

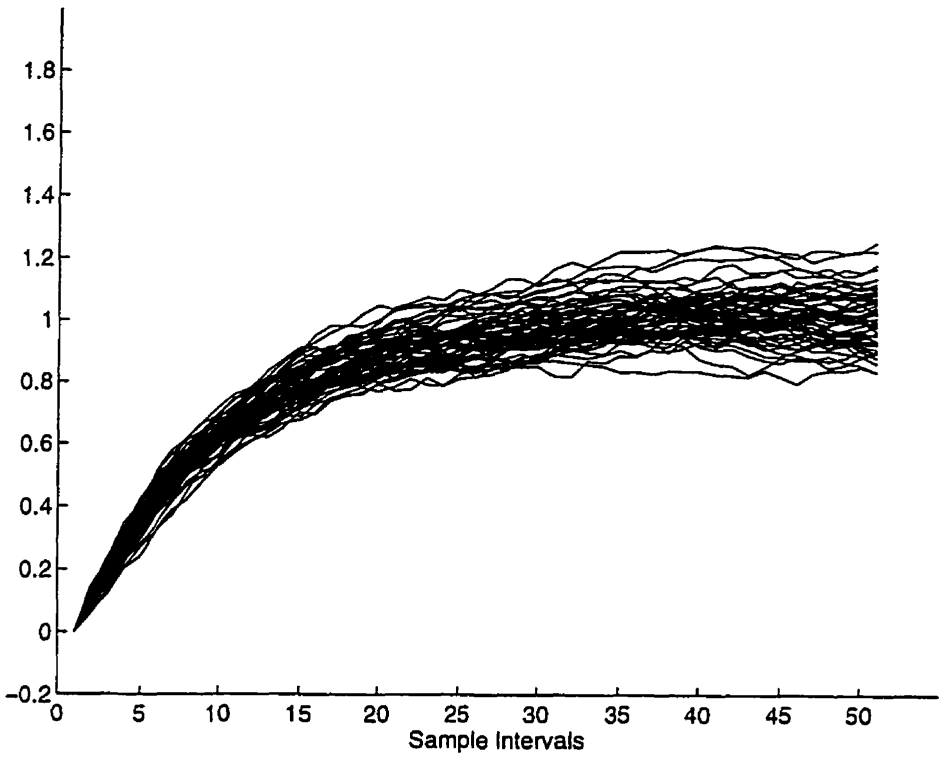

Figure 2.3: Estimated unit step responses with FIR model including unit delay (LIM= 6).

to Equation (2.16).

Although an unbiased estimate of the step response has been generated from an FIR model which includes the unit delay, the fact that $\hat{R}_{u_f a}(0) \approx 0$ would indicate that even if the unit delay had not been included the estimates would be unbiased. This result was verified by re-estimating 50 estimates of the impulse response model from the same 50 experiments used to generate Figure 2.3 (MATLAB ARX command with $NN = [0 \quad 50 \quad 0]$). The corresponding 50 step response estimates are plotted in Figure 2.5. By comparing with the true step response shown in Figure 2.4, the estimates are seen to be unbiased. Compared with the estimation results shown in Figure 2.3, the only difference is that the first term of the step response estimate $\hat{g}(0) = \hat{h}(0)$ is no longer exactly zero but has its own distribution with zero mean.

These results indicate that under the closed-loop conditions described in simu-

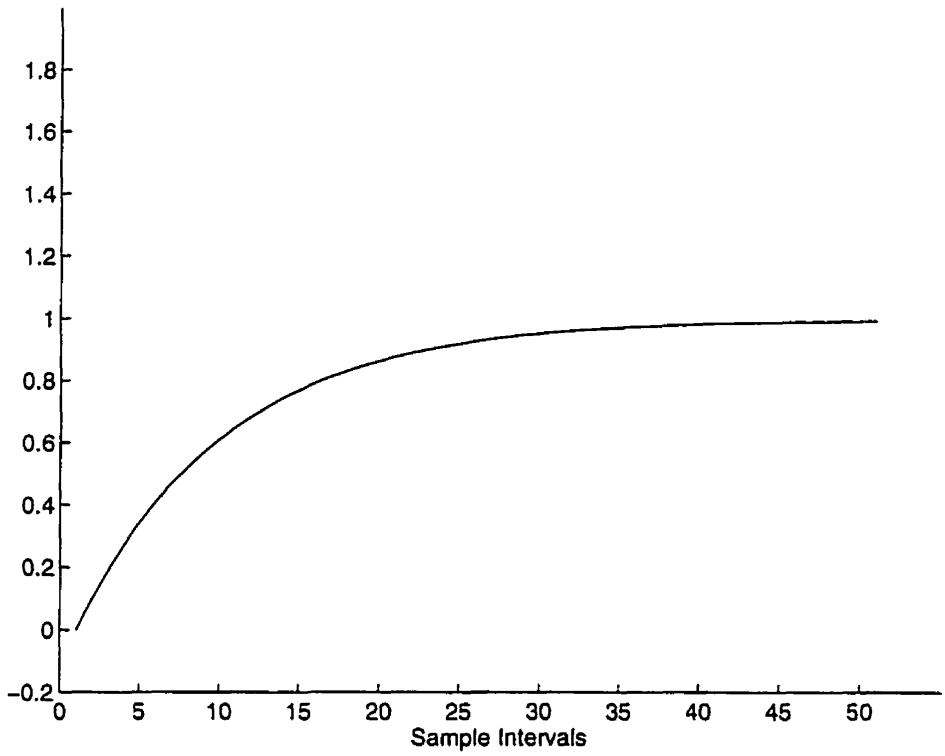

Figure 2.4: True unit step response

lation example 2.2.1, unbiased estimates of the process step response can be obtained using correlation analysis or equivalently the LS estimates of the FIR model provided the input-output data have been prefiltered with the inverse of the correct noise model.

In addition, we are also interested in investigating the identifiability of parametric models to see if they provide significantly different results. From the same 50 experiments used above, 50 estimates of a lower order transfer function model were obtained using the MATLAB OE command with $NN = [1 \quad 1 \quad 1]$ and $NN = [2 \quad 1 \quad 0]$ after the input-output data was prefiltered with the inverse of the correct noise model (see Appendix B). The corresponding 50 step response estimates are plotted in Figure 2.6 and 2.7 for $NN = [1 \quad 1 \quad 1]$ and $NN = [2 \quad 1 \quad 0]$, respectively. By comparing Figure 2.3 with Figure 2.6 and Figure 2.5 with 2.7, it is clear that the non-parametric estimates and the parametric estimates have similar distribution properties, the only difference being that the parametric estimates are smoother.

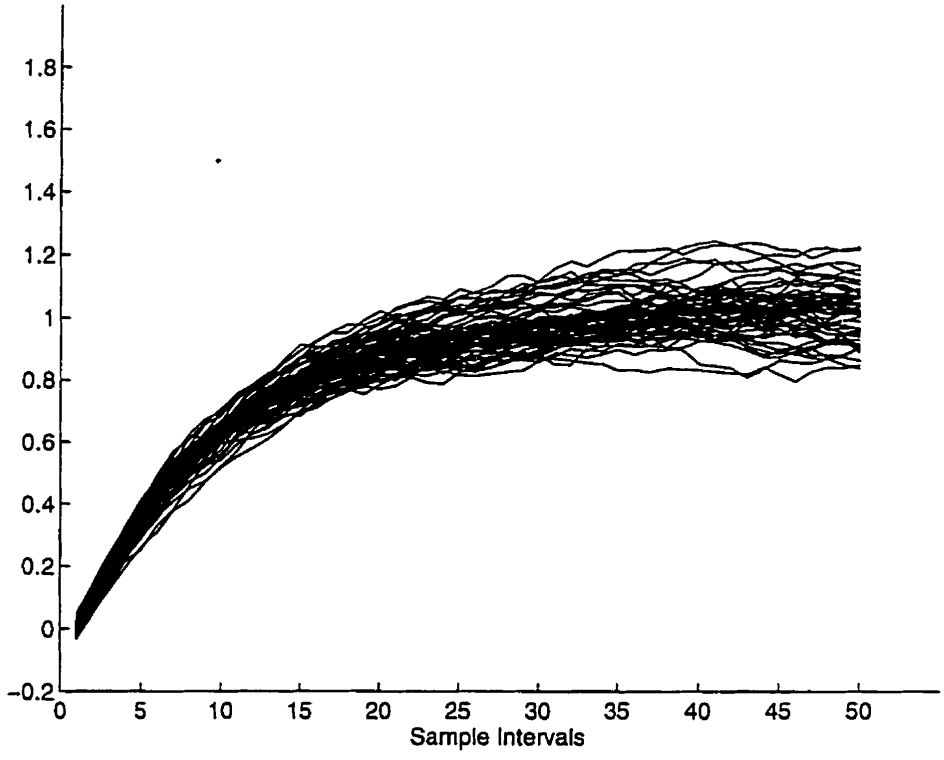

Figure 2.5: Estimated unit step responses with FIR model not including unit delay (LIM= 6).

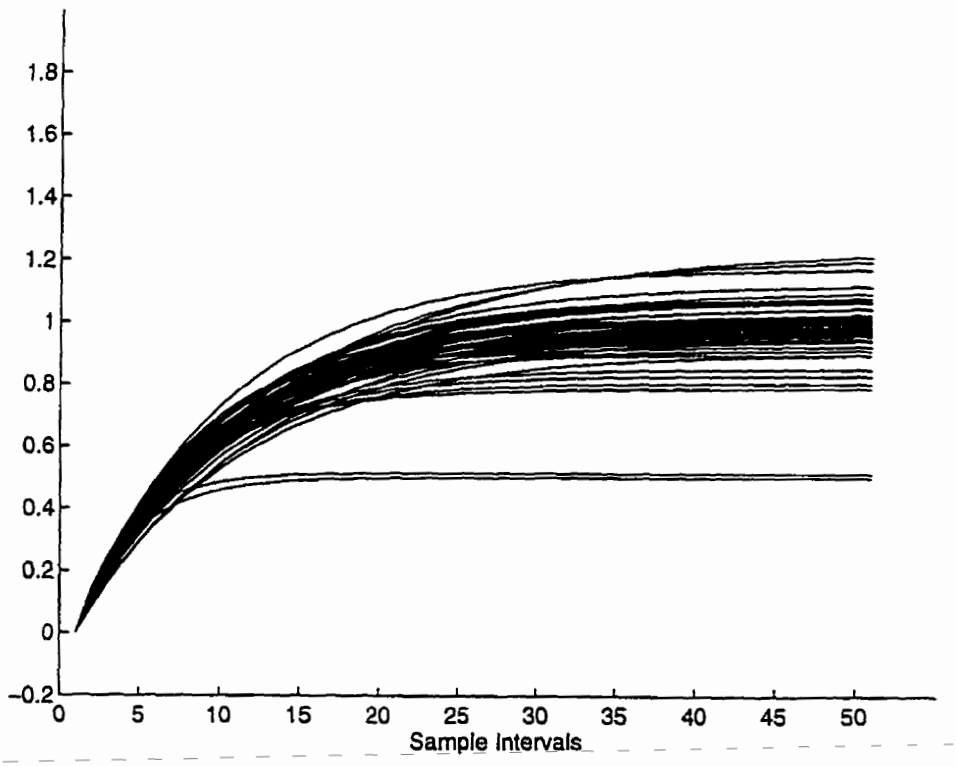

Figure 2.6: Estimated unit step responses with OE model including unit delay (LIM= 6).

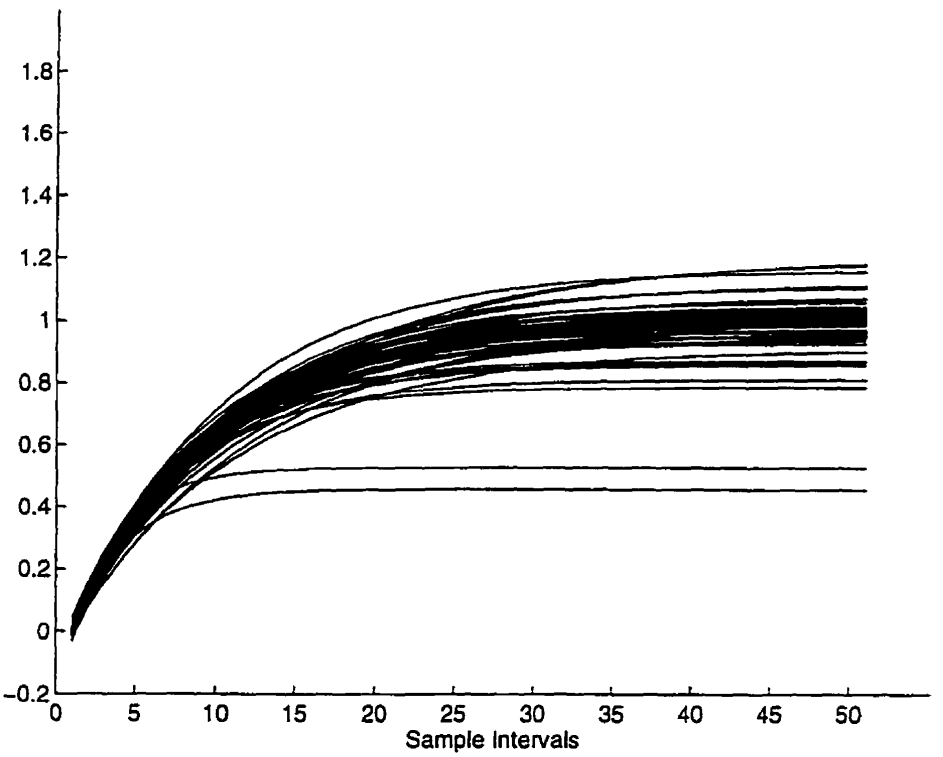

Figure 2.7: Estimated unit step responses with OE model not including unit delay (LIM= 6).

2.3.4 Convergence of Estimated Models

With the previous simulation results, in all cases we assumed a process model structure which was sufficiently complex to capture the true process transfer function. Ljung's (1987) asymptotic results tell us that the model estimates will converge to the true process as the data length, $M \rightarrow \infty$. To evaluate the convergence behaviour, 500 000 sets of input-output data were collected in one simulation experiment. Then, this data sequence was cut into different lengths by taking the first 10 000 data points, the first 20 000 data points, etc. up to the entire data length. This results in 50 data sets of different lengths. Based on the 50 data sets, unit step responses were estimated from the impulse response model with the LS method (MATLAB ARX command with $NN = [0 \;\; 50 \;\; 1]$) and from a low order transfer function model with the output error method (MATLAB OE command with $NN = [1 \;\; 1 \;\; 1]$) with the data correctly prefiltered. The results are

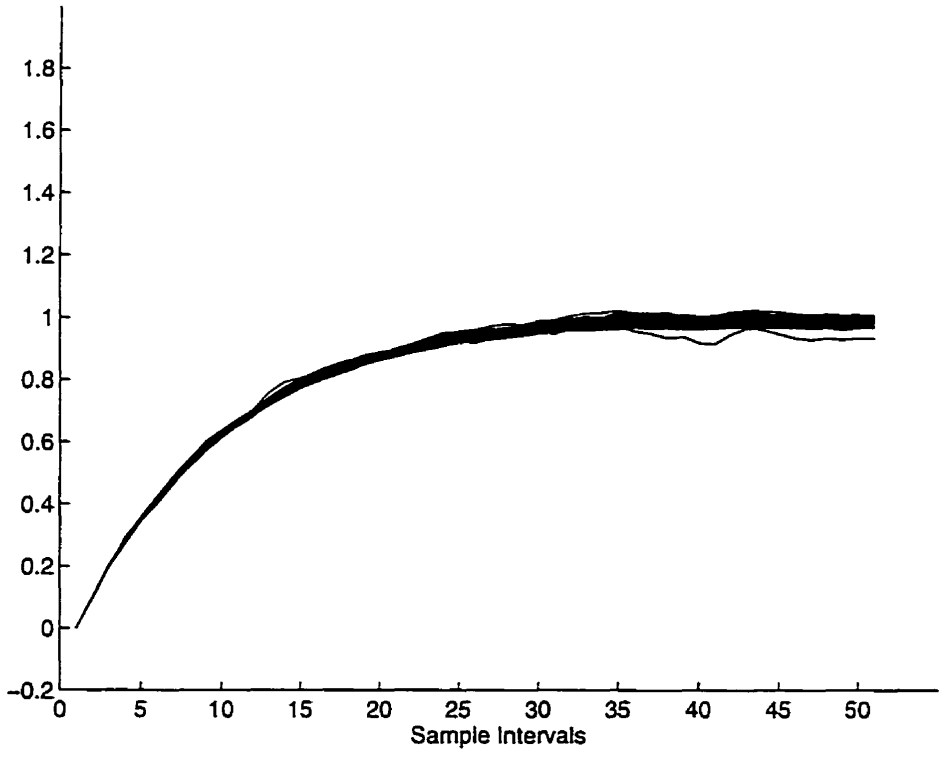

Figure 2.8: Convergence of Estimated Models: FIR model including unit delay (LIM= 6).

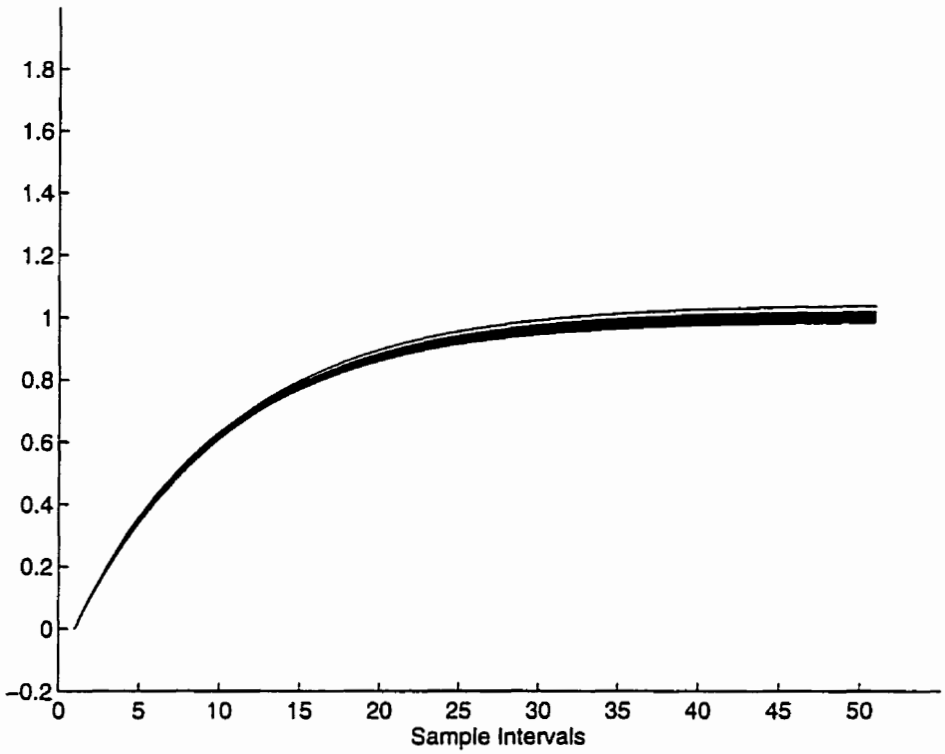

Figure 2.9: Convergence of Estimated Models: OE model including unit delay (LIM= 6).

shown in Figure 2.8 and 2.9, respectively.

By comparing Figure 2.4 with 2.8, and Figure 2.4 with 2.9, it is clear that both FIR generated estimates and the low order transfer function generated estimates converge to the true step response. In addition, by comparing Figure 2.3 with 2.8 and Figure 2.6 with 2.9, it is also clear that two estimates have similar convergence behaviour, the only difference being that the low order transfer function generated estimates are somewhat smoother.

2.4 The Effect of Operator Intervention on Model Quality

In industry, data which contains feedback operation is often discarded when a FIR model is to be estimated. This is because of the well-known result that non-parametric methods such as correlation analysis lead to biased estimates of the process model when applied to process input-output data which contains feedback. The results in section 2.3 clearly indicate that this need not be the case with proper data prefiltering. In this section, this issue is explored one step further by examining the effect of the frequency of the operator intervention on the model quality.

To carry out this study, two more sets of 50 experiments were performed under the conditions described in Example 2.2.1 with LIM set equal to 3 and 100. Example sections of 1000 sample periods for LIM= 3 and 100 are shown in Figure 2.10 and Figure 2.11, respectively. From comparing Figure 2.2, Figure 2.10 and Figure 2.11, it

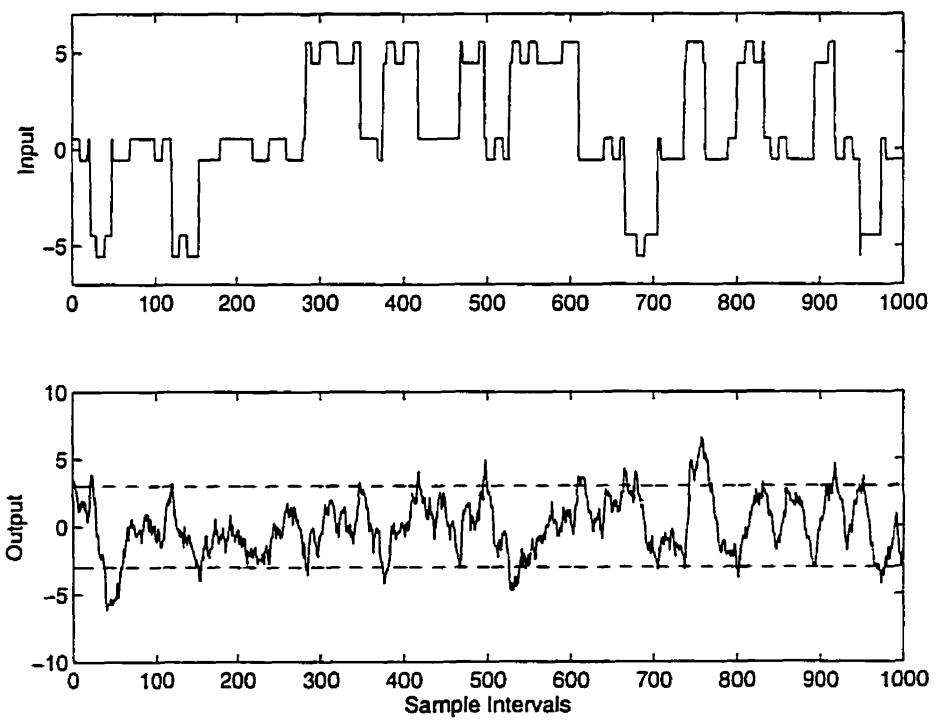

Figure 2.10: Precess input-output data with LIM= 3.

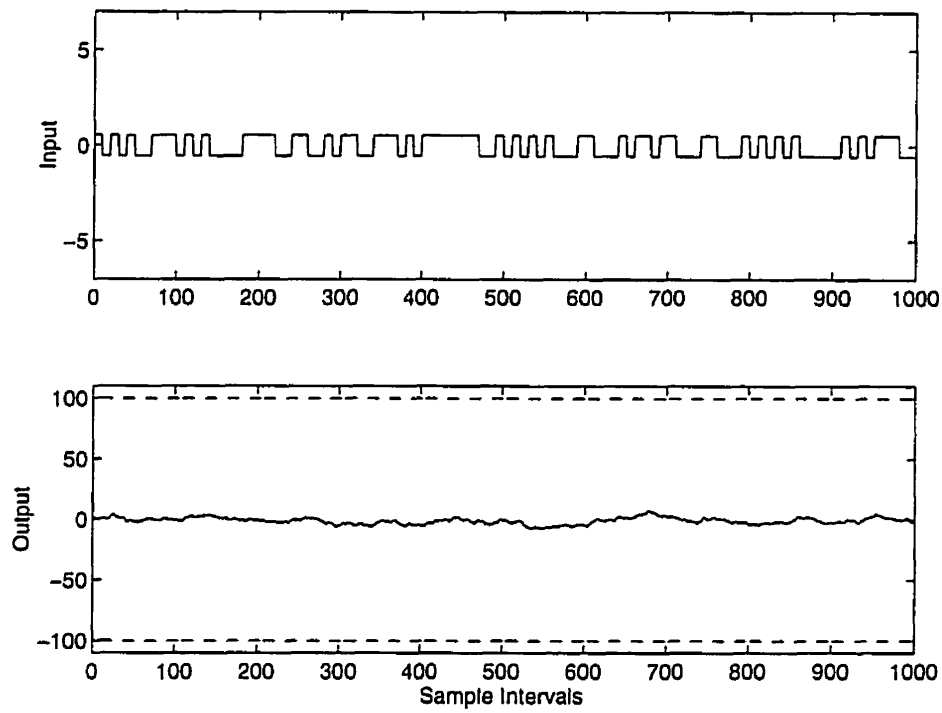

Figure 2.11: Process input-output data with LIM= 100.

is clear that the value of LIM directly determines the amount of operator intervention. For instance with LIM=100, the process output never drifts outside ±100, and the process input consists solely of the random binary signal with no operator intervention. This is equivalent to the open-loop situation. On the other hand, with LIM= 3, the process output is frequently outside the acceptable range of ±3, resulting in frequent interventions from the operator. With LIM= 6, the process output drifts less frequently outside the acceptable range of ±6 leading to fewer operator moves. Impulse response models were estimated using the LS method with u_t and y_t replaced by $u_{f,t}$ and $y_{f,t}$ in Equation (2.21) (MATLAB ARX command with $NN = [0\ \ 50\ \ 1]$). The corresponding 50 step response estimates are shown in Figure 2.12 and Figure 2.13 for LIM= 3 and 100, respectively.

In addition, using the same two sets of data as described above corresponding to LIM= 3 and 100, 50 estimates of a lower order transfer function model were obtained using the MATLAB OE command with $NN = [1\ \ 1\ \ 1]$, after the input-output data was

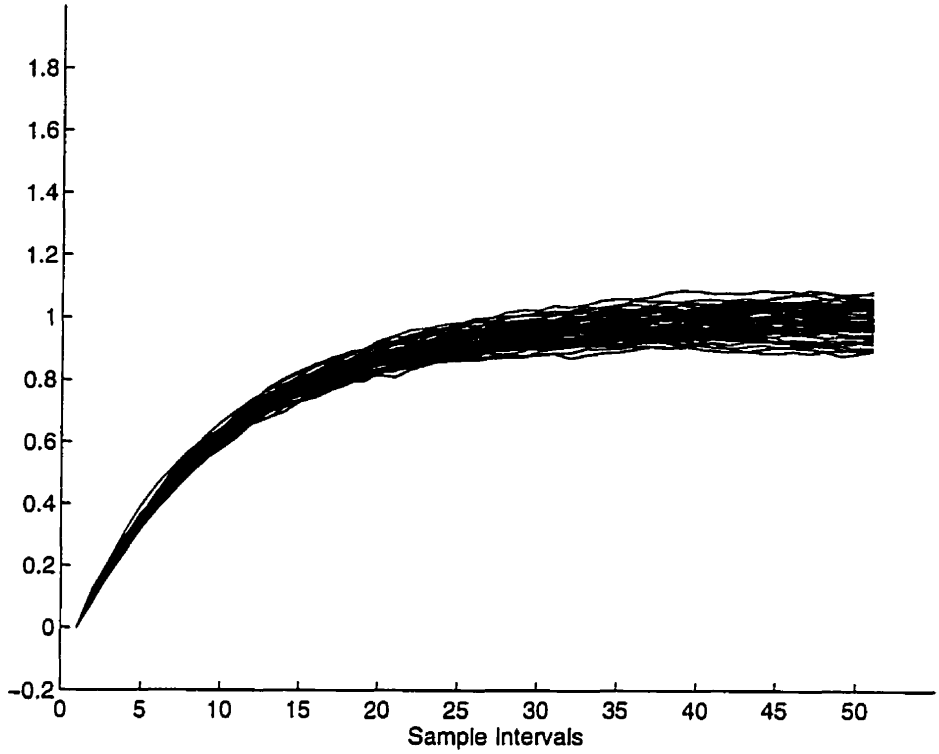

Figure 2.12: Estimated unit step responses with FIR model including unit delay (LIM= 3)..

prefiltered with the inverse of the correct noise model. The corresponding step response estimates are shown in Figure 2.14 and Figure 2.15, respectively.

By examining Figure 2.12, Figure 2.3 and Figure 2.13 for LIM= 3, 6 and 100, respectively, a very clear trend is present. Also, by examining Figure 2.14, Figure 2.6 and Figure 2.15 for LIM = 3, 6 and 100, respectively, the same trend can be seen. First, all three cases yield unbiased estimates. Second, the more frequent the operator intervention, the tighter is the distribution of the estimates around the true step response. Third, in all three cases, the distribution of the estimates broadens as steady-state is approached with the largest uncertainty being associated with the steady-state gain estimate. With LIM= 3, 6 and 100, the step response estimates are approximately within $\pm 10\%$, $\pm 20\%$ and $\pm 80\%$ of the true gain. The results indicate that the operator intervention can actually produce input-output data sets which subsequently lead to better

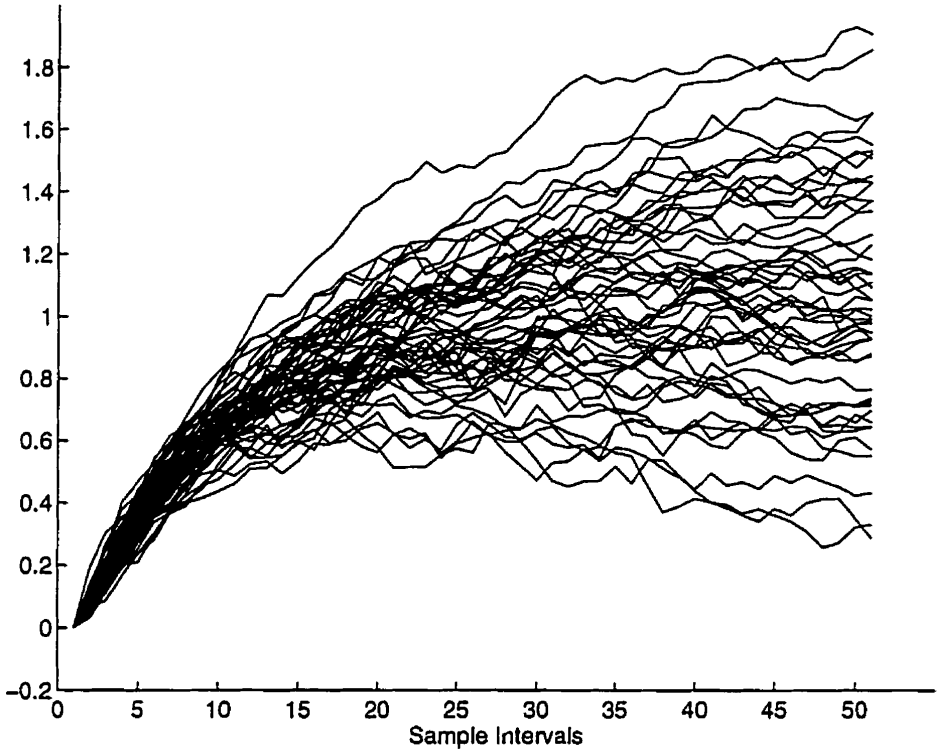

Figure 2.13: Estimated unit step responses with FIR model including unit delay (LIM= 100).

models, particularly with respect to estimation of the steady-state gains. This has important practical implications because the steady-state gain is one of the more important pieces of information to be determined from the identification experiment.

To explain these results, we may use a frequency domain interpretation of the asymptotic process model estimate or limit model. It has been shown in Ljung (1987) that, for the open-loop case, when prefiltering with the inverse of the correct noise model, the limit model is a best mean-square approximation of the true process with a frequency weighting $Q(w)$ given by

$$Q(w) = \frac{\Phi_u(w)}{|H_0(e^{jw})|^2} \tag{2.22}$$

where $\Phi_u(w)$ is the power spectrum of the process input $\{u_t\}$. When the process is under continuous feedback control with an external dither signal, the limit model becomes a function of the sensitivity function associated with the true and modelled closed-loop

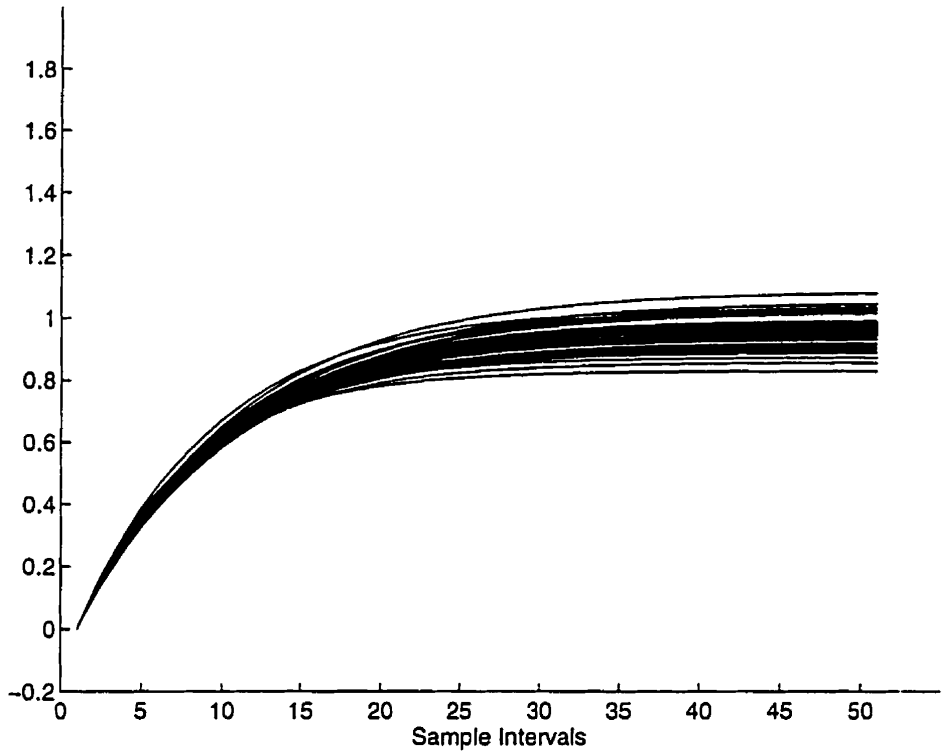

Figure 2.14: Estimated unit step responses with OE model including unit delay (LIM= 3).

system in addition to the power spectrum of the dither signal (MacGregor and Fogal, 1995). With operator intervention, where a mixture of open-loop and feedback operation exists, it seems reasonable to treat the power spectrum of the filtered process input $\{u_{f,t}\}$ as the weighting function where the process input in this case is the combination of a dither signal plus intermittent operator moves.

In all of our simulation work, we use finite data sets. However, we believe that we can still use the limit model results to explain the differences in the distribution of the various step response estimates. For instance, the larger the frequency weighting is in a given frequency region, the more accurate the model should be in that same frequency region. The frequency response of the noise model $H_0(z)$ in Equation (2.2) has a large magnitude at the low and median frequencies and a small magnitude at the higher frequencies. Therefore, the frequency weighting function in Equation (2.22) will

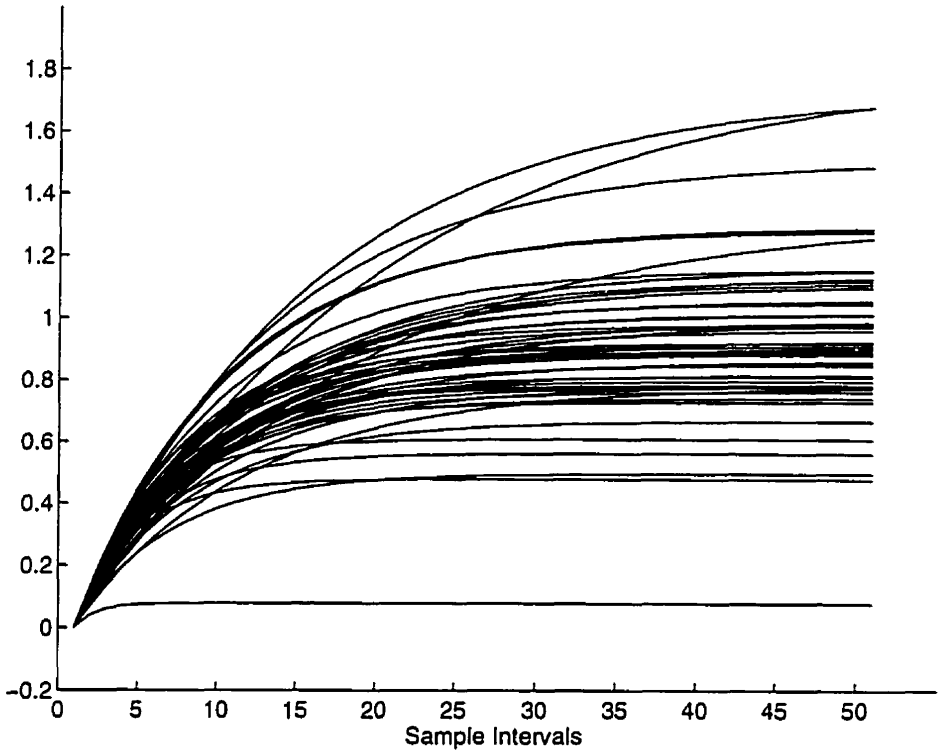

Figure 2.15: Estimated unit step responses with OE model including unit delay (LIM= 100).

tend to de-emphasize the low and medium frequency regions and emphasize the high frequency region. This explains why all of the distributions in Figure 2.12, Figure 2.3 and Figure 2.13, and Figure 2.14, Figure 2.6 and Figure 2.15 broaden as steady-state is approached. In addition, for a given experimental time, if the input signal has a larger power spectrum at all frequencies, then the estimated model will be more accurate because of the larger signal-to-noise ratio. Figure 2.16 shows a comparison of the three discrete power spectrums of the filtered process input $\{u_{f,t}\}$ taken from the sets of simulations with LIM= 3, 6 and 100. It is clear that as the operator intervention becomes more frequent, the magnitude of the filtered process input power spectrum increases leading to tighter distributions of the estimates around the true step response. This explains why the distribution becomes tighter as LIM goes from 3 to 6 to 100.

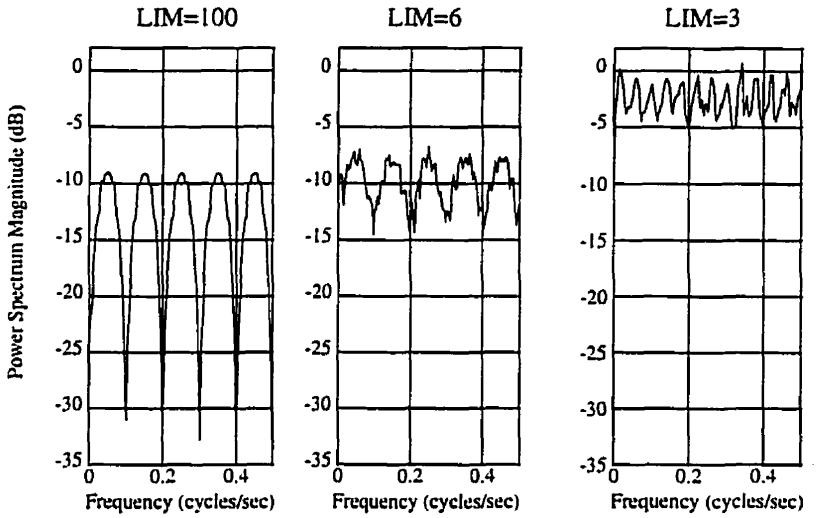

Figure 2.16: Power spectra of filtered process input with LIM= 3, 6 and 100.

2.5 The Effect of Intervention Strategies on Identifiability

2.5.1 Delayed vs. Immediate Intervention

"Delayed intervention" refers to the case where the operator makes an adjustment one sampling instant after the unacceptable deviation is detected. "Immediate intervention" refers to the case where the operator makes an adjustment of the process input at the same sampling instant that the unacceptable deviation in the process output occurs. It is believed that the delayed intervention described in Example 2.2.1 is more typical of what happens with human intervention where an operator needs a minimum response time (say one sampling period) to make an adjustment to the process input. However, the immediate intervention strategy is closer to what happens with an automatic feedback control mechanism which adjusts the process input at the current sampling instant based

on the current deviation of the process output from its target value. The objective in this section is to study the effect that this subtle difference might have on the accuracy of both estimated FIR and low order transfer function models.

Simulation Example 2.5.1

This simulation example is identical to simulation example 2.2.1 except that when the process output moves more than ±LIM (LIM= 6) away from its target value at a given sampling instant, a step change of magnitude ±5 is superimposed on the random binary signal at the same sampling instant to attempt to bring the process back to its target value. This is what is referred to as an immediate intervention strategy. The impulse response model in Equation (2.18) was estimated using the lease squares method with u_t and y_t replaced by $u_{f,t}$ and $y_{f,t}$ in Equation (2.21) (MATLAB ARX command with $NN = [0 \;\; 50 \;\; 1]$). Fifty different experiments with 50 different seeds for the white noise sequence were performed yielding 50 estimates of the impulse response model. The corresponding unit step response estimates were generated and the results are plotted in Figure 2.17. Compared with the true step response, the estimation results are unbiased. Due to the nature of the operator intervention in Example 2.5.1, correlation exists between $\{u_t\}$ and $\{v_t\}$ and as a result correlation also exists between $\{u_{f,t}\}$ and $\{a_t\}$. However, because $\{a_t\}$ is a white noise sequence, $\hat{R}_{u_f a}(\tau) \approx 0$ for all $\tau \geq 1$. Therefore, because the unit delay has been included in the FIR model, the estimates are unbiased. On the other hand, if models are estimated without including the unit delay, the estimates should be biased since $\hat{R}_{u_f a}(0) \neq 0$. The 50 estimates generated from the same 50 experiments using instead the MATLAB ARX command with $NN = [0 \;\; 50 \;\; 0]$ are plotted in Figure 2.18 where it is clear that the estimates are biased. These are in fact the conditions under which correlation between the process input and the disturbance cause identifiability problems.

However, these problems exist not only for the FIR models but also for the low order transfer function models. From the same 50 experiments used above, 50 estimates of a low order transfer function model were obtained using the MATLAB OE command with $NN = [2 \;\; 1 \;\; 0]$ after the input-output data was prefiltered with the inverse of

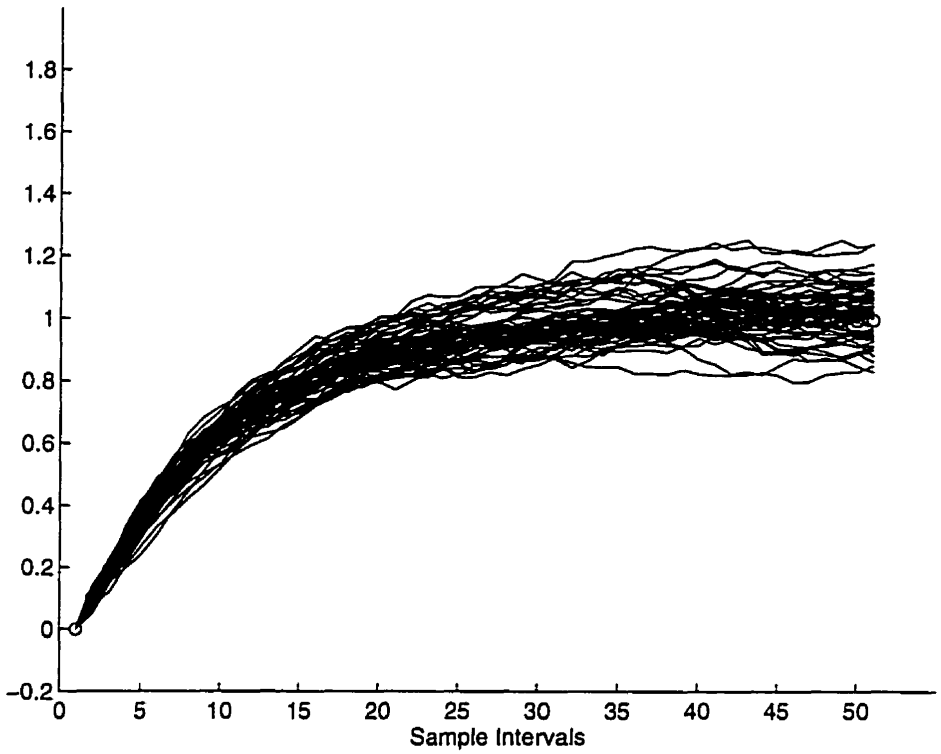

Figure 2.17: Estimated unit step responses with FIR model including unit delay for immediate operator intervention (circles denote the true process step response).

the correct noise model. This means that we have not included the unit delay in the output error model structure. The corresponding 50 step response estimates are plotted in Figure 2.19. By comparing Figure 2.18 and Figure 2.19, it is clear that the two sets of estimates have similar distribution properties (both are biased) with the only difference being that the low order transfer function generated estimates are smoother.

2.5.2 Waiting for Consecutive Unacceptable Deviations

Another situation which might happen during the identification experiment is that the output may drift outside the acceptable region due to a disturbance at one sampling instant, but may return to within the acceptable operating region at the subsequent sampling instant without requiring any intervention. Therefore, it may be the case that the operator intervenes only if there are several consecutive unacceptable deviations.

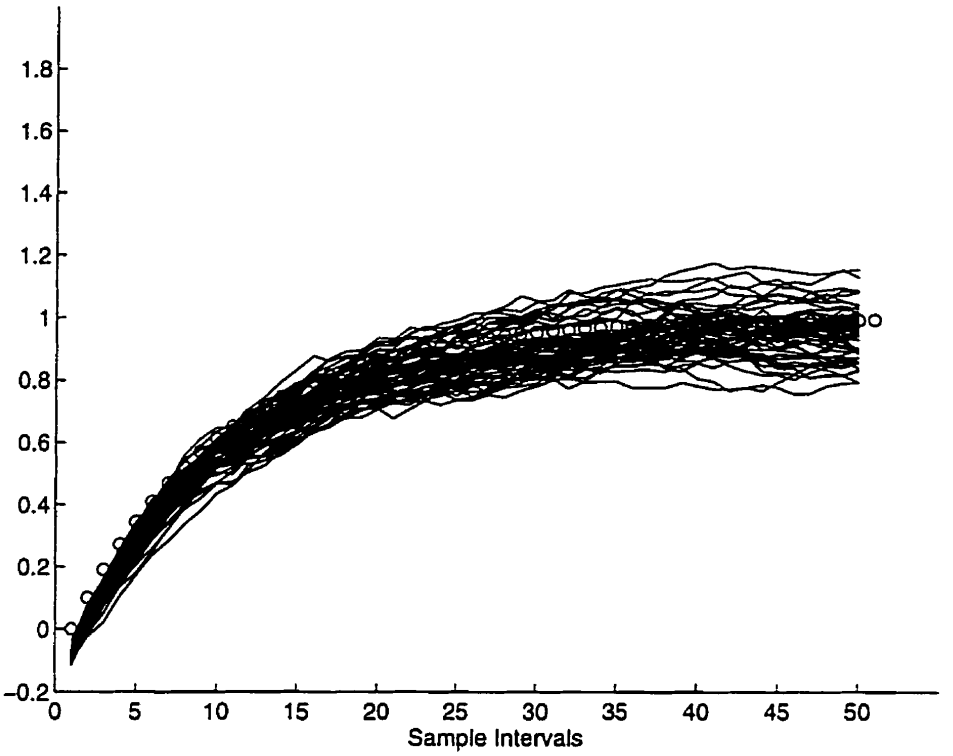

Figure 2.18: Estimated unit step responses with FIR model not including unit delay for immediate operator intervention (circles denote the true process step response).

Here we investigate what will happen to the estimated model under these circumstances.

Simulation Example 2.5.2

This simulation example is identical to Example 2.2.1 except now the operator does not intervene until there have been a certain number of consecutive process output samples outside either +LIM or −LIM. In this simulation example, the operator intervenes after two consecutive unacceptable output deviations have occurred.

Fifty experiments were performed using 50 different seeds for generating the white noise sequence yielding 50 sets of input-output data. Impulse response models were estimated using the LS method with u_t and y_t replaced by $u_{f,t}$ and $y_{f,t}$ in Equation 2.21 (MATLAB ARX command with $NN = [0 \;\; 50 \;\; 0]$). The corresponding 50 step response estimates are shown in Figure 2.20. Also, using the same data sets, low order transfer function models were estimated using the MATLAB OE command with $NN = [2 \;\; 1 \;\; 0]$

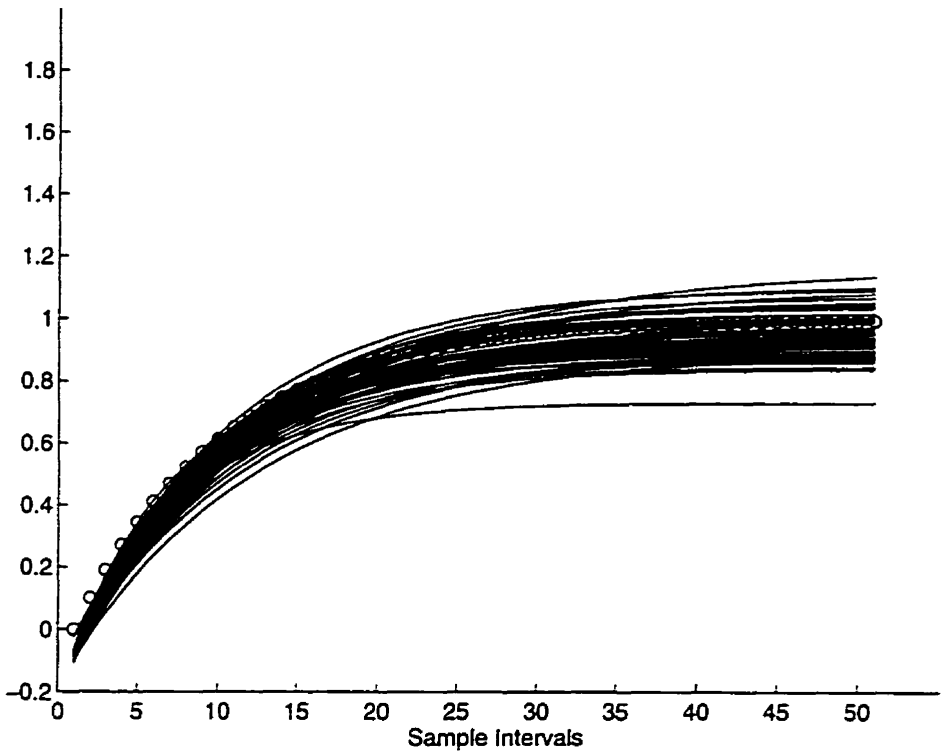

Figure 2.19: Estimated unit step responses with OE model not including unit delay for immediate operator intervention (circles denote the true process step response).

after the input-output data were properly prefiltered. The results are shown in Figure 2.21. Comparing Figure 2.20 with 2.5, and Figure 2.21 with 2.7, it is clear that the only difference is that the distributions of the estimates around the true step response are tighter with the earlier results. This can be explained by comparing the number of operator interventions that occurred for these two cases. The number of interventions that occurred in the first 9 simulations for the two cases are shown in Table 2.1. It is clear that waiting for two unacceptable consecutive output deviations decreases the number of interventions. As explained in section 2.5.1, less frequent operator intervention decreases the magnitude of the filtered process input power spectrum. Therefore the signal-to-noise ratio is lower with fewer interventions and the distribution of the estimates around the true step response broadens. However, the estimates remain unbiased.

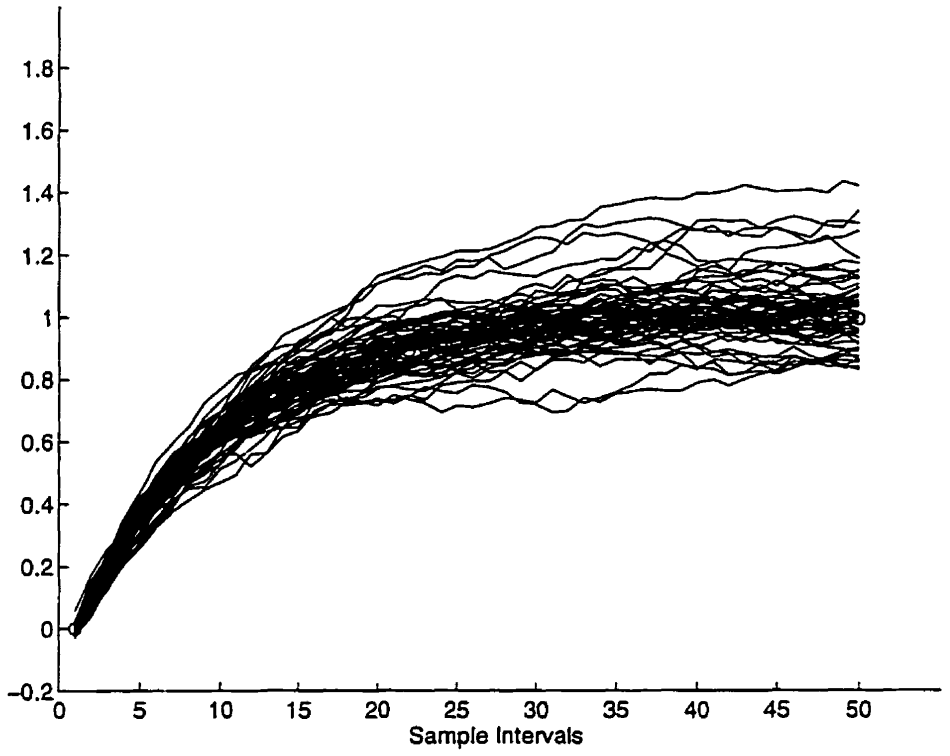

Figure 2.20: Estimated unit step responses with FIR model not including unit delay (circles denote the true process step response).

Operator Intervention Strategy	Number of interventions								
Intervene after one deviation	21	26	22	23	23	34	22	24	23
Intervene after two consecutive deviations	17	21	15	18	18	20	12	19	19

Table 2.1: Number of interventions in first 9 simulation experiments

2.6 Concluding Remarks

In this chapter, the identification of FIR models and low order transfer function models under closed-loop operation conditions was studied. Several conclusions can be made from this work:

1. Operator intervention may improve the overall signal-to-noise ratio, thereby leading to better models, particularly with respect to estimation of the steady-state gains. With proper data prefiltering, there is certainly no need to discard data which contains feedback .

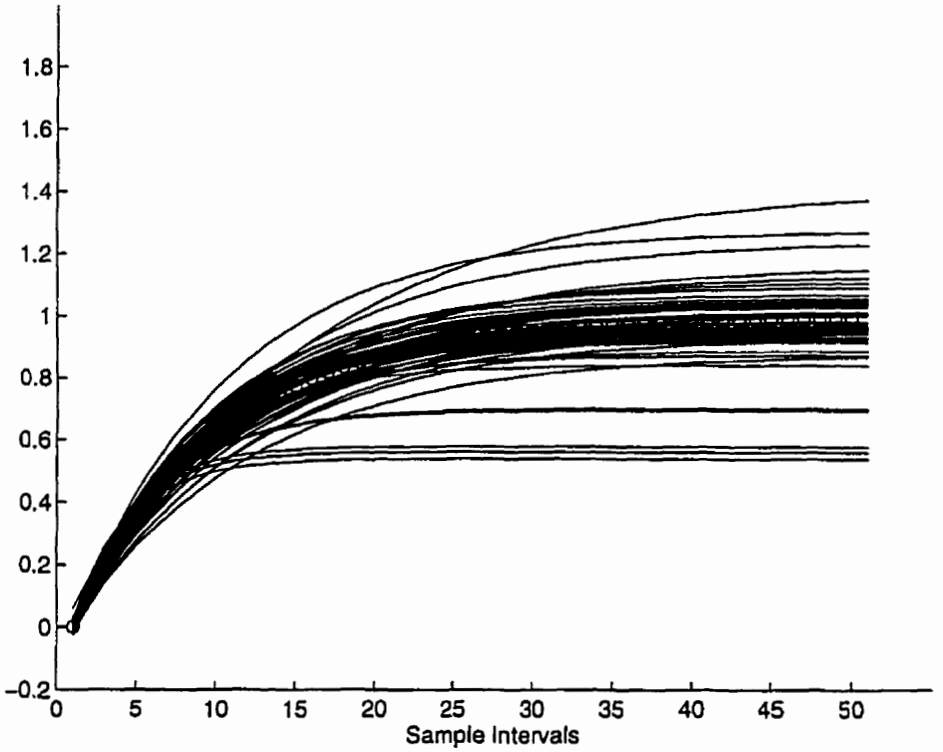

Figure 2.21: Estimated unit step responses with OE model not including unit delay (circles denote the true process step response).

2. With delayed operator intervention, the least squares estimate of a finite impulse response (FIR) model is unbiased after prefiltering data with the correct noise model. This conclusion holds regardless of whether the unit delay is included in the FIR model. The estimates of lower order transfer function models after prefiltering with the correct noise model have similar distribution properties to the FIR estimates, the only difference being that the lower order model estimates are smoother.

3. With immediate operator intervention, both FIR and low order transfer function model estimates are unbiased after prefiltering with the correct noise model if the unit delay is included in the model. If the unit delay is not included in the model, both models lead to biased estimates.

Chapter 3

Issues in the Design of the Prefilter

3.1 Introduction

In this chapter, the role of prefilters in closed-loop process identification is examined. This study is an extension of chapter 2, and therefore the identification results are obtained by combining the FIR model structure with a least squares estimator (LS). In section 3.2, the LS estimate of a simple FIR process under feedback control is theoretically analyzed. Also, a comparison is made between the case where the correct noise model is used in data prefiltering, and the case where no data prefiltering is performed. In addition, the asymptotic expression for the least squares objective function is used to further explain the role of noise model. In section 3.3, a study which looks at the relative importance of the components of an autoregressive-integrated-moving average (ARIMA) noise model in the design of the prefilter is carried out. Further study is then carried out to evaluate the effect of errors in the parameters of these components on the estimation results. Concluding remarks are given in section 3.4.

3.2 Theoretical Analysis

3.2.1 Without Data Prefiltering

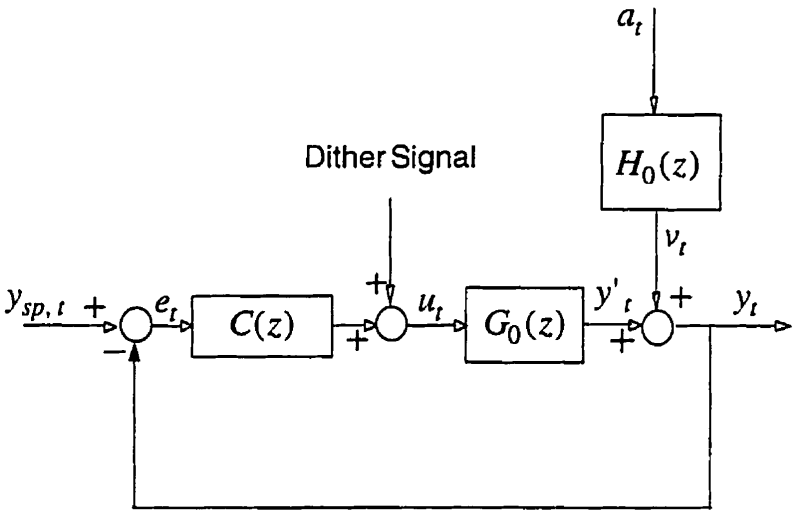

Figure 3.1: Closed-loop process with dither signal

The true system is assumed to be described by Equations (2.3) and (2.4). For a general closed-loop system in Figure 3.1, the process input u_t, with $y_{sp}(t) = 0 \ \forall \ t$ and dither signal, d_t, is given by

$$u_t = -C(z)y_t + d_t \tag{3.1}$$

where $C(z)$ is a time invariant, linear feedback controller. Combining Equations (2.3), (2.4) and (3.1) results in

$$u_t = \frac{1}{1 + C(z)G_0(z)}(d_t - C(z)v_t) \tag{3.2}$$

Here we can see that the process input signal u_t is correlated to the process disturbance v_t. Now we examine what will happen to the estimated model when the process input is in the form of Equation 3.2.

If the process is represented by an FIR model structure, the process given in Equation (2.3) can be equivalently written in its linear regression form:

$$y_t = \phi_t^T \theta_0 + v_t \tag{3.3}$$

and the parameter vector θ_0 can be estimated by

$$\hat{\theta} = [\frac{1}{M}\sum_{t=1}^{M}\phi_t\phi_t^T]^{-1}\frac{1}{M}\sum_{t=1}^{M}\phi_t y_t \tag{3.4}$$

where M denotes the number of data points.

The error between the true and the estimated parameter vector is derived in Söderström and Stoica (1989) as

$$\begin{aligned}\hat{\theta} - \theta_0 &= [\frac{1}{M}\sum_{i=1}^{M}\phi_t\phi_t^T]^{-1}[\frac{1}{M}\sum_{i=1}^{M}\phi_t y_t - \{\frac{1}{M}\sum_{i=1}^{M}\phi_t\phi_t^T\}\theta_0] \\ &= [\frac{1}{M}\sum_{i=1}^{M}\phi_t\phi_t^T]^{-1}[\frac{1}{M}\sum_{i=1}^{M}\phi_t v_t]\end{aligned} \tag{3.5}$$

This expression indicates that a consistent estimate is obtained under the conditions that

$$E[\phi_t\phi_t^T] \text{ is nonsingular} \tag{3.6}$$

$$E[\phi_t v_t] = 0 \tag{3.7}$$

Condition 3.6 requires that the data be sufficiently exciting. Condition 3.7 will be satisfied if v_t is uncorrelated with ϕ_t. If v_t is not white noise, it will normally be correlated with past inputs u_t through Equation (3.2) and past outputs y_t through Equation 3.3. Hence 3.7 will in general not hold and the LS estimate $\hat{\theta}$ will be biased. Let us examine the bias issue in more detail using the following example.

Example 3.2.1

The true process is given by the following FIR model

$$y_t = b_1 u_t + b_2 u_{t-1} + v_t \tag{3.8}$$

where u_t is generated according to the control law.

$$u_t = -C(z) y_t \tag{3.9}$$

With delayed intervention as described in chapter 2, there is a unit delay between when a unacceptable deviation occurs and when the operator intervenes. To impose the same delayed correlation structure on this example, we will take the controller to be of the form

$$C(z) = K z^{-1} \tag{3.10}$$

Now, we want to examine the LS estimate of the process on the data collected under the above experimental conditions. First, we want to use y' to denote the noise-free process output shown in Figure 3.1. Then

$$y_t = y'_t + v_t \tag{3.11}$$

Equation (3.9), (3.10) and (3.11) result in

$$u_t = -K y'_{t-1} - K v_{t-1} \tag{3.12}$$

The process given in Equation(3.8) can be expressed in its linear regression form by defining

$$\phi_t^T = [u_t \;\; u_{t-1}] \tag{3.13}$$

$$\theta_0^T = [b_1 \;\; b_2] \tag{3.14}$$

The LS estimate of θ_0 can be obtained by Equation (3.4)

$$\hat{\theta} = \begin{bmatrix} \hat{b}_1 \\ \hat{b}_2 \end{bmatrix} = \begin{bmatrix} \frac{1}{M}\sum_{t=1}^{M} u_t^2 & \frac{1}{M}\sum_{t=1}^{M} u_{t-1}u_t \\ \frac{1}{M}\sum_{t=1}^{M} u_{t-1}u_t & \frac{1}{M}\sum_{t=1}^{M} u_{t-1}^2 \end{bmatrix}^{-1} \begin{bmatrix} \frac{1}{M}\sum_{t=1}^{M} u_t y_t \\ \frac{1}{M}\sum_{t=1}^{M} u_{t-1} y_t \end{bmatrix} \tag{3.15}$$

The summations in Equation (3.15) converge in quadratic mean and hence in probability to their expected values (Goldberger, 1964), i.e.

$$\begin{bmatrix} \frac{1}{M}\sum_{t=1}^{M} u_t^2 & \frac{1}{M}\sum_{t=1}^{M} u_{t-1}u_t \\ \frac{1}{M}\sum_{t=1}^{M} u_{t-1}u_t & \frac{1}{M}\sum_{t=1}^{M} u_{t-1}^2 \end{bmatrix} \longrightarrow \begin{bmatrix} \hat{R}_{uu}(0) & \hat{R}_{uu}(1) \\ \hat{R}_{uu}(1) & \hat{R}_{uu}(0) \end{bmatrix}$$

$$\begin{bmatrix} \frac{1}{M}\sum_{t=1}^{M} u_t y_t \\ \frac{1}{M}\sum_{t=1}^{M} u_{t-1} y_t \end{bmatrix} \longrightarrow \begin{bmatrix} \hat{R}_{uy}(0) \\ \hat{R}_{uy}(1) \end{bmatrix}$$

Where

$$\hat{R}_{\alpha\beta}(\tau) = E[\alpha_{t-\tau}\beta_t]$$

Hence from Frechet's theorem (Goodwin and Payne, 1977, p. 224)

$$\begin{bmatrix} \hat{b}_1 \\ \hat{b}_2 \end{bmatrix} \longrightarrow \begin{bmatrix} \hat{R}_{uu}(0) & \hat{R}_{uu}(1) \\ \hat{R}_{uu}(1) & \hat{R}_{uu}(0) \end{bmatrix}^{-1} \begin{bmatrix} \hat{R}_{uy}(0) \\ \hat{R}_{uy}(1) \end{bmatrix} \tag{3.16}$$

Since

$$\begin{bmatrix} \hat{R}_{uu}(0) & \hat{R}_{uu}(1) \\ \hat{R}_{uu}(1) & \hat{R}_{uu}(0) \end{bmatrix}^{-1} = \frac{1}{\Delta} \begin{bmatrix} \hat{R}_{uu}(0) & -\hat{R}_{uu}(1) \\ -\hat{R}_{uu}(1) & R_{uu}(0) \end{bmatrix} \tag{3.17}$$

where

$$\Delta = \hat{R}_{uu}^2(0) - \hat{R}_{uu}^2(1) \tag{3.18}$$

Then, substituting Equation (3.17) into Equation (3.16) yields

$$\begin{bmatrix} \hat{b}_1 \\ \hat{b}_2 \end{bmatrix} \longrightarrow \frac{1}{\Delta} \begin{bmatrix} \hat{R}_{uu}(0)\hat{R}_{uy}(0) - \hat{R}_{uu}(1)\hat{R}_{uy}(1) \\ -\hat{R}_{uu}(1)\hat{R}_{uy}(0) + \hat{R}_{uu}(0)\hat{R}_{uy}(1) \end{bmatrix} \tag{3.19}$$

For simplicity, we assume that $\hat{R}_{vv}(\tau)$ is zero for $|\tau| \geq 2$. Then, from Equations (3.8) and (3.12), we get

$$\hat{R}_{uy}(0) = b_1\hat{R}_{uu}(0) + b_2\hat{R}_{uu}(1) - K\hat{R}_{vv}(1) \tag{3.20}$$

$$\hat{R}_{uy}(1) = b_1 u u(1) + b_2\hat{R}_{uu}(0) \tag{3.21}$$

Substituting (3.20) (3.21) into (3.19), yields

$$\begin{bmatrix} \hat{b}_1 \\ \hat{b}_2 \end{bmatrix} \longrightarrow \begin{bmatrix} b_1 - K\hat{R}_{vv}(1)\hat{R}_{uu}(0)/\Delta \\ b_2 + K\hat{R}_{vv}(1)\hat{R}_{uu}(1)/\Delta \end{bmatrix} \tag{3.22}$$

Thus, $\hat{b}_1$ and $\hat{b}_2$ do not converge in probability to the true parameters b_1 and b_2, unless the noise is white, i.e., $\hat{R}_{vv}(1)$ is zero.

3.2.2 With Data Prefiltering Using the True Noise Model

Choosing $H(z) = H_0(z)$ as a user selected prefilter, alternative forms of the process and controller equations are

$$y_{f,t} = G(z,\theta)u_{f,t} + a_t \tag{3.23}$$

$$u_{f,t} = -C(z)y_{f,t} + d_{f,t} \tag{3.24}$$

where $y_{f,t} = H(z)^{-1}y_t$, $u_{f,t} = H(z)^{-1}u_t$, $d_{f,t} = H(z)^{-1}d_t$.

The above Equations (3.23) and (3.24) result in

$$u_{f,t} = \frac{1}{1 + C(z)G_0(z)}(d_{f,t} - C(z)a_t) \tag{3.25}$$

With Equation (3.10), Equation (3.25) becomes

$$u_{f,t} = \frac{1}{1 + KG_0(z)z^{-1}}(d_{f,t} - Ka_{t-1}) \tag{3.26}$$

The process in its linear regression form is given by

$$y_{f,t} \;=\; \phi_{f,t}^T\theta_0 + a_t \tag{3.27}$$

where $\phi_{f,t} = H^{-1}(z)\phi_t$. The error associated with the LS estimate of θ_0 is

$$\hat{\theta} - \theta_0 = [\frac{1}{M}\sum_{i=1}^{M}\phi_{f,t}\phi_{f,t}^T]^{-1}[\frac{1}{M}\sum_{i=1}^{M}\phi_{f,t}a_t] \tag{3.28}$$

To check for correlation between $\phi_{f,t}$ and a_t (Condition 3.7), we must look at the definition of $\phi_{f,t}$ for an FIR model, where

$$\phi_{f,t}^T = [u_{f,t} \;\; u_{f,t-1} \;\; \ldots \;\; u_{f,t-N}] \tag{3.29}$$

Equation (3.26) shows that $u_{f,t}$ is not correlated with a_t. Therefore, $\phi_{f,t}^T$ is not correlated with a_t. Then, as long as Condition (3.6) is satisfied, an unbiased LS estimate should be obtained.

Example 3.2.2

Continuing on with example 3.2.1, with the data now prefiltered by the inverse of the true noise model $H_0(z)$, the process model is :

$$y_{f,t} = b_1 u_{f,t} + b_2 u_{f,t-1} + a_t \tag{3.30}$$

$$u_{f,t} = -K y'_{f,t-1} - K a_{t-1} \tag{3.31}$$

Applying the same analysis, the LS estimate behaves as

$$\begin{bmatrix} \hat{b}_1 \\ \hat{b}_2 \end{bmatrix} \longrightarrow \begin{bmatrix} b_1 - K\hat{R}_{aa}(1)\hat{R}_{u_f u_f}(0)/\Delta \\ b_2 + K\hat{R}_{aa}(1)\hat{R}_{u_f u_f}(1)/\Delta \end{bmatrix} \tag{3.32}$$

where

$$\Delta = \hat{R}^2_{u_f u_f}(0) - \hat{R}^2_{u_f u_f}(1) \tag{3.33}$$

Since a_t is white noise, $\hat{R}_{aa}(\tau) = 0$ for $\tau \geq 1$. Therefore, the error terms $K\hat{R}_{aa}(1)\hat{R}_{u_f u_f}(0)/\Delta$ and $K\hat{R}_{aa}(1)\hat{R}_{u_f u_f}(1)/\Delta$ are equal to zero, which yields that $\hat{\theta}$ converges to θ_0, i.e., the estimate is unbiased.

3.2.3 General Asymptotic Results

Asymptotic expressions developed by MacGregor and Fogal (1995) can be used to further explain the effect of prefiltering on identification results. The prediction errors of the estimated model are defined as, for the case of data prefiltering using $H(z)$,

$$e_t(\theta) = H^{-1}(z)[y_t - G(z,\theta)u_t] \tag{3.34}$$

where y_t is given by

$$y_t = \frac{1}{1 + C(z)G_0(z)}(G_0(z)d_t + v_t) \tag{3.35}$$

Defining

$$S_0(z) = \frac{1}{1 + C(z)G_0(z)} \tag{3.36}$$

as the sensitivity function of the true closed-loop system, and substituting Equations (3.2), (3.35) and (3.36) into Equation (3.34) gives

$$e_t(\theta) = \frac{S_0(z)}{H(z)}[(G_0(z) - G(z,\theta))d_t + (1 + C(z)G(z,\theta))v_t] \tag{3.37}$$

Consequently, the power spectrum of the prediction errors is

$$\Phi_e(\omega,\theta) = [|G_0(e^{j\omega}) - G(e^{j\omega},\theta)|^2\Phi_d(\omega) + |1 + C(e^{j\omega})G(e^{j\omega},\theta)|^2\Phi_v(\omega)]\frac{|S_0(e^{j\omega})|^2}{|H(e^{j\omega})|^2} \tag{3.38}$$

Using a prediction error method, the estimated model $G(z,\theta)$ is determined by minimizing the sum of squares of $e_t(\theta)$. The least squares objective function is then given by

$$\begin{aligned} J(\theta) &= E[e_t^2(\theta)] = \frac{1}{2\pi}\int_{-\pi}^{\pi}\Phi_e(\omega,\theta)d\omega \\ &= \frac{1}{2\pi}\int_{-\pi}^{\pi}|G_0(e^{j\omega}) - G(e^{j\omega},\theta)|^2\frac{|S_0(e^{j\omega})|^2\Phi_d(\omega)}{|H(e^{j\omega})|^2}d\omega \quad \text{bias term} \\ &+ \frac{1}{2\pi}\int_{-\pi}^{\pi}\frac{|S_0(e^{j\omega})|^2}{|S(e^{j\omega},\theta)|^2}\frac{|H_0(e^{j\omega})|^2\sigma_a^2}{|H(e^{j\omega})|^2}d\omega \quad \text{sensitivity ratio term} \end{aligned} \tag{3.39}$$

where $S(e^{j\omega},\theta) = \frac{1}{1+C(e^{j\omega})G(e^{j\omega},\theta)}$ is the sensitivity function of the modeled closed-loop system (MacGregor and Fogal, 1995).

As defined in MacGregor and Fogal (1995), the two terms in the objective function are the bias term and the sensitivity ratio term. The minimum of $J(\theta)$ is σ_a^2 when the bias term is equal to zero and the ratio of the frequency dependent terms in the sensitivity ratio term is equal to unity. This requires that the prefilter $H(e^{j\omega})$ be selected identical to the true noise model $H_0(e^{j\omega})$. If $H(e^{j\omega}) \neq H_0(e^{j\omega})$, then the ratio of the frequency dependent terms in the sensitivity ratio term cannot be equal to unity if the process model is correct (i.e. if $G(z,\theta) = G_0(z)$). This results in an objective function that is larger than its minimum (σ_a^2). Therefore a bias of $(G_0(z) - G(z,\theta))$ exists. This theoretically confirms that an unbiased estimate of the process model can be obtained provided that the prefilter is the exact inverse of the true noise model.

3.3 Importance of the Accuracy of the Noise Model

According to the analysis in section 3.2, an unbiased estimate of the true process model can be obtained from data containing feedback if the data are first prefiltered by the inverse of the true noise model. Mismatch between the true noise model, $H_0(z)$ and the assumed noise model, $H(z)$ would be expected to produce a biased estimate. In this section, the effect of the accuracy of noise model on the identification results is investigated under two headings, structure mismatch and parameter mismatch.

3.3.1 Structure Mismatch

This study is carried out using simulation example 2.2.1 with LIM = 6, but with different disturbance characteristics.

Simulation Example 3.3.1

The true noise model has an ARIMA structure

$$H_0(z) = \frac{(1 - \theta_0 z^{-1})}{(1 - \varphi_0 z^{-1})(1 - z^{-1})} \tag{3.40}$$

with $\theta_0 = 0.3$ and $\varphi_0 = 0.7$. There are three terms in this expression, which are called the autoregressive or AR-term $(1 - \phi_0 z^{-1})$, the integrated or I-term $(1 - z^{-1})$, and the moving average or MA-term $(1 - \theta_0 z^{-1})$.

Based on the data collected from this simulation experiment, the impulse response model was estimated using the LS method with u_t and y_t replaced by $u_{f,t}$ and $y_{f,t}$ in Equation 2.21 (MATLAB ARX command with $NN = [0 \;\; 50 \;\; 1]$) according to

$$u_{f,t} = H(z)^{-1} u_t \tag{3.41}$$

$$y_{f,t} = H(z)^{-1} y_t \tag{3.42}$$

where $H(z)$ is a user-selected prefilter. The following choices for $H(z)$ were considered: (a) $H(z) = \frac{1}{(1-0.7z^{-1})(1-z^{-1})}$ (MA mismatch); (b) $H(z) = \frac{1-0.3z^{-1}}{1-z^{-1}}$ (AR mismatch); (c) $H(z) = \frac{1-0.3z^{-1}}{1-0.7z^{-1}}$ (I mismatch); (d) $H(z) = \frac{1}{1-z^{-1}}$ (ARMA mismatch); (e)

$H(z) = \frac{1}{1-0.7z^{-1}}$ (IMA mismatch); and (f) $H(z) = \frac{1-0.3z^{-1}}{1}$ (ARI mismatch). We estimated the process step response models using the same set of raw data prefiltered by these different choices of $H(z)$.

The study in chapter 2 showed that there is a distribution of the estimated results arising from different choices of the random number seed used to generate a_t. Therefore, forty experiments with forty different seeds for the white noise sequence were performed yielding 40 estimates of the step response model for each choice of prefilter. When looking at the 40 estimation results, one might also want to look at the average model. For ease of comparison of the effect of using different prefilters, we compare only the average estimated models with the true process step response. The results are plotted in Figure 3.2 and Figure 3.3.

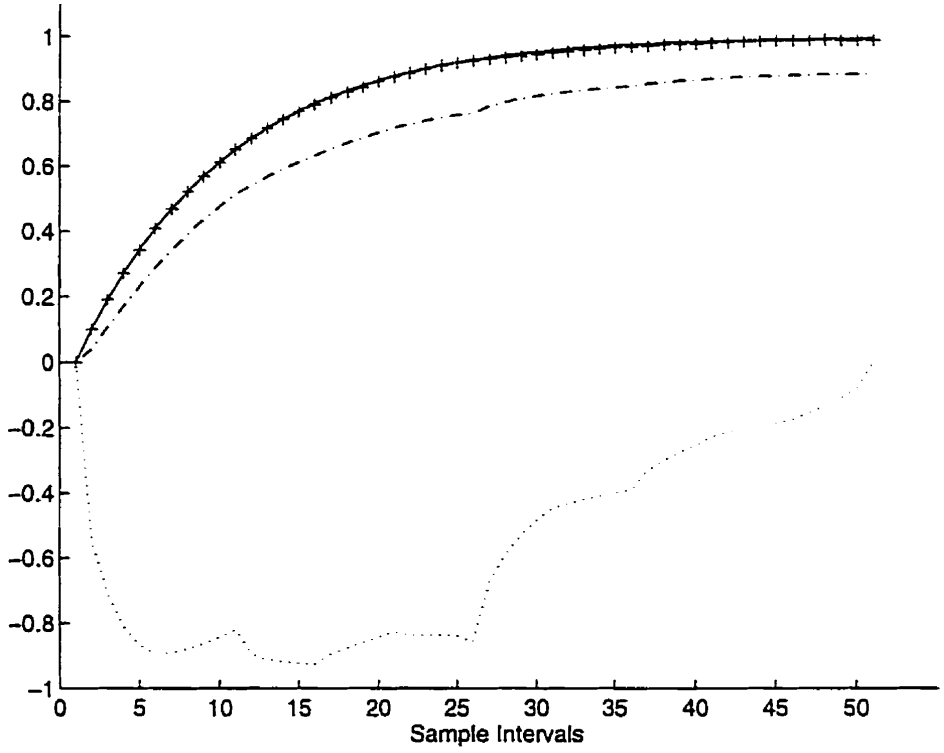

Figure 3.2: Average step response estimated with user-selected prefilters (Solid line: true process step response; Plus: $H(z) = H_0(z)$; Dashed: MA mismatch, Dashdot: AR mismatch; Dotted: I mismatch)

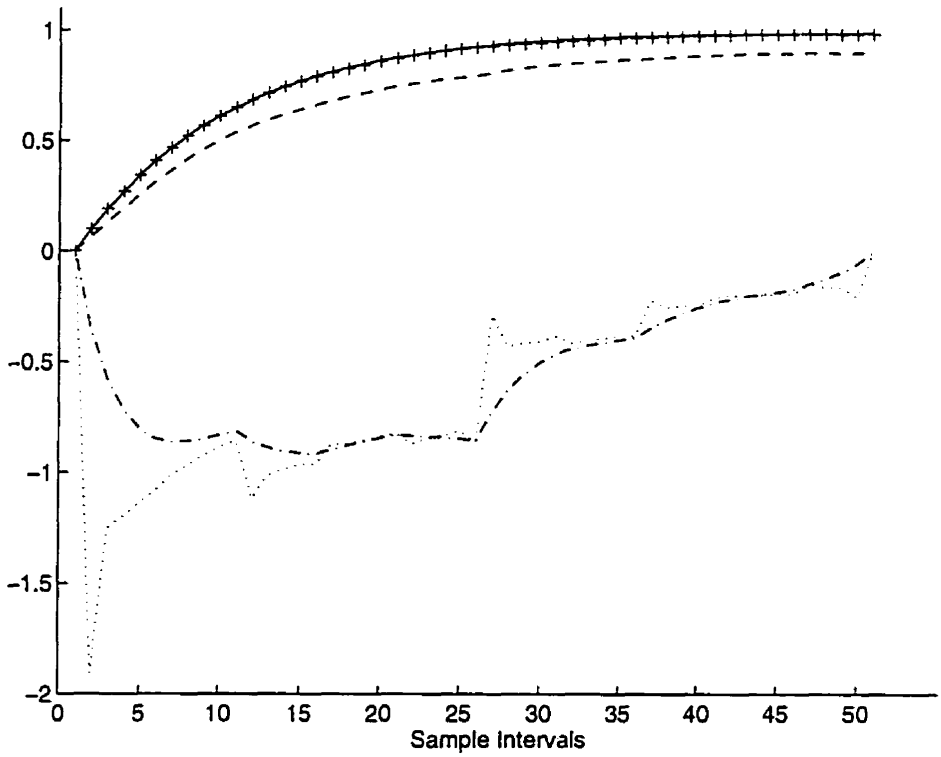

Figure 3.3: Average step response estimated with user-selected prefilters (Solid line: true process step response; Plus: $H(z) = H_0(z)$; Dashed: ARMA mismatch; Dashdot: IMA mismatch; Dotted: ARI mismatch)

Comparing the average estimation results for different prefilters with the true process step response in Figure 3.2 and Figure 3.3, we can see that any combination of structure mismatch between the true noise model and prefilter results in estimation problems except in the case where there is only MA mismatch. The fact that MA mismatch does not affect the estimation results is somewhat unique to this simulation example. More detailed discussion about this particular point will be given below. In general, the mismatch between the true noise model and the prefilter causes estimation problems because Condition (3.7) is not satisfied. For prefiltered data, Condition (3.7) requires that $E[\phi_{f,t}v_{f,t}] = 0$.

For the case of MA mismatch, the average of the estimated models in Figure 3.2 is virtually identical to the true process step response model. This result seems to contradict the earlier analysis that the prefilter must be exactly equal to the true noise

model if one wants to get an unbiased estimate of the process model. However, this can be explained by looking at the correlation between $u_{f,t}$ and $v_{f,t}$. The process unit step response model was obtained from the LS estimated FIR model with u_t and y_t replaced by $u_{f,t}$ and $y_{f,t}$ in Equation (2.21) (MATLAB ARX command with $NN = [0 \;\; 50 \;\; 1]$). Due to the nature of the operator intervention, correlation exists between $\{u_{t+1}\}$ and $\{v_t\}$ and as a result correlation also exists between $\{u_{f,t+1}\}$ and $\{v_{f,t}\}$. In the case of MA mismatch between $H(z)$ and $H_0(z)$, $\{v_{f,t}\}$ has moving average dynamics only. i.e. $v_{f,t} = a_t - 0.3a_{t-1}$. However, because $\{a_t\}$ is a white noise sequence, $\hat{R}_{u_f a}(\tau) \approx 0$ for all $\tau \geq 1$. Therefore, because the unit delay is included in the FIR model, the estimates remain unbiased. On the other hand, if models were estimated without including the unit delay in the FIR model, the estimates would be biased. The 40 estimates, generated from the same 40 experiments using the MATLAB ARX command with $NN = [0 \;\; 50 \;\; 0]$, were obtained after the data were prefiltered with $H(z) = \frac{1}{(1-0.7z^{-1})(1-z^{-1})}$. The average of the 40 estimates in each case is plotted in Figure 3.4 and compared with the true process unit step response. It is clear that the estimates are now biased.

In summary, looking at the estimation problems caused by various combinations of structure mismatches between the true noise model and the prefilter, we can write these different mismatches in descending order according to the importance of their negative effect on the estimation results: (1) ARI mismatch, (2) I mismatch, (3) IMA mismatch, (4) AR mismatch, (5) ARMA mismatch and (6) MA mismatch. In fact, since both the AR and I terms appear in the denominator of the general ARIMA model in Equation (3.40), we can think of the I term as a special case of the AR term. Therefore, we can conclude that the AR term is the most important term in the prefilter design.

3.3.2 Parameter Mismatch

It has been identified in the previous subsection that AR-type noise model terms are the most important in terms of the data prefilter design. In this subsection, we are going to evaluate the sensitivity of the estimation results to parameter mismatch in the autoregressive term between the true noise model and the assumed noise model. The

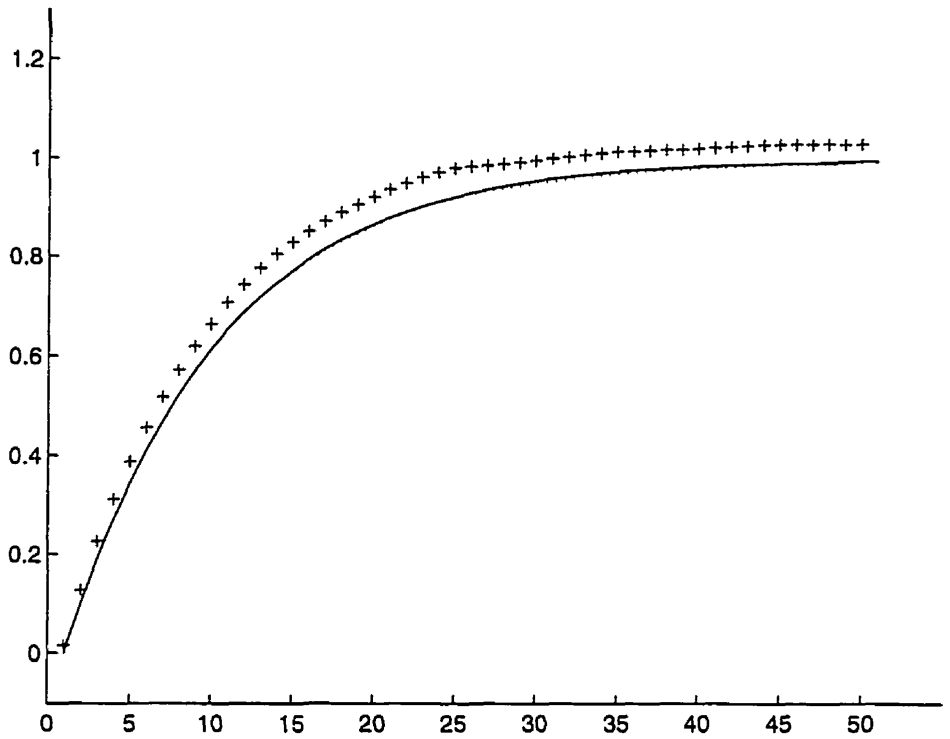

Figure 3.4: Average estimated unit step response with FIR model not including unit delay on data prefiltered by user-selected prefilters (Solid line: true process step response; Dotted: $H(z) = H_0(z)$; Plus: MA mismatch)

study is carried out using two simulation examples.

Simulation Example 3.3.2 (Noise Model Parameter Underestimated)

The simulation example is identical to Example 3.3.1 except that the true noise model has an AR structure

$$H_0(z) = \frac{1}{1 - 0.99z^{-1}}$$

and the prefilter was selected to have the same model structure

$$H(z) = \frac{1}{1 - \varphi z^{-1}}$$

but with the value of φ taken to be different and smaller than 0.99. We have examined the following choices for φ: 0.5, 0.6, 0.7, 0.8, 0.9, 0.95 and 0.97. As mentioned in simulation example 3.3.1, due to the distribution of the estimated results arising from

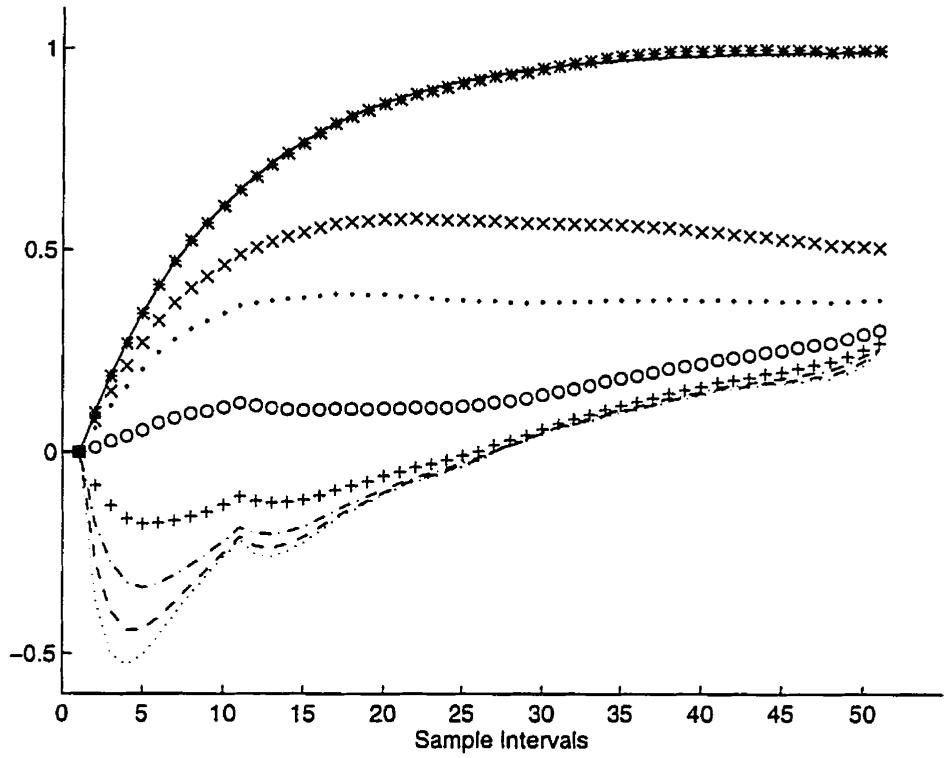

Figure 3.5: Example 3.3.2: Average step responses estimated with different prefilters ($H(z) = \frac{1}{1-\varphi z^{-1}}$) (Solid: true process step response; Star: $\varphi = 0.99$; X-mark: $\varphi = 0.97$; Point: $\varphi = 0.95$; Circle: $\varphi = 0.90$ Plus: $\varphi = 0.80$; Dashdot: $\varphi = 0.70$; Dashed: $\varphi = 0.60$; Dotted: $\varphi = 0.50$).

different choices of the random number seed used to generate a_t, 40 experiments with 40 different seeds for the white noise sequence were performed yielding 40 estimates of the step response model for each prefilter. The average estimated models are compared with the true process step response. The results are plotted in Figure 3.5. It is clear that a larger parameter mismatch between the true noise model and prefilter produces a greater difference between the true process and the estimated model. Moreover, the estimation results are very sensitive to even subtle differences.

In order to quantitatively evaluate the error between true process step response and the estimated response caused by the parameter mismatch, the sum of squared errors in the estimated step response coefficients for each case was calculated and plotted in Figure 3.6.

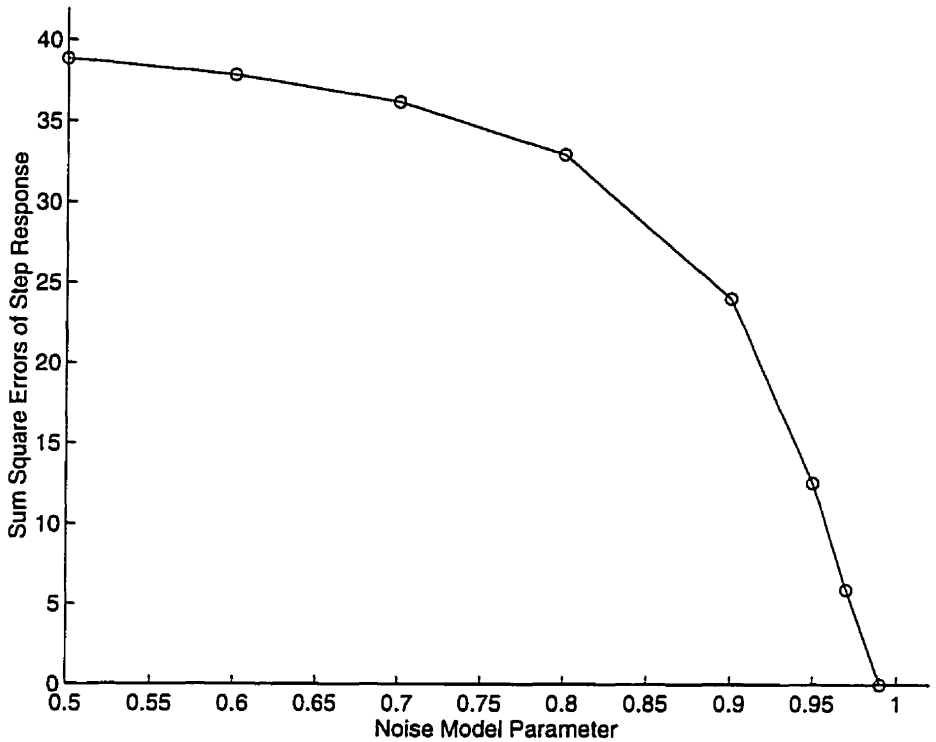

Figure 3.6: Estimation Error as a Function of Assumed Noise Model Parameter

Simulation Example 3.3.3 (Noise Model Parameter Overestimated)

In simulation example 3.3.2, the parameter in each prefilter had a smaller value compared with the true value. In this example, we want to look at the case where the prefilter has a larger parameter value than the true one. We constructed simulation experiments identical to those in simulation example 3.3.2, except that the true noise model is given by $H_0(z) = \frac{1}{1-0.97z^{-1}}$. The prefilter was selected to have the same model structure as before, with the following values for φ: 0.95, 0.96, 0.98, 0.985, 0.99 and 1.0. The same approach for obtaining the step response estimates as used in simulation example 3.3.2 was used. The results are plotted in Figure 3.7. It is clear that as the parameter mismatch grows, the estimation error increases.

From simulation examples 3.3.2 and 3.3.3, we can conclude that either an under-estimation or over-estimation of the parameter in the autoregressive term of the assumed noise model results in identifiability problems. Even for a subtle difference in the pa-

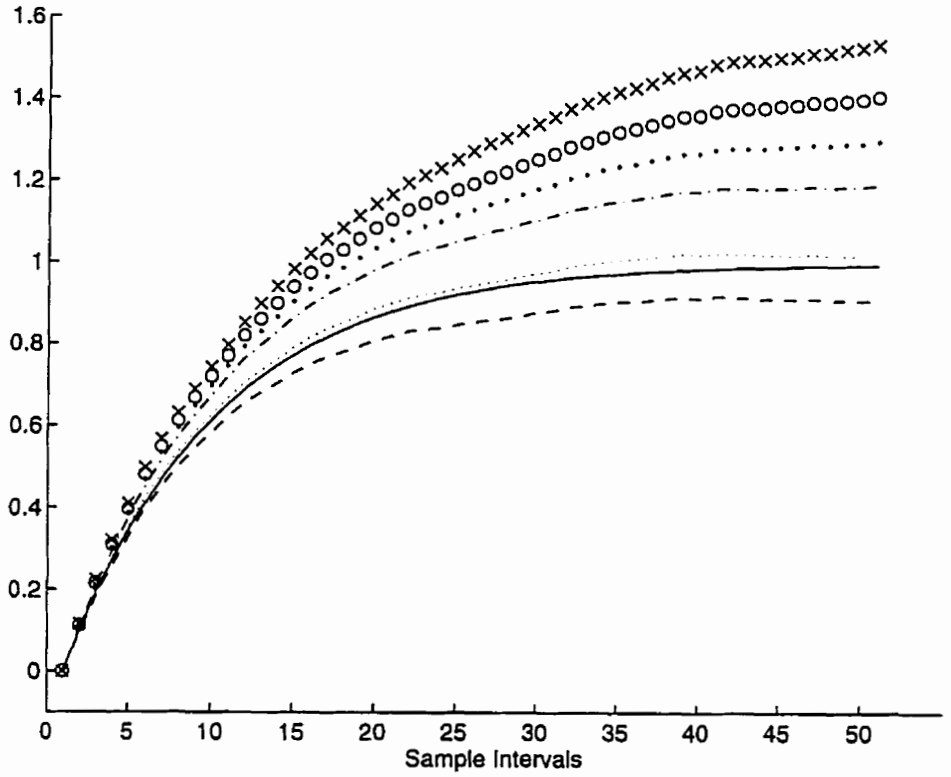

Figure 3.7: Example 3.3.3: Average step responses estimated with different prefilters ($H(z) = \frac{1}{1-\varphi z^{-1}}$) (Solid: true step response; Dashed: $\varphi = 0.96$; Dotted: $\varphi = 0.97$; Dashdot: $\varphi = 0.98$ Point: $\varphi = 0.985$; Circle: $\varphi = 0.99$; X-mark: $\varphi = 1.0$).

rameter, the estimation problems are obvious. Therefore, an accurate estimation of the autoregressive terms of the noise model is required in order to obtain a good estimate of the process model.

3.4 Concluding Remarks

In this chapter, the use of the noise model in prefilter design is studied. Results confirm that prefiltering data which contains feedback using the correct noise model is necessary to achieve unbiased estimates of the process dynamics. Specific conclusions from this chapter are:

1. Unbiased process model estimation using data containing feedback requires that the data be prefiltered by the inverse of an accurate noise model. Structure mismatch or

parameter mismatch between the true noise model and assumed noise model causes process model estimation problems.

2. Mismatch in the autoregressive component between the assumed noise model and the true noise model causes the most serious identifiability problems. The process estimate is very sensitive even to a subtle parameter mismatch in this component.

Chapter 4

Simultaneous Identification of Process and Noise Models

4.1 Introduction

In this chapter, a generalized least squares (GLS) algorithm is developed for simultaneous identification of both the process and noise models. The FSF model structure is used to represent the process model and in section 4.2, an introduction to the FSF model structure and its properties is given. In section 4.3, the least squares estimate of the FSF model parameters and calculation of the statistical confidence bounds for the FSF-based step response estimate are presented. Section 4.3 also briefly explains the concept of the sum of squared true prediction errors (PRESS) and its computation. The use of the PRESS criterion for selection of both the process model structure and the noise model structure is a unique feature of the GLS algorithm presented in section 4.4. In section 4.5 and 4.6, the proposed algorithm is applied to some simulation examples and an industrial data set, respectively. Concluding remarks are given in section 4.7.

4.2 FSF Process Model Structure and Its Properties

4.2.1 FSF Model Structure

A single input, single output (SISO) process, assumed to be stable, linear and time-invariant, can be represented by the following discrete-time FIR model

$$G(z) = \sum_{i=0}^{N-1} h_i z^{-i} \tag{4.1}$$

where N is the model order with the impulse response coefficients $h_i = 0$ for all $i \geq N$ and z^{-1} is the backward shift operator. Practically, N is chosen according to $N \approx \frac{T_s}{\Delta t}$, where T_s is the process settling time and Δt is the chosen sampling interval.

With the assumption that N is an odd number, the inverse Discrete Fourier Transform (DFT) of $G(z)$ is

$$h_i = \frac{1}{N} \sum_{k=-\frac{N-1}{2}}^{\frac{N-1}{2}} G(e^{j\frac{2\pi k}{N}}) e^{j\frac{2\pi ki}{N}} \tag{4.2}$$

This expression relates the frequency response of the process with its impulse response coefficients. Substituting Equation (4.2) into (4.1) gives

$$G(z) = \sum_{i=0}^{N-1} \frac{1}{N} \sum_{k=-\frac{N-1}{2}}^{\frac{N-1}{2}} G(e^{j\frac{2\pi k}{N}}) e^{j\frac{2\pi ki}{N}} z^{-i} \tag{4.3}$$

Interchanging the summations

$$G(z) = \sum_{k=-\frac{N-1}{2}}^{\frac{N-1}{2}} G(e^{j\frac{2\pi k}{N}}) \frac{1}{N} \frac{1 - z^{-N}}{1 - e^{j\frac{2\pi k}{N}} z^{-1}} \tag{4.4}$$

gives the frequency sampling filter model form.

Defining

$$F_k(z) = \frac{1}{N} \frac{1 - z^{-N}}{1 - e^{j\frac{2\pi k}{N}} z^{-1}} \tag{4.5}$$

for $k = 0, \pm 1, \pm 2, ..., \pm\frac{N-1}{2}$ gives the frequency sampling filters (FSF) and $G(e^{j\frac{2\pi k}{N}})$ are the parameters of the FSF model. Figure 4.1 shows a block diagram of the FSF model,

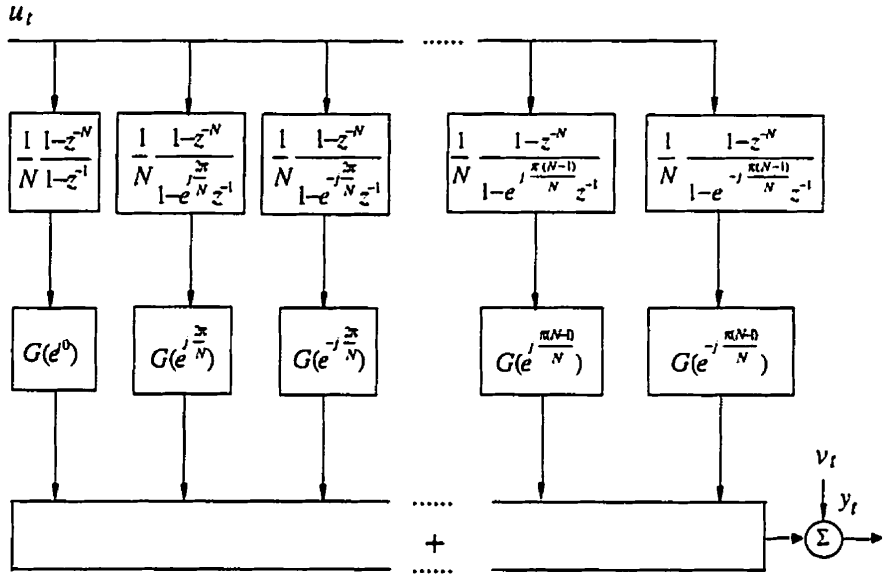

Figure 4.1: Schematic diagram of FSF model

where u_t is the process input and y_t is the measured process output.

The process step response can be obtained directly through

$$g_m = \sum_{i=0}^{m} h_i \tag{4.6}$$

for $m = 0, 1, ..., N-1$. Substituting Equation (4.2) into (4.6), we get

$$g_m = \sum_{k=-\frac{N-1}{2}}^{\frac{N-1}{2}} G(e^{j\frac{2\pi k}{N}}) \frac{1}{N} \frac{1 - e^{j\frac{2\pi k}{N}(m+1)}}{1 - e^{j\frac{2\pi k}{N}}} \tag{4.7}$$

which gives the step response in terms of the process frequency response $G(e^{j\frac{2\pi k}{N}})$.

4.2.2 Properties of the FSF Model

- With fast sampling, the FSF model parameters converge to their continuous-time counterparts at $\omega = 0, \frac{2\pi}{T_s}, ..., \frac{\pi}{\Delta t}$ for a fixed T_s. As sampling interval (Δt) decreases,

the number of parameters associated with the model increases but only in the high frequency region.

- Based on the above property, there exists an odd integer n such that for all k where $\frac{n-1}{2} < |k| \leq \frac{N-1}{2}$, the magnitudes of the FSF model parameters, $G(e^{j\frac{2\pi k}{N}})$, are approximately equal to zero. As $\Delta t \to 0$, n becomes independent of the choice of the sampling interval and is called the effective model order which is generally much less than N. This reduced *nth* order FSF model can be written in the following form

$$G(z) \approx \sum_{k=-\frac{n-1}{2}}^{\frac{n-1}{2}} G(e^{j\frac{2\pi k}{N}}) \frac{1}{N} \frac{1 - z^{-N}}{1 - e^{j\frac{2\pi k}{N}} z^{-1}} \tag{4.8}$$

and the step response model obtained from the reduced order FSF model is given by:

$$g_m \approx \sum_{k=-\frac{n-1}{2}}^{\frac{n-1}{2}} G(e^{j\frac{2\pi k}{N}}) \frac{1}{N} \frac{1 - e^{j\frac{2\pi k}{N}(m+1)}}{1 - e^{j\frac{2\pi k}{N}}} \tag{4.9}$$

- Due to the reduction in the number of parameters that need to be estimated from N to n and the narrow bandpass nature of the frequency sampling filters, the general conditioning of the correlation matrix associated with the least squares estimate of the FSF model is improved. On the other hand, the correlation matrix associated with the least squares estimate of an FIR model is only well-conditioned when the periodogram of the input signal is approximately equal at all frequencies. However, input signals with only low and medium frequency content are typically used in the process industries which means the correlation matrix for the FIR model will almost always be ill-conditioned. This leads to inflation of the covariance matrix and noisy step response estimates.

4.3 Least Squares Estimate of the FSF Model

4.3.1 Least Squares Formulation

The frequency sampling filter model of the system to be identified can be written as

$$y_t = \sum_{k=-\frac{n-1}{2}}^{\frac{n-1}{2}} G(e^{j\frac{2\pi k}{N}}) \frac{1}{N} \frac{1-z^{-N}}{1-e^{j\frac{2\pi k}{N}}z^{-1}} u_t + v_t \tag{4.10}$$

where v_t is the output disturbance which is assumed to be uncorrelated with the process input u_t. The process output can be expressed in an equivalent linear regression form by defining a parameter vector as

$$\theta = [G(0) \;\; G(e^{j\frac{2\pi}{N}}) \;\; G(e^{-j\frac{2\pi}{N}}) \;\; \ldots \;\; G(e^{j\frac{(n-1)\pi}{N}}) \;\; G(e^{-j\frac{(n-1)\pi}{N}})]^T \tag{4.11}$$

and its corresponding regressor vector as

$$\phi_t = [f_t^0 \;\; f_t^1 \;\; f_t^{-1} \ldots \;\; f_t^{\frac{n-1}{2}} \;\; f_t^{-\frac{n-1}{2}}]^T \tag{4.12}$$

where

$$f_t^r = \frac{1}{N} \frac{1-z^{-N}}{1-e^{j\frac{2\pi r}{N}}z^{-1}} u_t \tag{4.13}$$

for $r = 0, \pm 1, \ldots, \pm\frac{n-1}{2}$. Then we can rewrite Equation (4.10) as

$$y_t = \phi_t^T \theta + v_t \tag{4.14}$$

and in matrix form for M sets of process input-output data

$$Y = \Phi\theta + V \tag{4.15}$$

where $Y^T = [y_0 \;\; y_1 \;\; \ldots \;\; y_{M-1}]$, $V^T = [v_0 \;\; v_1 \;\; \ldots \;\; v_{M-1}]$ and

$$\Phi = \begin{bmatrix} f_0^0 & f_0^1 & f_0^{-1} & \cdots & f_0^{-\frac{n-1}{2}} \\ f_1^0 & f_1^1 & f_1^{-1} & \cdots & f_1^{-\frac{n-1}{2}} \\ \vdots & & & & \\ f_{M-1}^0 & f_{M-1}^1 & f_{M-1}^{-1} & \cdots & f_{M-1}^{-\frac{n-1}{2}} \end{bmatrix}$$

The least squares estimate of θ in Equation (4.15) is given by

$$\hat{\theta} = (\Phi^*\Phi)^{-1}\Phi^*Y \tag{4.16}$$

where (*) denotes the complex conjugate transpose, which minimizes the sum of squared prediction errors

$$E = (Y - \Phi\theta)^T(Y - \Phi\theta) \tag{4.17}$$

4.3.2 Confidence Bounds

Confidence bounds for the FSF model-based estimate in both the frequency and time domains are discussed in Cluett et al. (1996). In this thesis, the identification results are presented using the unit step response. Therefore, the derivation of the confidence bounds for the process step response estimate is presented here. The basic idea is to first represent the step response coefficients as a linear transformation of the estimated FSF parameters and then map the covariance matrix from the frequency domain to the time domain. Some assumptions are required to guaranteed that $\hat{\theta}$ is an unbiased and normally distributed estimate of θ.

(A1) The process has finite settling time T_s and the parameter N is chosen to be greater than or equal to $\frac{T_s}{\Delta t}$.

(A2) The disturbance is a zero mean, white and normally distributed random sequence.

(A3) $n = N$. For the truncated FSF model with $n < N$, Wang and Cluett (1996b) and Patel et al. (1996) state that the use of PRESS as a criterion in model structure selection attempts to ensure that the bias in the model due to unmodelled dynamics is small relative to the variance error caused by the presence of noise in the measured process output.

Let the estimated step response be represented by

$$\hat{g}_m = S(m)\hat{\theta} \tag{4.18}$$

where $S(m) = [s_0(m) \;\; s_1(m) \;\; \ldots \;\; s_{\frac{N-1}{2}}(m)]$ with $s_k(m)$ defined by

$$s_k(m) = \frac{1}{N}\frac{1 - e^{j\frac{2\pi k}{N}(m+1)}}{1 - e^{j\frac{2\pi k}{N}}} \tag{4.19}$$

Under assumption A1, the true process step response can be represented by

$$g_m = S(m)\theta \tag{4.20}$$

We need to calculate the variance of the estimated step response coefficients to obtain a confidence bound for the estimate. The variances are given by

$$\begin{aligned} E[(\hat{g}_m - g_m)^2] &= E[S(m)(\hat{\theta} - \theta)(\hat{\theta} - \theta)^* S(m)^*] \\ &= S(m)(\Phi^*\Phi)^{-1} S(m)^* \sigma^2 \\ &= \delta(m)^2 \end{aligned} \tag{4.21}$$

Then, the error between the true process step response weight g_m and the estimated step response weight $\hat{g}_m$ is bounded by

$$|\hat{g}_m - g_m| \leq \rho \times \delta(m) \tag{4.22}$$

with probability $P(\rho)$, i.e. the trajectory of the true step response g_m for $m = 0, 1, ..., N-1$ lies inside the envelope generated by $\hat{g}_m \pm \delta(m)$ with probability $P(\rho)$. $P(1) = 0.683$, $P(2) = 0.954$ and $P(3) = 0.997$ according to the specified level of the normal distribution.

4.3.3 The PRESS Statistic

Definition 1 PRESS residuals: The PRESS residuals, $e_{t,-t}$ are also called the true prediction errors. They are defined as

$$\begin{aligned} e_{t,-t} &= y_t - \phi_t^T \hat{\theta}_{-t} \\ &= y_t - \hat{y}_{t,-t} \end{aligned} \tag{4.23}$$

where $\hat{\theta}_{-t}$ is the estimate obtained using the least squares algorithm without including ϕ_t and y_t. This definition ensures that y_t and $\hat{y}_{t,-t}$ are independent. Therefore $e_{t,-t}$ represents the true prediction error.

Definition 2 PRESS: The PREdiction Sum of Squares is defined as

$$PRESS = \sum_{t=1}^{M} e_{t,-t}^2 \tag{4.24}$$

which provides a measure of the predictive capability of the estimated model. For model structure selection, the value of n which corresponds to the smallest PRESS is adopted.

Using an orthogonal decomposition algorithm, the PRESS residuals $e_{t,-t}$, where $t = 1, 2, ..., M$, defined in Equation (4.23) can easily be calculated (Wang and Cluett, 1996b).

An important feature of the PRESS is that it does not always decrease as more terms are added to the model. If the PRESS increases when a term is added to the model, this indicates that the predictive capability of the model is better without that term. On the other hand, the sum of squares of the conventional residuals always decreases as more terms are added.

4.4 GLS Algorithm and the Development

Chapters 2 and 3 showed that an accurate estimate of the noise model is required for the design of a data prefilter in order to remove the effect of any feedback on the process step response estimate. In addition, one of the conditions needed to evaluate the confidence bounds is that the disturbance be a zero mean, white and normally distributed sequence. The generalized least squares algorithm (GLS) described in Goodwin and Payne (1977) provides an approach for iteratively determining estimates of the process and noise models in such a way that an appropriate prefilter is constructed and the "disturbance" associated with the prefiltered system is close to "white". In this section, the standard GLS algorithm is reviewed and then the modified GLS algorithm proposed in this thesis is presented.

Consider the process description given by

$$y_t = G(z)u_t + v_t \tag{4.25}$$

where the disturbance term v_t is assumed to be represented by

$$v_t = H(z)a_t \tag{4.26}$$

where $H(z)$ is the noise model and a_t is a zero mean, white noise sequence.

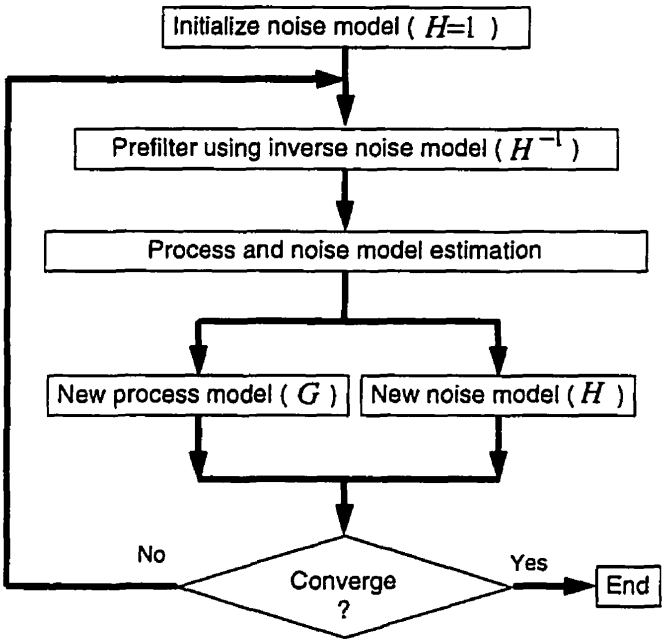

Figure 4.2: Conceptual block diagram of GLS

The original GLS algorithm consists of the following steps (see Fig. 4.2):

(i) Set $\hat{H}(z) = 1$

(ii) Form $y_{f,t} = \hat{H}(z)^{-1} y_t$ and $u_{f,t} = \hat{H}(z)^{-1} u_t$

(iii) Obtain the least squares estimate $\hat{G}$ using $y_{f,t}$ and $u_{f,t}$

(iv) Construct an estimate of the disturbance term, $\hat{v}_t = y_t - \hat{G} u_t$

(v) Obtain $\hat{H}(z)$ from $\hat{v}_t$

(vi) If $\hat{G}$ has converged, stop; otherwise, go to (ii)

Note that the structures of both process and noise models ($G(z)$ and $H(z)$) must be selected before applying this method. The modified GLS algorithm proposed in this thesis will include the model structure selection procedures inside the iteration loop, so that the parameters and orders of the process and noise models are identified simultaneously.

In the proposed GLS algorithm, the FSF model is used to represent the process ($G(z)$) due to its many advantages. Based on the estimated FSF model parameters, the

process step response model is estimated and presented as the final process identification results. In addition, an important assumption in the proposed algorithm is that the noise model ($H(z)$) can be described by an autoregressive type model (AR). Based on Chapter 3, we know that the AR terms are the most important in terms of the design of the prefilter. This assumption on the type of noise model ensures that the most important noise model terms will be identified. Clark (1967) used the same assumption on the noise model type in his application of the original GLS algorithm. The noise model is given by

$$v_t = \frac{1}{F(z)} a_t \tag{4.27}$$

where $F(z) = 1 + f_1 z^{-1} + ... + f_{n_f} z^{-n_f}$ and a_t is assumed to be a zero mean, white noise sequence. Therefore, we have

$$(1 + f_1 z^{-1} + ... + f_{n_f} z^{-n_f}) v_t = a_t$$

$$v_t = -f_1 v_{t-1} - ... - f_{n_f} v_{t-n_f} + a_t \tag{4.28}$$

Here, the issue of the selection of a proper noise model structure becomes a decision on the best choice for n_f.

A unique feature of the proposed GLS is the use of the PRESS statistic as a criterion for both process and noise model structure selection in steps (iii) and (v). The modified steps (iii)-(v) are illustrated in Figure 4.3. To begin the algorithm, we need to provide N based on an estimate of the process settling time, the maximum FSF process model order (n), and the maximum AR noise model order (n_f). We then choose the process model order which corresponds to the minimum PRESS as the best FSF process model order and use the LS method to estimate the process model parameters. Based on the residuals the noise model order which corresponds to the minimum PRESS is chosen as the best AR noise model order and the LS method is used to estimate the noise model parameters.

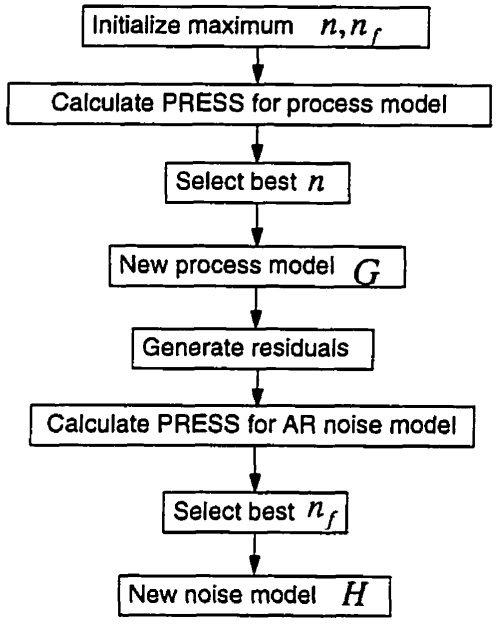

Figure 4.3: Process and noise model estimation

4.5 Simulation Examples

In this section, two simulation examples are used to assess the convergence of the proposed GLS algorithm. In the simulations, we will use two different noise models. In the first simulation, the noise model can be exactly represented by an AR structure and in the second simulation the noise model is taken to be a more complicated structure.

Simulation Example 4.5.1

In this simulation example, the true system is given by

$$y_t = \frac{0.8e^{-45s}}{3600s^2 + 120s + 1}u_t + v_t \tag{4.29}$$

The simulation duration is 2040 seconds. The sampling interval is chosen to be 3 seconds. The input signal is specified to be a random binary signal with a magnitude of ± 5 units and a minimum switching time of 120 seconds.

The noise sequence v_t is generated by passing a zero mean, white noise sequence

a_t with variance of 0.0138 filtered by the true noise model $H_0(z)$ given by

$$H_0(z) = \frac{1}{1 - z^{-1}} \tag{4.30}$$

To apply the GLS method to the process input-output data generated from this simulation experiment, we selected the maximum process FSF model order, n, to be 27 and the maximum AR noise model order, n_f, to be 14. N is estimated to be 170 sampling intervals. The number of iterations performed by the algorithm was set to 6, i.e. no convergence stopping criterion was used. The results are shown in Figures 4.4 to 4.7. Figure 4.4 shows the PRESS corresponding to different FSF process model orders from 1 up to 27. The figure shows that the PRESS picks 23 as the best process model order in the first iteration and 7 as the best process model order in the last iteration. Actually, the results in the last 3 iterations are almost the same as those in the 3rd

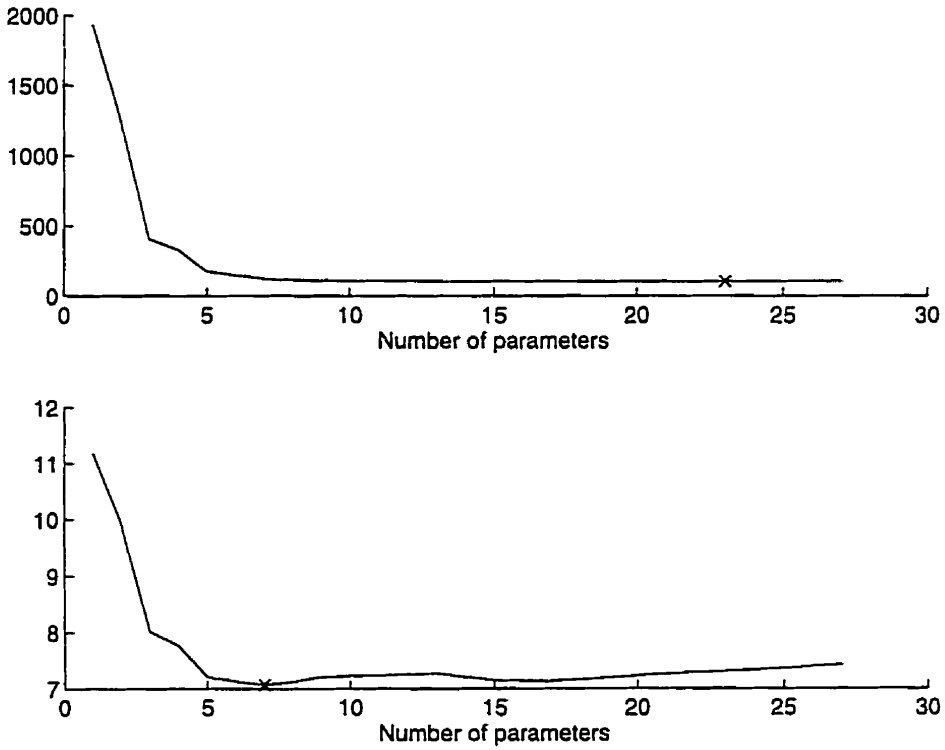

Figure 4.4: Example 4.5.1: Behaviour of PRESS for process model structure selection in first iteration (top) and last iteration (bottom) ('x' denotes the number of parameters corresponding to the minimum PRESS)

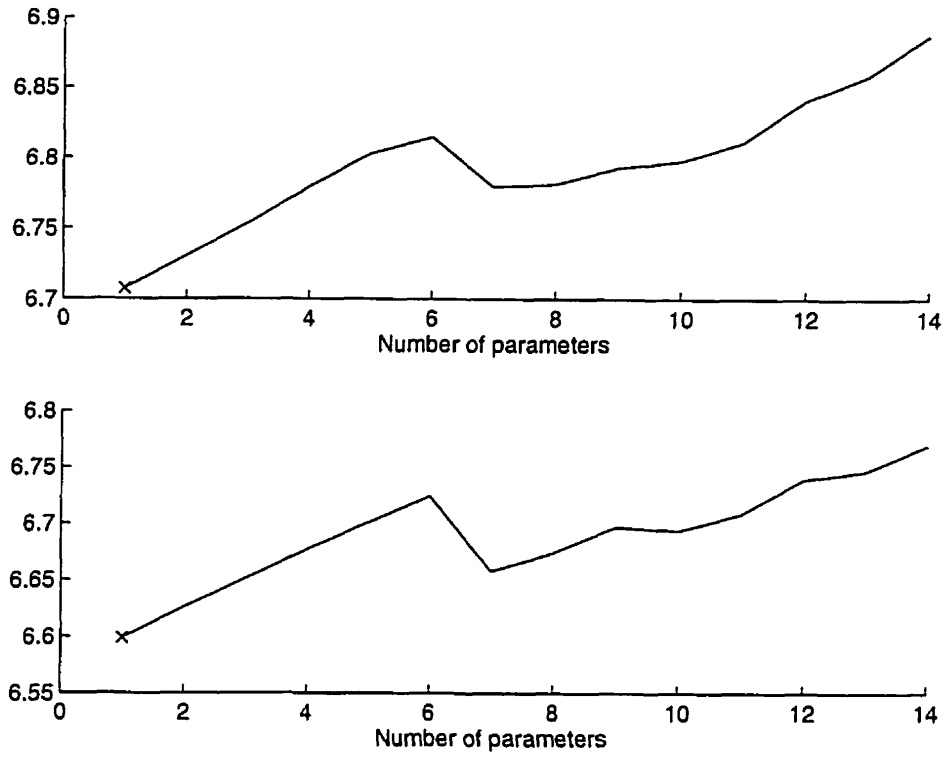

Figure 4.5: Example 4.5.1: Behaviour of PRESS for noise model structure selection in first iteration (top) and last iteration(bottom) ('x' denotes the number of parameters corresponding to the minimum PRESS)

iteration, i.e., the results converged in 3 iterations. Figure 4.5 shows the behaviour of the PRESS corresponding to AR noise model orders from 1 up to 14. The figure shows that PRESS picks 1 as the best noise model order in the first iteration and the same order is chosen in the last iteration. The result exactly matches the order of the true noise model used in the simulation. The noise model in the last iteration is given by: $\hat{F}(z) = 1.000 - 0.984z^{-1}$, which is very close to the true noise model. The process step response estimate obtained in the last iteration is shown in Figure 4.6 along with its 99% confidence bounds.

To check whether the prefilter designed from the estimated noise model produces white residuals, autocorrelation (ACF) analysis is carried out on the initial residuals obtained after step (iv) of the first iteration ($y_t - \hat{G}u_t$) and on the final residuals

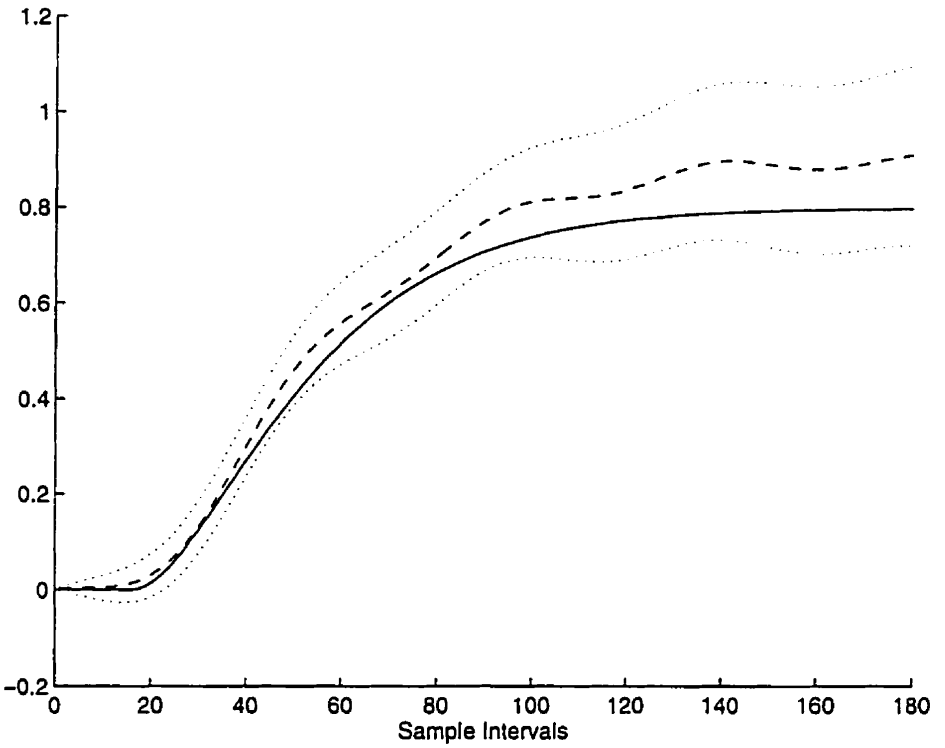

Figure 4.6: Example 4.5.1: Process unit step response (Solid: true step response; Dashed: estimated step response; Dotted: 99 % confidence bounds)

obtained after step (v) of the last iteration ($\hat{a}_t = \frac{1}{H}\hat{v}_t$). The results are shown in Figure 4.7. Graph (2) in the figure shows that the ACF is well inside the 2σ confidence bounds after the first lag, and thus the final residuals have the same characteristics as white noise. For comparison, the ACF of the initial residuals is shown in graph (1). These results in Figures 4.4 to 4.7 confirm that the proposed GLS provides an unbiased estimate of the process step response while constructing an accurate noise model.

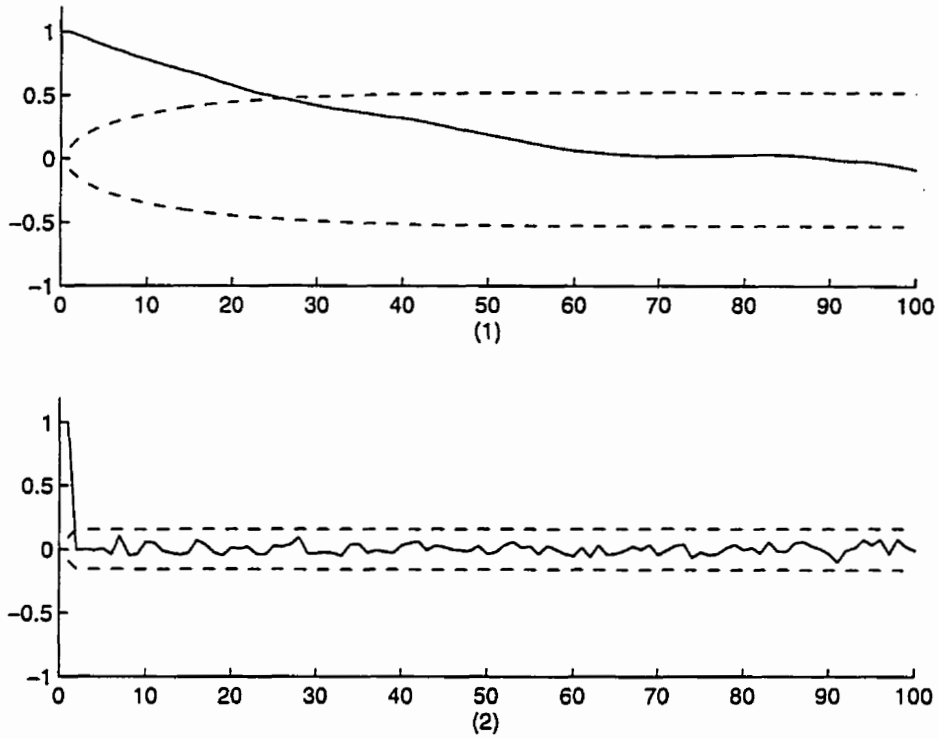

Figure 4.7: Example 4.5.1: ACF of residuals with 2σ confidence bounds: (1) first iteration; (2) last iteration

Simulation Example 4.5.2

This example is the same as example 4.5.1 except that the disturbance model is now given by

$$H_0(z) = \frac{1 - 0.8z^{-1}}{(1 - z^{-1})(1 - 0.5z^{-1})} \tag{4.31}$$

As in example 4.5.1, N is estimated to be 170 sampling intervals. The maximum FSF process model order, n, has been initialized to be 27 and the maximum AR noise model order, n_f, has been initialized to be 14. The number of iterations preformed by the algorithm was set to 6. The estimation results are shown in Figures 4.8 to 4.11. Figure 4.8 shows the PRESS corresponding to different FSF process model orders from 1 up to 27. The figure shows that the PRESS picks 21 as the best process model order in the first iteration and 17 as the best process model order in the last iteration. In

fact, the results converged in 3 iterations. Figure 4.9 shows the behaviour of the PRESS corresponding to AR noise model orders from 1 up to 14. The figure shows that the PRESS picks 9 as the best noise model order in the first iteration and the same order is chosen at the last iteration. The noise model estimated in the last iteration is given by $\hat{F}(z) = 1.000 + 0.6551z^{-1} + 0.0516z^{-2} + 0.0242z^{-3} + 0.0502z^{-4} - 0.0106z^{-5} + 0.1587z^{-6} - 0.0801z^{-7} + 0.0121z^{-8} + 0.1111z^{-9}$ The process step response estimate obtained in the last iteration is shown in Figure 4.10 along with the 99% confidence bounds.

As in example 4.5.1, we also check whether the prefilter designed from the estimated noise model produces white residuals using autocorrelation (ACF) analysis on the initial residuals obtained after step (iv) of the first iteration ($y_t - \hat{G}u_t$) and on the final residuals obtained after step (v) of the last iteration ($\hat{a}_t = \frac{1}{\hat{H}}\hat{v}_t$). The results are

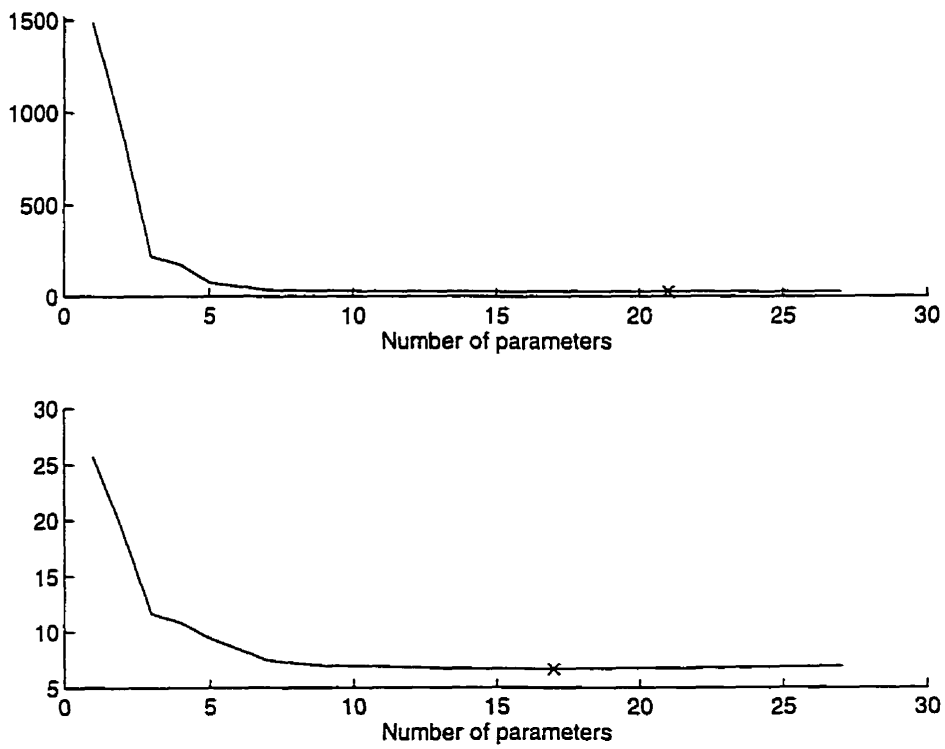

Figure 4.8: Example 4.5.2: Behaviour of PRESS for process model structure selection in first iteration (top) and last iteration (bottom) ('x' denotes the number of parameters corresponds to the minimum PRESS)

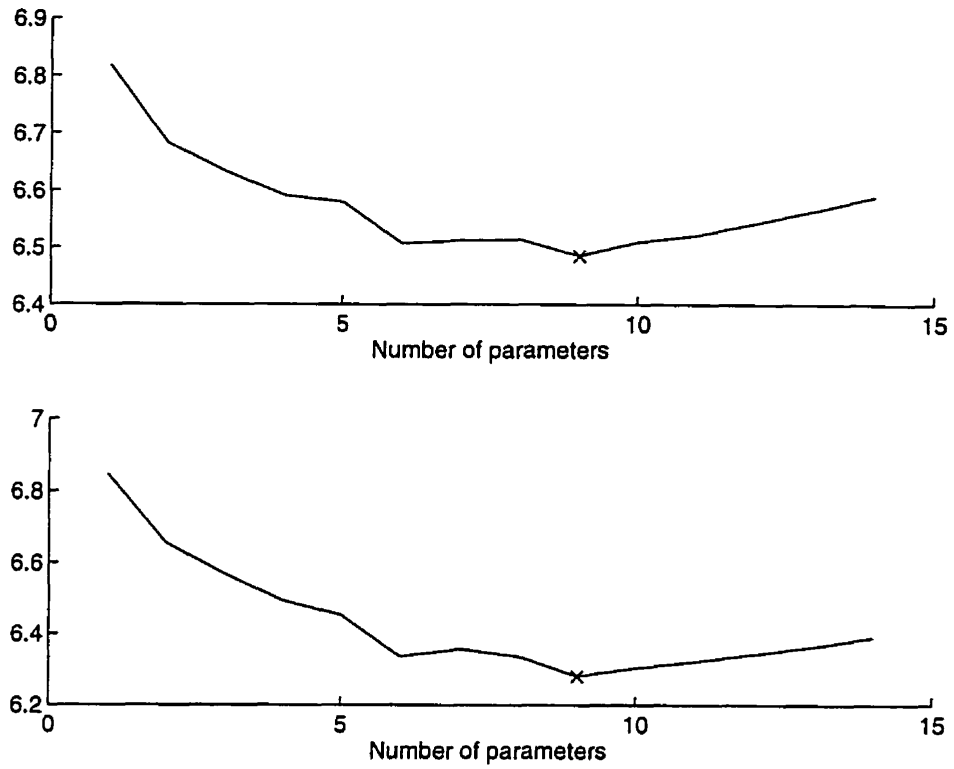

Figure 4.9: Example 4.5.2: Behaviour of PRESS for noise model structure selection in first iteration (top) and last iteration(bottom) ('x' denotes the number of parameters corresponds to the minimum PRESS)

shown in Figure 4.11. Graph (2) in this figure shows that the ACF is well inside the 2σ confidence bounds after the first lag, and thus the final residuals have the same characteristics as white noise. For comparison, the ACF of the initial residuals is shown in graph (1). The results of this simulation example again confirm that the proposed GLS provides an unbiased estimate of the process step response while constructing an accurate noise model.

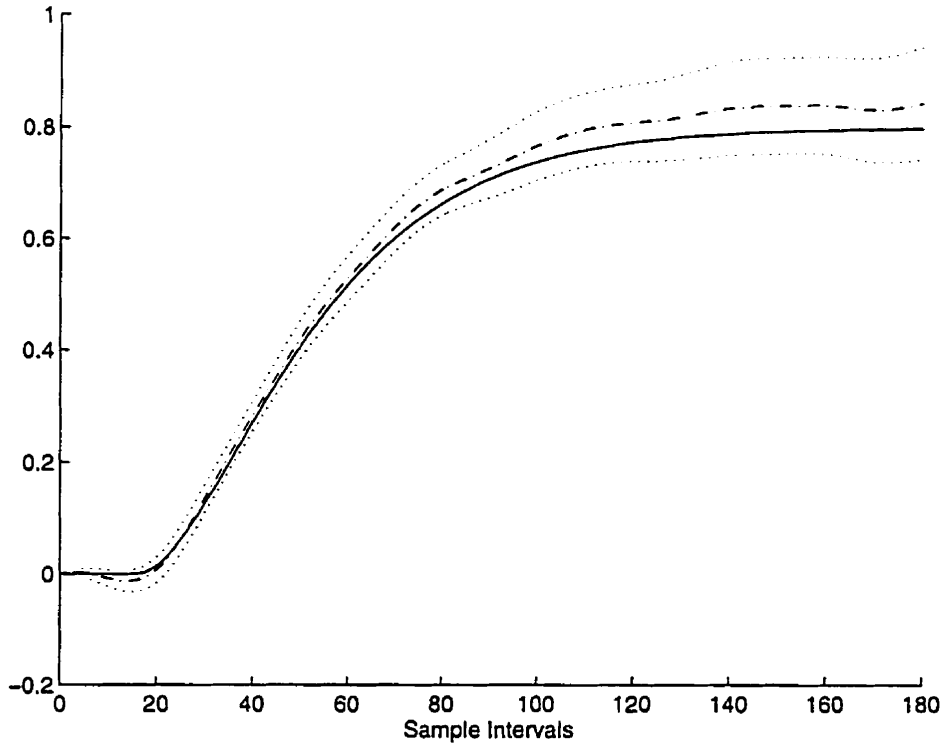

Figure 4.10: Example 4.5.2: Process step responses (Solid: true step response; Dashdot: estimated step response; Dotted: 99 % confidence bounds)

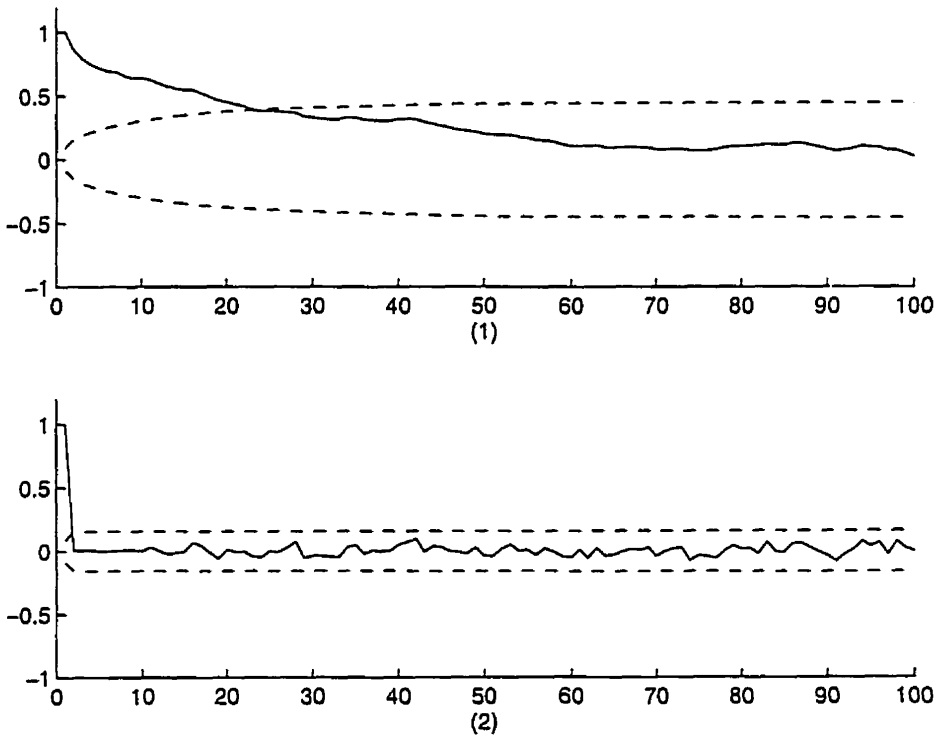

Figure 4.11: Example 2: ACF of residuals with 2σ confidence bound: (1) first iteration; (2) last iteration

4.6 Application to an Industrial Data Set

The proposed improved GLS algorithm is further investigated by applying it to an industrial data set obtained from an alkylation unit at Imperial Oil's Nanticoke refinery. The data set is a subset of a larger data set and consists of three input ($[u_1 \quad u_2 \quad u_3]$) and two output ($[y_1 \quad y_2]$) variables. For the purposes of this thesis, the system can be represented using by a simple block diagram (See Figure 4.12).

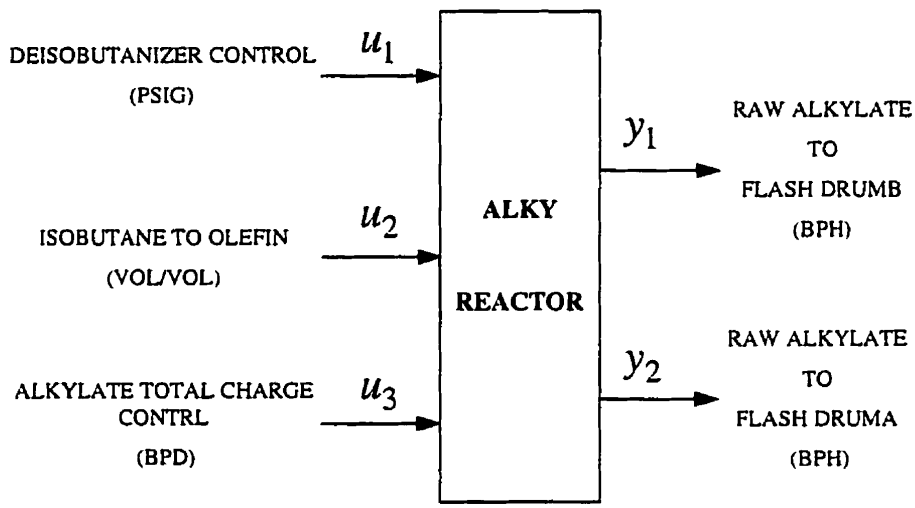

Figure 4.12: Block diagram for the industrial process

The input-output data, plotted in Appendix A, was provided in four segments. The data was recorded at one minute intervals and the settling time (N) for each input-output subprocess was estimated to be 60. For a multivariable system, we prefer to

treat the process as two 3-input, single output identification problems. The identification algorithm described in this thesis has been extended to multi-input, single-output (MISO) systems in Patel et.al. (1996). This MISO algorithm was applied to the data set. We set up a criterion for checking the convergence of the process model parameters. If the sum of the squared differences between parameter estimates in two consecutive iterations is less than 0.001, the algorithm stops. In this particular application, the algorithm stopped after 3 iterations. The final results are shown in Figure 4.13 to 4.19. The FSF-based process model orders are found to be [9 5 1] and [5 5 1] for y_1 and y_2, respectively. The final values of the PRESS associated with each output variable are shown in Figure 4.13. The final noise models are given by:

$$\begin{aligned}\hat{F}_1(z) &= 1.000 + 0.5204z^{-1} + 0.3235z^{-2} + 0.2164z^{-3} + 0.0901z^{-4} \\ &- 0.0214z^{-5} - 0.0964z^{-6} \end{aligned} \tag{4.32}$$

$$\begin{aligned}\hat{F}_2(z) &= 1.000 + 0.6551z^{-1} + 0.0516z^{-2} + 0.0242z^{-3} + 0.0502z^{-4} \\ &- 0.0106z^{-5} + 0.1587z^{-6} - 0.0801z^{-7} + 0.0121z^{-8} + 0.1111z^{-9} \end{aligned} \tag{4.33}$$

where $\hat{F}_1$ and $\hat{F}_2$ are the noise models associated with y_1 and y_2, respectively.

4.6.1 Discussion of results

We compared the process step responses estimated by the aforementioned algorithm with those estimated by the following approaches:

(I) Estimate of FSF model using the same order found by using the proposed GLS algorithm, but without noise model estimation.

(II) Estimate of full order FSF model without any noise model estimation.

(III) Estimate of full order FSF model with noise model estimation.

These estimates are also shown in Figures (4.14) to (4.19). Note that full order FSF model estimates are equivalent to the FIR model estimates. Based on these results, we can make the following observations.

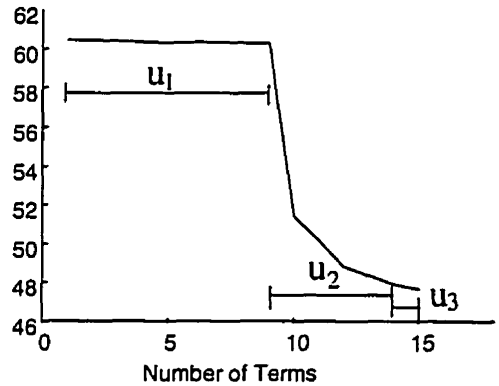

(a) PRESS for process output y_1

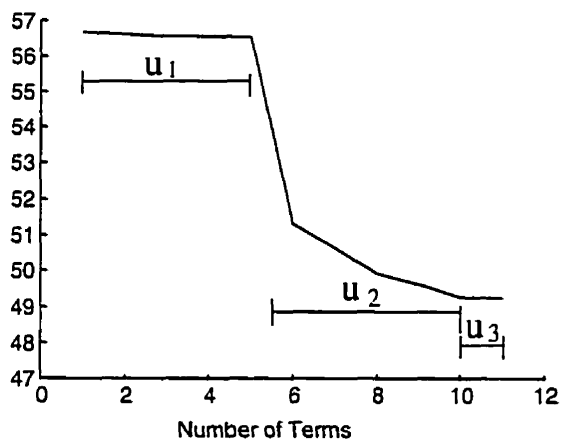

(b) PRESS for process output y_2

Figure 4.13: PRESS for process FSF model-based MISO system structure selection

1. Comparison of estimation results between filtered and unfiltered data

From Figures 4.14, 4.16, 4.17 and 4.19, we can see differences between the step response models obtained from filtered and unfiltered data corresponding to the pairs u_1 and y_1, u_3 and y_1, u_1 and y_2 and u_3 and y_2. This might indicate that there are feedback connections within these data pairs. However, by examining Figures 4.15 and 4.18, there

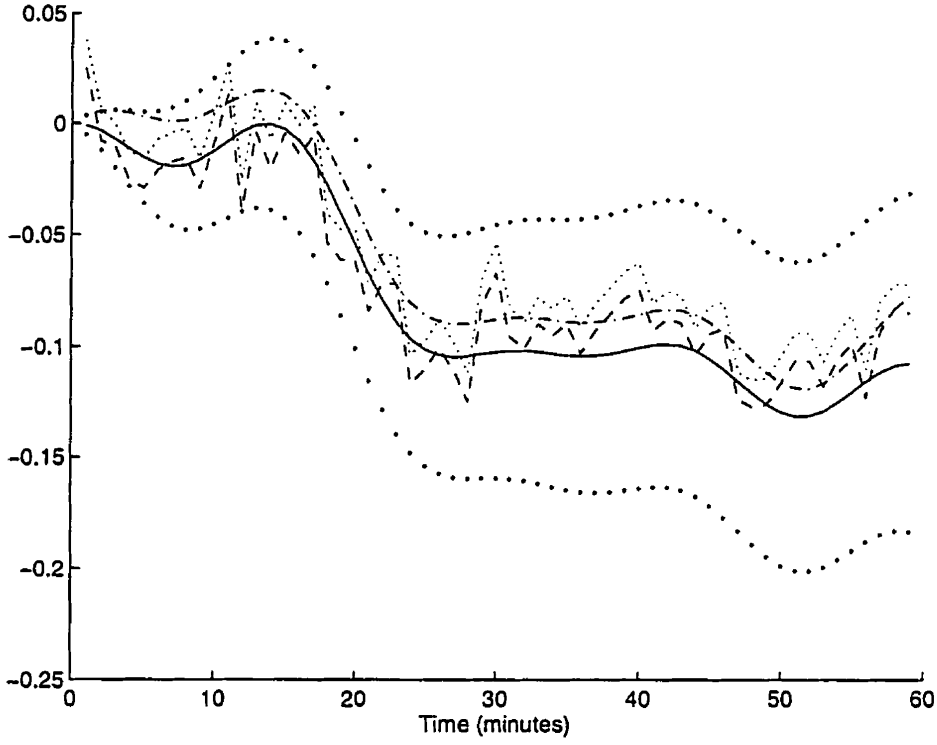

Figure 4.14: Step response models relating u_1 to y_1 (Solid: FSF model with optimized order and noise modelling; Large dots: 99 % confidence bounds; Dashdot: FSF model with optimized order but without noise modelling; Dotted: full order FSF model without noise modelling; Dashed: full order FSF with noise modelling)

is little difference between the various step response models corresponding to the pairs u_2 and y_1, and u_2 and y_2. This could indicate that the process input u_2 is not dependent on the process outputs y_1 and y_2 through any feedback connections.

2. Comparison of the noise models obtained from the FIR and FSF model structures

By approach (III), the noise models are given by:

$$\hat{F}_1'(z) = 1.0000 + 0.4958z^{-1} + 0.2918z^{-2} + 0.1607z^{-3} \tag{4.34}$$

$$\begin{aligned} \hat{F}_2'(z) &= 1.0000 + 0.4150z^{-1} + 0.2353z^{-2} + 0.0896z^{-3} - 0.0481z^{-4} \\ &- 0.1805z^{-5} - 0.1966z^{-6} - 0.1359z^{-7} - 0.1168z^{-8} \end{aligned} \tag{4.35}$$

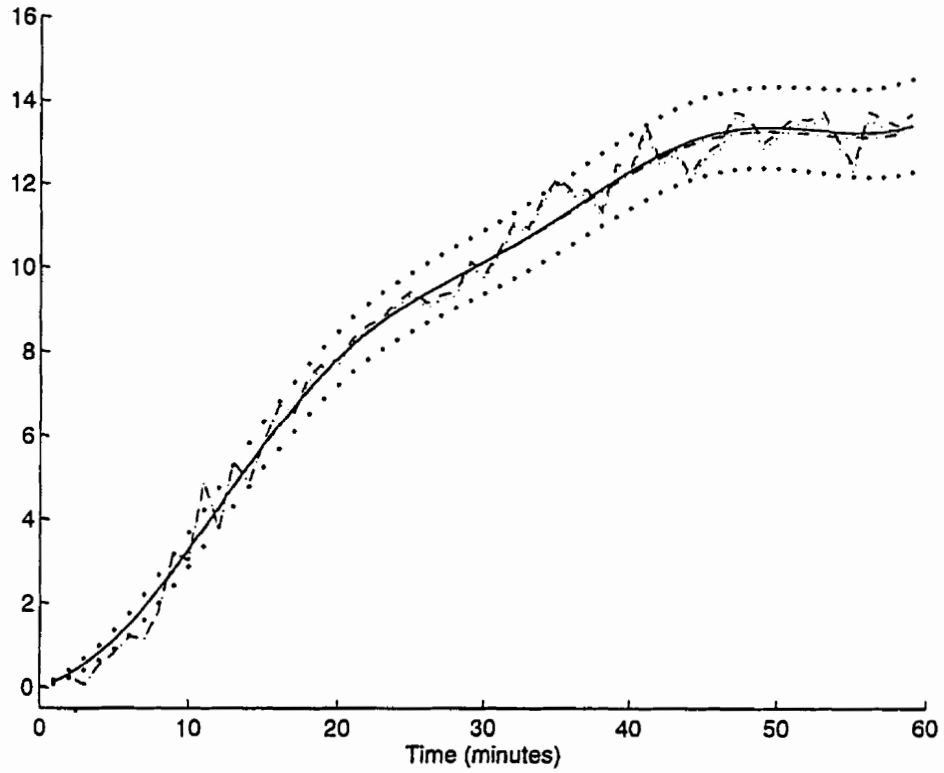

Figure 4.15: Step response models relating u_2 to y_1 (Solid: FSF model with optimized order and noise modelling; Large dots: 99 % confidence bounds; Dashdot: FSF model with optimized order but without noise modelling; Dotted: full order FSF model without noise modelling; Dashed: full order FSF with noise modelling)

The residuals for outputs y_1 and y_2 from the estimated models are not white noise sequences, which is evident from the estimated noise models given by Equations (4.32) and (4.33) for the FSF model and Equations (4.34) and (4.35) for the FIR model. The discrepancy between the two sets of noise models can be explained by the fact that the reduced order FSF models are approximations of the FIR models and therefore the neglected high frequency dynamics of the process in the FSF model are included in the noise models associated with Equation (4.32) and (4.33).

3. Comparison of the smoothness between the FSF and FIR model estimates

From Figures 4.14 to 4.19, we can see that the estimated step response models using the FSF model structure are much smoother than the estimated ones using the

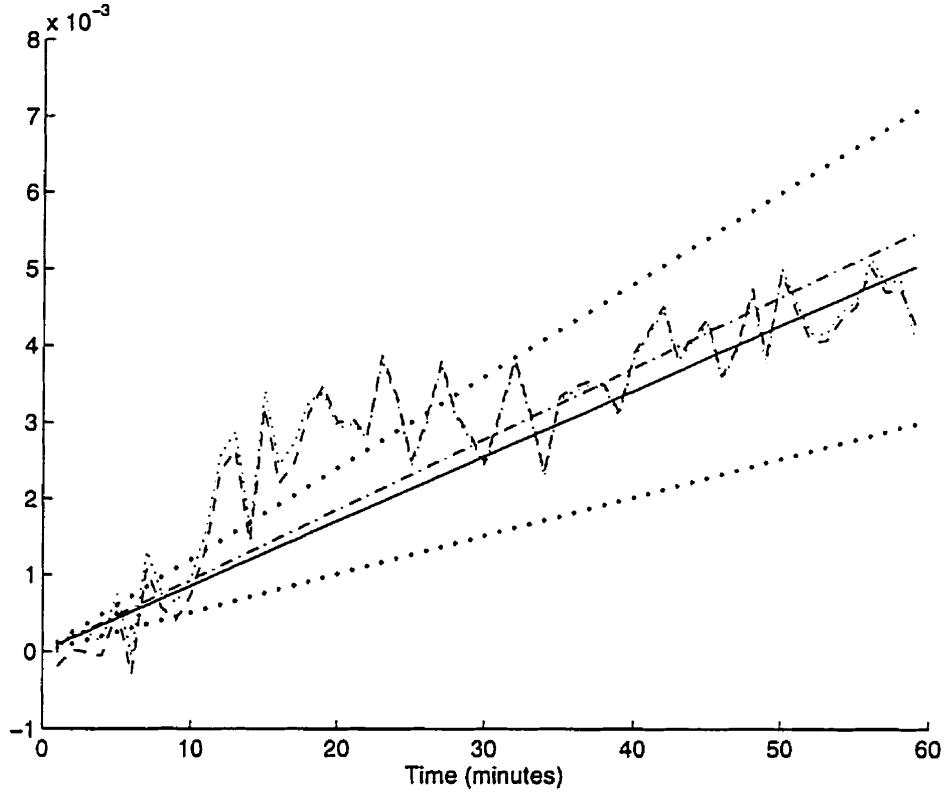

Figure 4.16: Step response models relating u_3 to y_1 (Solid: FSF model with optimized order and noise modelling; Large dots: 99 % confidence bounds; Dashdot: FSF model with optimized order but without noise modelling; Dotted: full order FSF model without noise modelling; Dashed: full order FSF with noise modelling)

FIR model structure. This is because the reduced order FSF model neglected the high frequency dynamics of the process. In contrast, the FIR model estimates the parameters in the high frequency region of the process where we typically face a lower signal to noise ratio resulting in larger variances of the estimated parameters. Large variances on the high frequency estimates are reflected by the lack of smoothness of the step response models. Note that the lower signal to noise ratio in the high frequency region is caused by the infrequent moves made in the process input signals (see Appendix A).

4. Comparison between the estimation results of extremely low order FSF model and FIR model

Figure 4.16 and 4.19 show the estimation results obtained from the FIR model

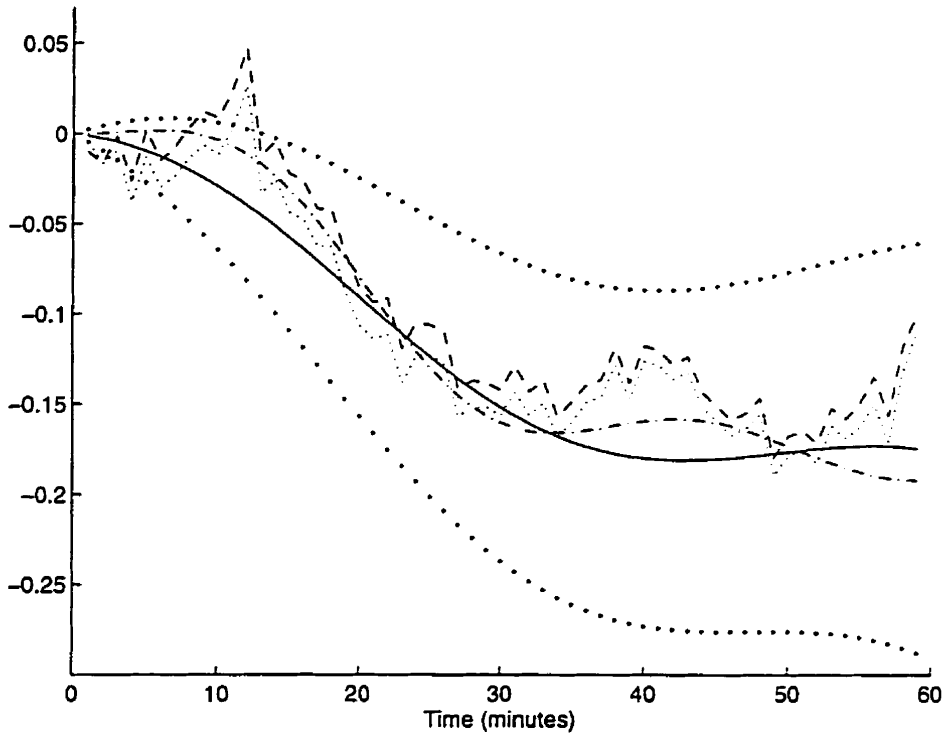

Figure 4.17: Step response models relating u_1 to y_2 (Solid: FSF model with optimized order and noise modelling; Large dots: 99 % confidence bounds; Dashdot: FSF model with optimized order but without noise modelling; Dotted: full order FSF model without noise modelling; Dashed: full order FSF with noise modelling)

and the FSF model with order of 1, which was chosen to be the best order by the PRESS. The reasons for such extremely low FSF model orders needs some further investigation. This result may be caused by the presence of only pure gain relationships between these input-output pairs. If this is the case, the PRESS has chosen the correct model order. However, this result may also be caused by a lack of sufficient excitation in the input signal (u_3). If this is the case, then increasing the frequency content and the magnitude of the movement in the input signal u_3 would increase the FSF model order and provide more accurate step response estimates.

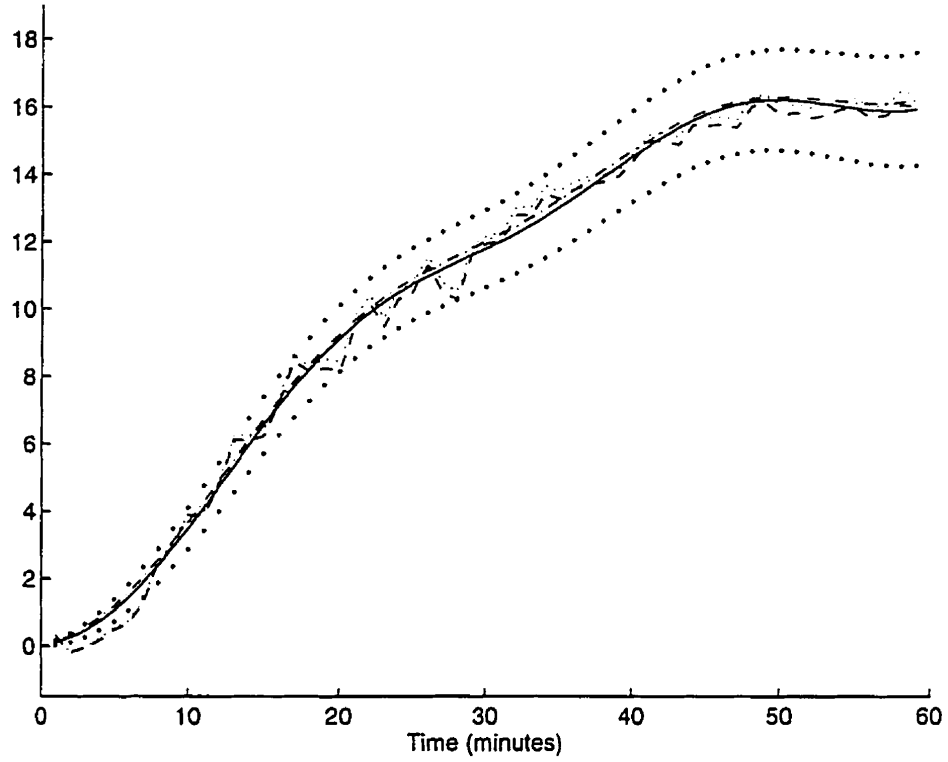

Figure 4.18: Step response models relating u_2 to y_2 (Solid: FSF model with optimized order and noise modelling; Large dots: 99 % confidence bounds; Dashdot: FSF model with optimized order but without noise modelling; Dotted: full order FSF model without noise modelling; Dashed: full order FSF with noise modelling)

4.7 Concluding Remarks

A generalized least squares algorithm (GLS) has been developed in this chapter for simultaneous identification of both the process and noise models. Convergence of the algorithm was illustrated through simulation examples. The proposed procedure was also applied to an industrial data set. The benefits of this algorithm are:

1. Simultaneous estimation of the process and noise models ensures that the biasing effect of any feedback in the data on the process identification results is removed.

2. The proposed algorithm is able to drive the residuals to behave like white noise so that statistical confidence bounds can be computed.

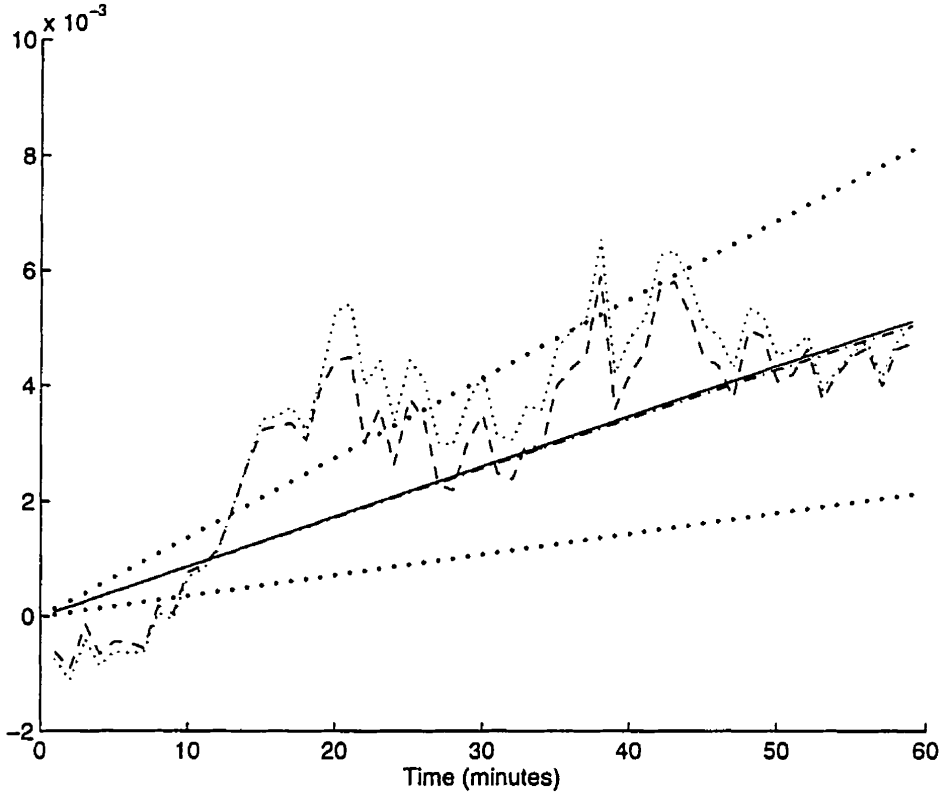

Figure 4.19: Step response models relating u_3 to y_2 (Solid: FSF model with optimized order and noise modelling; Large dots: 99 % confidence bounds; Dashdot: FSF model with optimized order but without noise modelling; Dotted: full order FSF model without noise modelling; Dashed: full order FSF with noise modelling)

3. The use of the PRESS criterion for selection of both the FSF process model order and the AR noise model order makes the proposed algorithm an efficient approach to identify multivariable processes.

Chapter 5

Conclusions

In this thesis, issues in closed-loop system identification are revisited, where the feedback is introduced by operator intervention. Here, "open-loop" refers to the situation where a predetermined input signal is applied to the process without any concern about whether the process output moves outside the desired operating region. "Closed-loop" refers to the situation when the process input is a combination of a predetermined sequence plus additional moves made intermittently by an operator to bring the process output back within some desired region. The thesis consists of three main parts:

- The role of operator intervention in process identification
- Design of the data prefilter using noise model information
- Development of an algorithm for simultaneous identification of process and noise models

5.1 The Role of Operator Intervention in Process Identification

When identifying a process model using data containing feedback due to operator intervention under a delayed intervention strategy (where there exists one sampling interval of delay between when the unacceptable process output deviation occurs and when the operator adjusts the process input), the LS estimate of an FIR model is unbiased after

prefiltering the process data using the correct noise model, regardless of whether the unit delay is included in the model. The estimates of low order transfer function models have similar distribution properties, the only difference being that the lower order model estimates are smoother. This result indicates that with proper data prefiltering, there is certainly no need to discard data which contains feedback. Because operator intervention can improve the overall signal-to-noise ratio, data containing feedback may actually result in better models, particularly with respect to estimation of the steady-state gains.

With an immediate intervention strategy (where the operator adjusts the process input at the same sampling instant that the unacceptable process output deviation occurs), both the LS estimate of the FIR model and the estimate of a lower order transfer function model using an OE model remain unbiased provided the unit delay has been included in the model and the data have been prefiltered using the correct noise model. If the unit delay is not included, then both the LS estimate of the FIR model and the estimate of a low order transfer function model are biased. These are in fact the conditions under which correlation between the process input and the disturbance cause identifiability problems for both parametric and non-parametric models.

5.2 The Design of the Prefilter

The conclusions with respect to the design of the prefilters are:

1. It is extremely important to filter the process data prior to parameter estimation when using data that contains feedback. The design of the prefilter must be based on an accurate estimate of the true noise model.

2. In general, structural mismatch between the true noise model and the user-selected prefilter causes problems in process model estimation to a certain degree. In a relative sense, AR-type mismatch affects the accuracy of the estimated model more than MA-type mismatch. Furthermore, even when the assumed noise model structure exactly matches the true noise model structure, small errors in the parameters themselves can also lead to estimation problems.

5.3 Simultaneous Identification of Process and Noise Models

An algorithm developed using a GLS approach has been presented to simultaneously identify process and noise models. The unique features of the algorithm are the combined application of the FSF model for process model identification, and the PRESS statistic for both process and noise model structure selection. The proposed algorithm has the ability to remove the effect of any feedback on the process model estimate as well as producing "white" residuals to allow for the development of statistical confidence bounds associated with the process model. This algorithm has been successfully applied to a data set from Imperial Oil's Nanticoke refinery for estimating step response models with statistical confidence bounds.

Bibliography

Anderson, B. D. O. and Gevers, M. R. (1982), 'Identifiability of linear stochastic systems operating under linear feedback', *Automatica* **Vol. 18**(No. 2), pp. 195–213.

Box, G. and Jenkins, G. (1976), *Time Series Analysis: Forecasting and Control*, Holden-Day Inc.

Chen, C.-W., Huang, J.-K., Phan, M. and Juang, J.-N. (1992), 'Integrated system identification and state estimation for control of flexible space structures', *Journal of Guidance, Control, and Dynamics* **Vol. 15**(No. 1), pp. 88–95.

Clarke, D. W. (1967), 'Generalized least-squares estimation of the parameters of a dynamic model', *Proc. IFAC symp. Identification Auto. Control Syst.* **Paper 3.17**. Prague, Czechoslovakia.

Cluett, W. R., Wang, L. and Zivkovic, A. (1996), 'Development of quality bounds for time and frequency domain models: application to the Shell distillation column', *Journal of Process Control (*to appear) .

Cutler, C. and Yocum, F. (1991), 'Experience with the dmc inverse for identification', *Proc. Fourth International Conference on Chemical Process Control, Padre Island, Texas*, pp. 297–317.

Fang, C. and Xiao, D. (1988), *Process Identification*, Tsinghua University Press, Beijing, China.

Goberdhansingh, E., Wang, L. and Cluett, W. R. (1992), 'Robust frequency domain identification', *Chemical Engineering Science* **Vol. 47**(No. 8), pp. 1989–1999.

Goldberger, A. S. (1964), *Econometric Theory*, Wiley, New York.

Goodwin, G. C. and Payne, R. L. (1977), *Dynamic System Identification-Experiment Design and Data Analysis*, Academic Press, Inc.

Gustavsson, I., Ljung, L. and Söderström, T. (1977), 'Survey paper', *Automatica* **Vol. 13**, pp. 59–75.

Huang, B. and Shah, S. L. (1996), 'Closed-loop identification: A two-step approach', *Submitted to Journal of Process Control* .

Juang, J.-N. and Phan, M. (1994), 'Identification of system, observer, and controller from closed-loop experimental data', *Journal of Guidance, Control, and Dynamics* **Vol. 17**(No. 1), 91–96.

Juang, J.-N., Phan, M., Horta, L. G. and Longman, R. W. (1993), 'Identification of observer/kalman filter markov parameters: Theory and experiments', *Journal of Guidance, Control, and Dynamics* **Vol. 16**(No. 2), 320–329.

Ljung, L. (1987), *System Identification -Theory for the User*, Prentice-Hall, Inc.

MacGregor, J. F. and Fogal, D. T. (1995), 'Closed loop identification: The role of the noise model and prefilters', *Journal of Process Control* **Vol. 5**, pp. 163–171.

MacGregor, J. F., Kourti, T. and Kresta, J. V. (1991), 'Multivariate identification: a study of several methods', *Proc. IFAC Advanced Control of Chemical Processes, Toulouse, France* pp. 101–107.

Patel, U. J., Wang, L., Foley, M. and Cluett, W. R. (1996), 'Application of the frequency sampling filter model in process identification: An industrial case study', *Submitted to ADCHEM '97* .

Phan, M., Juang, J.-N., Horta, L. G. and Longman, R. W. (1994), 'System identification from closed-loop data with known output feedback dynamics', *Journal of Guidance, Control and Dynamics* **Vol. 17**(No.4), pp. 661–669.

Prett, D. M. and Garcia, C. E. (1988), *Fundamental Process Control*, Butterworth-Heinemann.

Ricker, N. L. (1988), 'The use of biased least squares estimators for parameters in discrete-time pulse-response models', *Ind. Eng. Chem. Res.* **Vol. 27**, 343–350.

Söderström, T. C. and Stoica, P. (1989), *System Identification*, Prentice Hall, Englewood Cliffs, New Jersey 07632.

Stoica, P., Eydhoff, P., Janssen, P. and Söderström, T. (1986), 'Model-structure selection by cross-validation', *Int. J. Control* **Vol. 43**(No.6), pp. 1841–1878.

Van Den Hof, P. M. J. and Schrama, R. J. P. (1993), 'An indirect method for transfer function estimation from closed loop data', *Automatica* **Vol. 29**(No. 6), pp. 1523–1527.

Wang, L. and Cluett, W. R. (1996a), 'Frequency sampling filters: an improved model structure for step response identification', *to appear in Automatica; Proc. 13th IFAC World Congress, San Francisco* **Vol. I**, pp. 411–416.

Wang, L. and Cluett, W. R. (1996b), 'Use of PRESS residuals in dynamic system identification', *Automatica* **Vol. 32**, pp. 781–784.

Wellstead, P. E. (1977), 'Reference signals for closed-loop identification', *Int. J. Control* **Vol. 26**(No. 6), pp. 945–962.

Appendix A

Process Data Set from Imperial Oil's Nanticoke Refinery

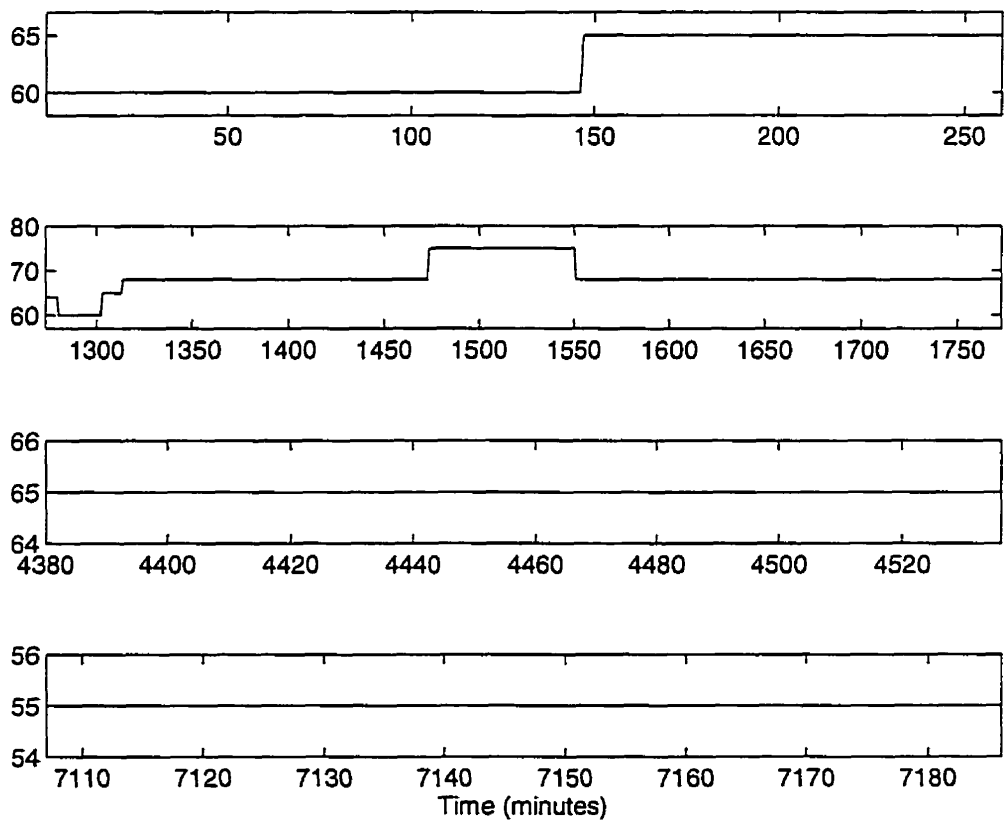

Figure A.1: Process input u_1

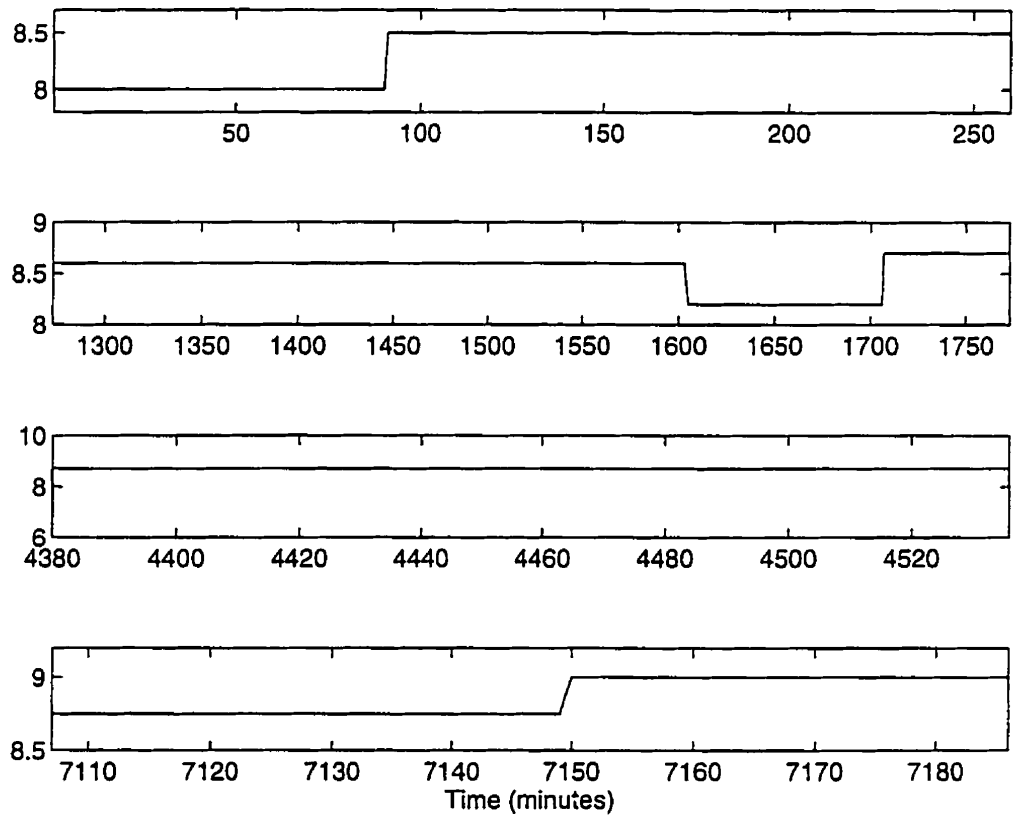

Figure A.2: Process input u_2

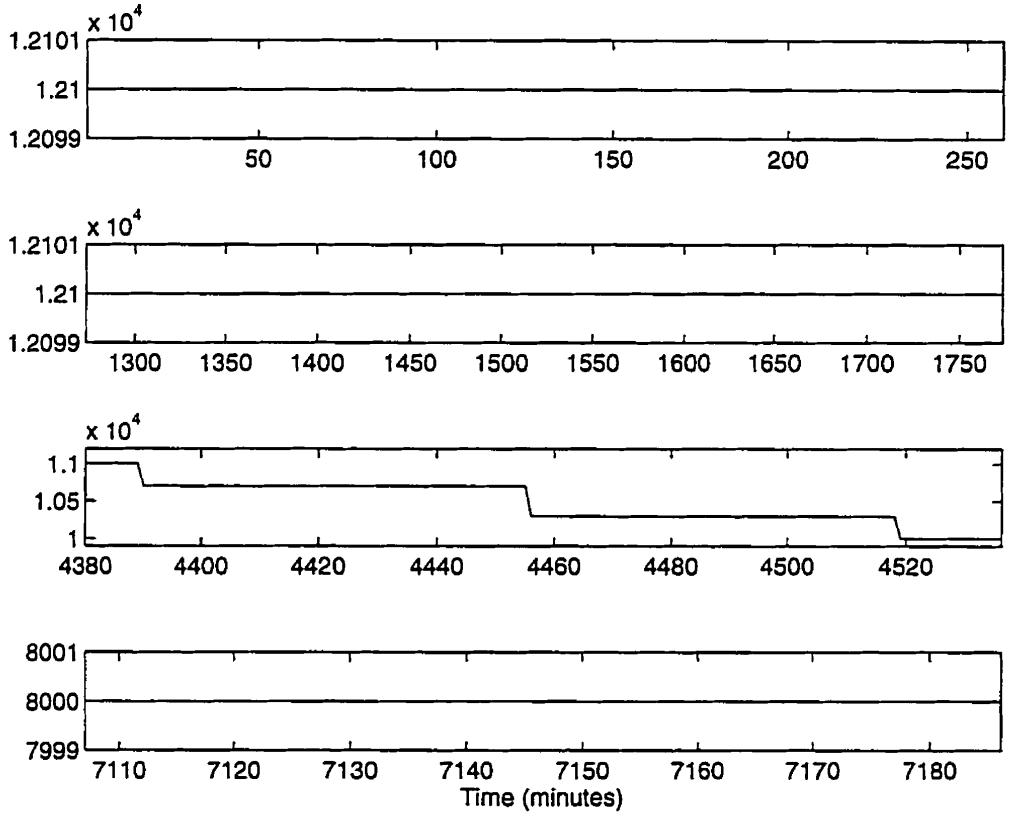

Figure A.3: Process input u_3

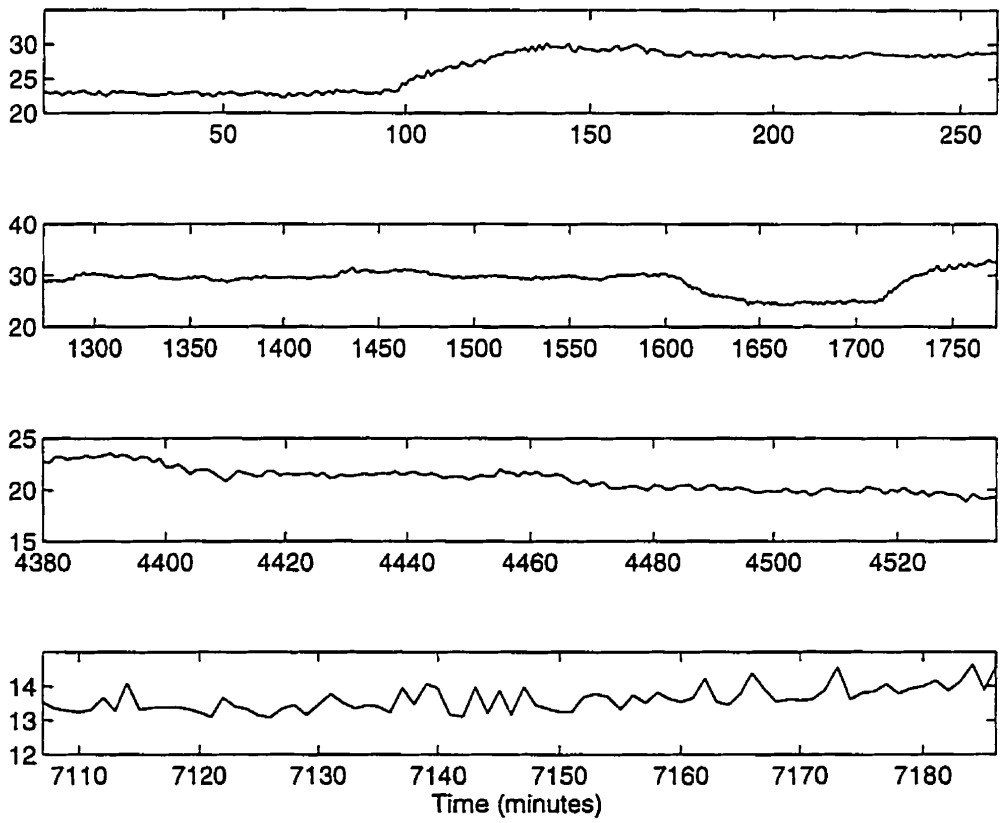

Figure A.4: Process output y_1

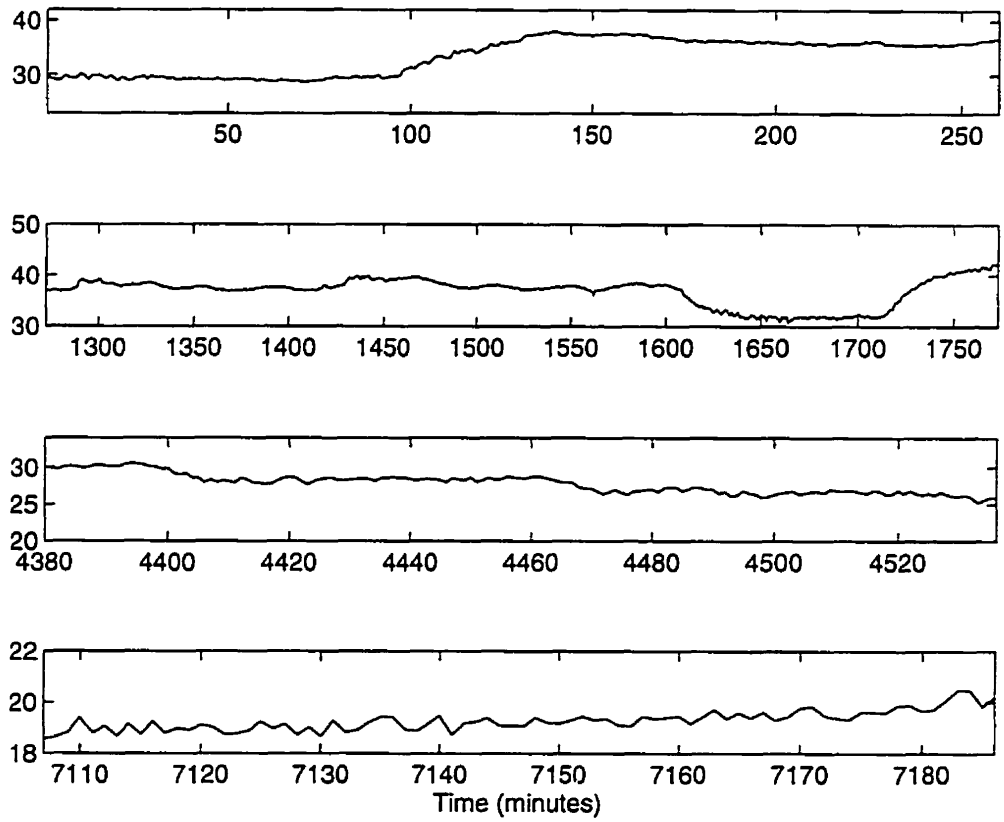

Figure A.5: Process output y_2

Appendix B

MATLAB Commands

B.1 $TH = \text{ARX}\ (Z, NN)$

Computes LS-estimates of ARX-models

$$A(z)y_t = B(z)u_{t-nk} + e_t$$

where $A(z) = 1 + a_1 z^{-1} + ... + a_{na} z^{-na}$; $B(z) = b_1 + b_2 z^{-1} + ... + b_{nb} z^{-nb+1}$.

TH: Returned as the estimated parameters of the ARX model.

Z : The output-input data $Z = [y \quad u]$, with y and u as being column vectors. For time series $Z = y$ only.

NN: $NN = [na \quad nb \quad nk]$. For AR models, $NN = na$ only.

B.2 $TH = \text{OE}(Z, NN)$

Computes the prediction error estimate of an output-error model

$$y_t = \frac{B(z)}{D(z)} u_{t-nk} + e_t$$

where $B(z) = b_1 + b_2 z^{-1} + ... + b_{nb} z^{-nb+1}$; $D(z) = 1 + d_1 z^{-1} + ... + d_{nd} z^{-nd}$.

TH: Returned as the estimated parameters of the output-error model.

Z : The output-input data $Z = [y \quad u]$, with y and u being column vectors.

NN: $NN = [nb \quad nd \quad nk]$.

TEST TARGET (QA-3)

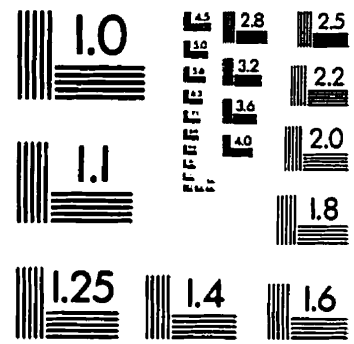

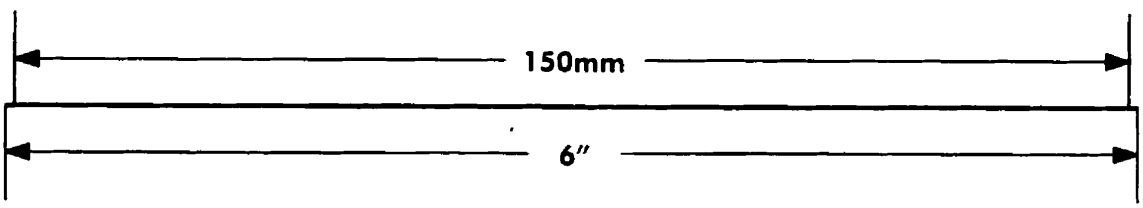

APPLIED IMAGE, Inc
1653 East Main Street
Rochester, NY 14609 USA
Phone: 716/482-0300
Fax: 716/288-5989